universität wien

MASTERARBEIT / MASTER'S THESIS

Titel der Masterarbeit / Title of the Master's Thesis

„Interaction of Vaccinia virus protein A46 with the mammalian proteins TRAM and TRIF"

verfasst von / submitted by

Nina Bobik, BSc

angestrebter akademischer Grad / in partial fulfilment of the requirements for the degree of

Master of Science (MSc)

Wien, 2017 / Vienna 2017

Studienkennzahl lt. Studienblatt / degree programme code as it appears on the student record sheet:	A 066 834
Studienrichtung lt. Studienblatt / degree programme as it appears on the student record sheet:	Masterstudium Molekulare Biologie
Betreut von / Supervisor:	ao. Univ.-Prof. Dr. Timothy Skern

Acknowledgements

I would like to thank Prof. Tim Skern for accepting me to his lab and for giving me the chance to work on this project, as well as for his helpful tips and advice concerning experiments.

My thanks go to Sofiya Fedosyuk for supervising me, for teaching me all the practical techniques of lab work, for giving me advice, for the interesting discussions in which I could learn a lot, and for answering my many questions.

I also want to thank all the nice people I had the pleasure of working with together in the lab: Gustavo Arruda Bezerra, Martina Aumayr, Daniel Azar, Karin Olek, Öykü Üzülmez and Amelie Schoenenwald. Thank you all for your helpful tips, for the friendly atmosphere you created and for the many enjoyable hours we spent together inside and outside of the lab. It is no matter of course to get along so well as colleagues, and you deserve the credit for making me feel welcome in the lab every day.

I am very grateful to Christina Wagner, who got me interested in molecular biology and without whom I probably would not be where I am today. Thank you for being both a friend and somebody to look up to.

I would like to thank Armin, who always knew that I would be a scientist.
Thank you for your encouraging words and your interest in what I do.

Last but not least, I want to thank my parents for their incredible support all along the way. Thank you for believing in me, for giving me advice when I need it, for pushing me to stand up to challenges that I probably would not have taken on by myself. Above all, thank you for encouraging me to walk my own path and to chase my dreams, wherever it is they may take me.

Table of content

Abstract

Vaccinia virus was used as the smallpox vaccine that led to the eradication of the devastating smallpox virus in 1980. It is known to encode for a vast variety of proteins that impede the function of the mammalian immune system. One of these proteins, A46, has been shown to bind to the TIR-domains of various adapter proteins within the TLR signaling pathway, a main component of the innate immune system that is responsible for the activation of the pro-inflammatory transcription factor NF-kB. Recently, the structures of both the C- and the N-terminus of A46 have been solved. These studies revealed a hydrophobic cavity formed by the N-terminus of the protein, which is capable of accommodating myristic acid. As one of the mammalian immune proteins targeted by A46, TRAM, is myristoylated in vivo, it can be speculated that this fatty acid is be used as a docking site by A46 in order to bind to TRAM and sequester its function. In this thesis, I present the purification of five mutants of the N-terminus of A46 that were subsequently shown to exhibit differences in their ability to bind fatty acids (Fedosyuk et al., 2016).

I also show the purification of an N-terminally deleted version of the TIR-domain of TRIF, another adaptor molecule involved in TLR signaling. However, the protein could not be obtained as a monomer in a purified state, emphasizing the instability of the protein and the difficulty to develop a suitable protocol for its purification.

Furthermore, I describe a way of purifying a C-terminally truncated variant of TRAM and investigate the ability of A46 to form a complex with TRAM both by co-expression in *E. coli* cells as well as by mixing the two purified proteins together *in vitro*. The results suggest that, under the conditions tested, the two proteins fail to form a complex, likely because the conditions they require for being soluble are very different. Moreover, I tried to elucidate possible effects of A46 on TRAM localization within mammalian cells by co-transfection of these constructs in mammalian cells and subsequent subcellular fractionation followed by visualization of the tagged proteins of interest by Western Blotting. A46 does not seem to have a significant effect on the relocalization TRAM, thus impairing this adaptor protein's function in TLR signaling in some other, still unknown way. Finally, I also investigate the localization of full-length A46 as well as the N- and C-termini alone in mammalian cells to gain an understanding of possible sites and modes of action of this viral protein. Surprisingly, my data suggests that it is not the N-terminus of A46 that targets it to the membrane, but the Bcl2-like C-terminus. Therefore, the hydrophobic cavity formed by A46 is likely not used to bind to membrane lipids in the cell but serves some other, to date unknown function.

Zusammenfassung

Das Vacciniavirus gehört zur Familie der Pockenviren und ist ein Bestandteil jener Impfung, durch die im Jahr 1980 die Pocken, eine Krankheit die im Lauf der Geschichte Millionen Menschenleben gefordert hat, weltweit als ausgerottet deklariert werden konnten. Das Virus ist unter anderem für seine Vielfalt an Proteinen bekannt, die das Immunsystem des Wirts beeinträchtigen, um dem Virus eine einfache Replikation in der Zelle zu ermöglichen. Eines dieser Proteine ist A46, das mit den TIR-Domänen zahlreicher Immunoadaptor-Proteine des TLR-Signalwegs interferiert. Dieser Signalweg stellt eine zentrale Komponente des angeborenen Immunsystems dar und löst die Aktivierung von NF-κB, einem pro-inflammatorischen Transkriptionsfaktor, aus. Sowohl die Struktur des N-Terminus als auch des C-Terminus von A46 wurde in den letzten Jahren aufgeklärt. Es zeigte sich, dass der N-Terminus einen hydrophoben Tunnel bildet, der Fettsäuren wie etwa Myristinsäure binden kann. Da TRAM, einer der Immunoadaptoren des TLR-Signalwegs, in vivo myristoyliert ist, kann spekuliert werden, ob A46 diese Modifikation nutzt, um spezifisch an TRAM zu binden und es zu inhibieren.

In dieser Arbeit präsentiere ich die Isolation von fünf Mutanten des N-Terminus von A46, die in weiteren Untersuchungen Unterschiede in ihrer Fähigkeit, Fettsäuren zu bilden, aufwiesen (Fedosyuk et al, 2016). Des Weiteren exprimierte und isolierte ich eine N-terminal verkürzte Variante der TIR-Domäne von TRIF, einem weiteren Immunoadaptor des TLR-Signalwegs. Allerdings konnte dieses Protein nicht als Monomer isoliert werden, was die Instabilität des Proteins und damit die Schwierigkeit unterstreicht, ein geeignetes Protokoll für seine Isolation zu etablieren. Weiters isolierte ich eine C-terminal verkürzte Variante von TRAM und untersuchte die Bindung zwischen diesem Protein und A46 sowohl durch Co-Expression in *E. coli* als auch durch *in vitro* Versuche mit beiden aufgereinigten Proteinen. Unter den getesteten Bedingungen konnte ich keinen Komplex zwischen TRAM und A46 nachweisen, vermutlich weil die Bedingungen, die die Proteine jeweils benötigen um löslich zu sein, zu unterschiedlich sind.

Außerdem co-transfizierte ich HEK293T-Zellen mit beiden Konstrukten und testete mithilfe von subzellulärer Fraktionierung und Western Blotting, inwieweit A46 einen Einfluss auf die subzellulare Lokalisation von TRAM in menschlichen Zellen hat. Es zeigte sich kein signifikanter Effekt, was darauf schließen lässt, dass A46 den TLR-Signalweg nicht durch Delokalisation von TRAM beeinträchtigt.

Schlussendlich untersuchte ich auch die subzelluläre Lokalisation der N- und C-terminalen Domänen von A46 im Vergleich zum vollständigen Protein. Überraschenderweise konnte ich nachweisen, dass A46 durch seinen Bcl2-ähnlichen C-Terminus und nicht über den N-Terminus an die Zellmembran bindet. Folglich verankert der hydrophobe Tunnel des N-Terminus das Protein nicht an Fettsäuren der Zellmembran, sondern besitzt eine andere, bis dato ungeklärte Funktion.

1. Introduction

Smallpox, an illness evoked by variola virus (VARV), was the most devastating disease in human history. It is believed to have emerged approximately 10.000 BC (Barquet and Domingo, 1997) and claimed millions of lives in wide parts of the world. VARV belongs to the genus *Orthopoxviridae* in the subfamily *Chordopoxvirinae* and the family *Poxviridae*. Symptoms of an infection include pustular rash, fever and headaches; the overall mortality rate was approximately 30% (Henderson et al., 1999; Belongia and Naleway, 2003). Following the development of a vaccine by Edward Jenner, it was found that exposure to vaccinia virus (VACV), a member of the same viral genus, provides cross-immunity against VARV, because the structural proteins of orthopoxviruses are highly conserved (Jacobs et al., 2009). After a worldwide vaccination campaign with VACV by the WHO, smallpox was declared eradicated in 1980. VACV remains a matter of scientific research for a variety of reasons, including its vast arsenal of proteins that interfere with the host's immune system and its potential as both an anti-tumor agent and a vector for other live vaccines. In this introduction, I will give an overview of the innate immune system and its major proteins and discuss vaccinia virus and how it can impede the host's immune system to facilitate its own replication.

1.1 Innate immune system

The immune system is responsible for detecting viral, fungal or prokaryotic pathogens that have entered an organism's body and for clearing them from the system by activating several defense mechanisms that combat the infection. It can broadly be differentiated into two parts: the innate immunity and the adaptive immunity. The adaptive immunity is a slow-acting, pathogen-specific system that is responsible for the formation of an "immune memory", which can be reactivated to clear pathogens rapidly from the organism's system in case of a recurring infection. In contrast, the innate immunity provides fast, unspecific protection against various infections, but cannot provide long-lasting immunity. The innate immunity is a multifunctional system that developed early in evolution and is found in almost all multicellular organisms (Medzhitov and Janeway, 2000). It provides fast protection against pathogens by recognizing them non-specifically through so-called pathogen-associated molecular patterns (PAMPs), molecular motifs typically found in or on the surface of pathogens (Medzhitov and Janeway, 2000). In the following chapters, I will briefly talk about the TLR signaling pathway, one of the main pathways through which the innate immune system detects and combats viruses that have infected an organism.

1.1.1 TLR signaling pathway

Toll-like receptors (TLRs) are a group of transmembrane proteins present on the endoplasmatic and the cellular membranes that recognize and bind to molecules characteristic for pathogens such as lipopolysaccharides (LPS) and dsDNA (Takeda et al., 2003). Such molecules are referred to as pathogen-associated molecular patterns (PAMPs) (Medzhitov and Janeway, 2000). Originally identified as a protein involved in ventralization in *Drosophila* by Christiane Nüsslein-Volhard, Toll has later been found to possess an immune function in the defense against fungi in the fly (Lemaitre et al., 1996).

In 1997, Medzhitov et al. discovered the first Toll-homologue in humans, the Toll-like receptor 4 (Medzhitov et al., 1997; Hansson and Edfeldt, 2005). So far, 13 different TLRs have been identified in mammals, of which TLRs 1-10 are functional in humans (Stack et al., 2005). TLRs contain an intracellular domain that closely resembles interleukin-1 receptors and an extracellular domain rich in leucine-rich repeats (Medzhitov et al., 1997; Slack et al., 2000; Akira and Takeda, 2004). Once a TLR binds a PAMP, it forms a homo- or heterodimer with another TLR protein and elicits an elaborate intracellular signalling cascade that ultimately results in the activation of the pro-inflammatory transcription factor NF-κB (Takeda et al., 2003). Different TLRs specifically recognize different PAMPs, as summarized by Yu et al. (Yu et al., 2010). A common feature of all TLRs and adaptor proteins involved in the signalling pathway is the Toll/IL-1R homologous region known as the TIR-domain (O'Neill and Bowie, 2007). This domain is approximately 200 amino acids long and has been shown to be crucial for signal propagation, as mutations in this region led to the loss of signalling (Slack et al., 2000). The structure of the TIR domains of human TLR1 and TLR2 have been solved. Both TIR domains consist of a central β-sheet surrounded by five alpha helices, but exhibit large conformational differences in certain loop regions. This structural diversity may be crucial for specificity in the signal transduction process (Xu et al., 2000). One of these loops, termed the BB loop, connects the second β-sheet to the second α-helix and has been found to be of particular importance to signalling, as mutations of conserved residues in this loop abolished downstream signal propagation (Xu et al., 2000; reviewed by Stack and Bowie, 2012).

For all TLRs except TLR3, the signal is first propagated via the adaptor protein MyD88. TLR2 and TLR4 additionally require the adaptor protein Mal to interact with MyD88 (Fitzgerald et al., 2001). The C-terminal region of MyD88 contains a TIR-domain, which interacts with the TIR-domains of the activated TLRs (Hultmark, 1994). MyD88 then recruits the interleukin-1 receptor associated kinases (IRAKs) IRAK1 and IRAK2 via its N-terminal death domain and IRAK4 via its intermediate domain (Wesche et al., 1997; Muzio et al., 1997; Burns et al., 2003). The activation of IRAK4, which functions as a kinase of other IRAK proteins, starts a cascade of phosphorylation and autophosphorylation of the IRAK proteins, which leads to the binding and subsequent oligomerization of TNFR-associated factor 6 (TRAF6) (Li et

al. 2002; Kollewe et al., 2004; Aderem and Ulevitch, 2000). TRAF6 and IRAK1 dissociate from the complex and recruit TAK-1 binding protein-1 (TAB-1) as well as TAK-1 and TAB-2, which leads to the degradation of IRAK1. Subsequent ubiquitylation and degradation of TRAF6 activate TAK-1, which in turn activates both mitogen activated protein kinases (MAPKs) and phosphorylates the inhibitor of κB kinase (IKK) complex consisting of the two kinases IKKα, IKKβ, and NEMO/IKKγ (Jain et al., 2014; Wang et al., 2001). Subsequently, both IKKα and IKKβ are able to phosphorylate the inhibitory IκB proteins, which form a complex with NFκB and mask its nuclear localization signal to keep it in an inactive form in the cytoplasm. This phosphorylation leads to the ubiquitylation and rapid degradation of the inhibitory IκB molecules (Karin and Ben-Neriah, 2000), which in turn allows for NFκB proteins to enter the nucleus and activate genes associated with inflammation and the fighting of pathogens.

Five proteins make up the family of the NF-κB transcription factors: NF-κB1 (p50), NF-κB2 (p52), REL-A (p65), REL-B and c-REL (Akira and Takeda, 2004). These proteins can associate with each other to form various homo-or heterodimers (Oeckinghaus and Ghosh, 2009). They all share an approximately 300 amino acid long region known as the rel homology domain (RHD), which mediates DNA binding, dimerization and interaction with IκB proteins (Ghosh et al., 1998). Over 150 target genes are regulated by NF-κB. These include a vast variety of cytokines and chemokines, major histocompatibility complex proteins, proteins involved in antigen presentation and neutrophil receptors (Pahl, 1999).

TLR3 does not use MyD88-dependent signaling pathway, but instead signals through the adaptor protein TRIF (also known as TICAM-1) to activate the expression of IFN-inducible genes, a pathway that can also be employed by TLR4. While TLR3 binds directly to TRIF, TLR4 requires another adaptor protein, TRAM (also known as TICAM-2), for the interaction with TRIF (Oshiumi et al., 2003a; Oshiumi et al., 2003b). TLR4 is therefore the only TLR which interacts with MyD88, Mal, TRIF and TRAM (Ullah et al., 2016). TRIF is a protein consisting of approximately 700 amino acids. Its N-terminal domain is capable of binding to TRAF6 and TBK-1, a kinase of IFN regulatory factor 3 (Sato et al., 2003), and has also been speculated to prevent oligomerization of TRIF molecules (Tatematsu et al., 2010). Its TIR-domain mediates interactions with TLR3 or TRAM, and its C-terminus has been observed to be involved in NF-κB activation and the initiation of apoptosis (Ullah et al., 2016). TRAM is a protein composed of 235 amino acids that specifically interacts with TLR4 for a MyD88-independent activation of inflammatory cytokines, but not with TLR3 and contains an N-terminal myristoylation site and a C-terminal TIR-domain (Fitzgerald et al., 2003a; Ullah et al., 2015). TRIF-dependent signaling has been shown to activate both NF-κB and interferon (IFN) regulatory factor-3 (IRF-3), an essential transcription factor for IFN-β expression (Sato et al., 2003; Oshiumi et al., 2003a). TRIF may bind either TBK-1 or TRAF6 through its N-terminal domain. While the latter leads to the activation of NF-κB through the pathway described earlier, the binding of TBK-1 leads to the phosphorylation and activation of IRF-3

(Fitzgerald et al., 2003b, Sharma et al., 2003), which in turn migrates to the nucleus, where it promotes the transcription of the IFN-β gene, which can activate the expression of various IFN-inducible genes associated with combating pathogens (Yoneyama et al., 1998).

A simplified summary of the steps in TRAF6-dependent TLR signaling is given in Fig. 1.

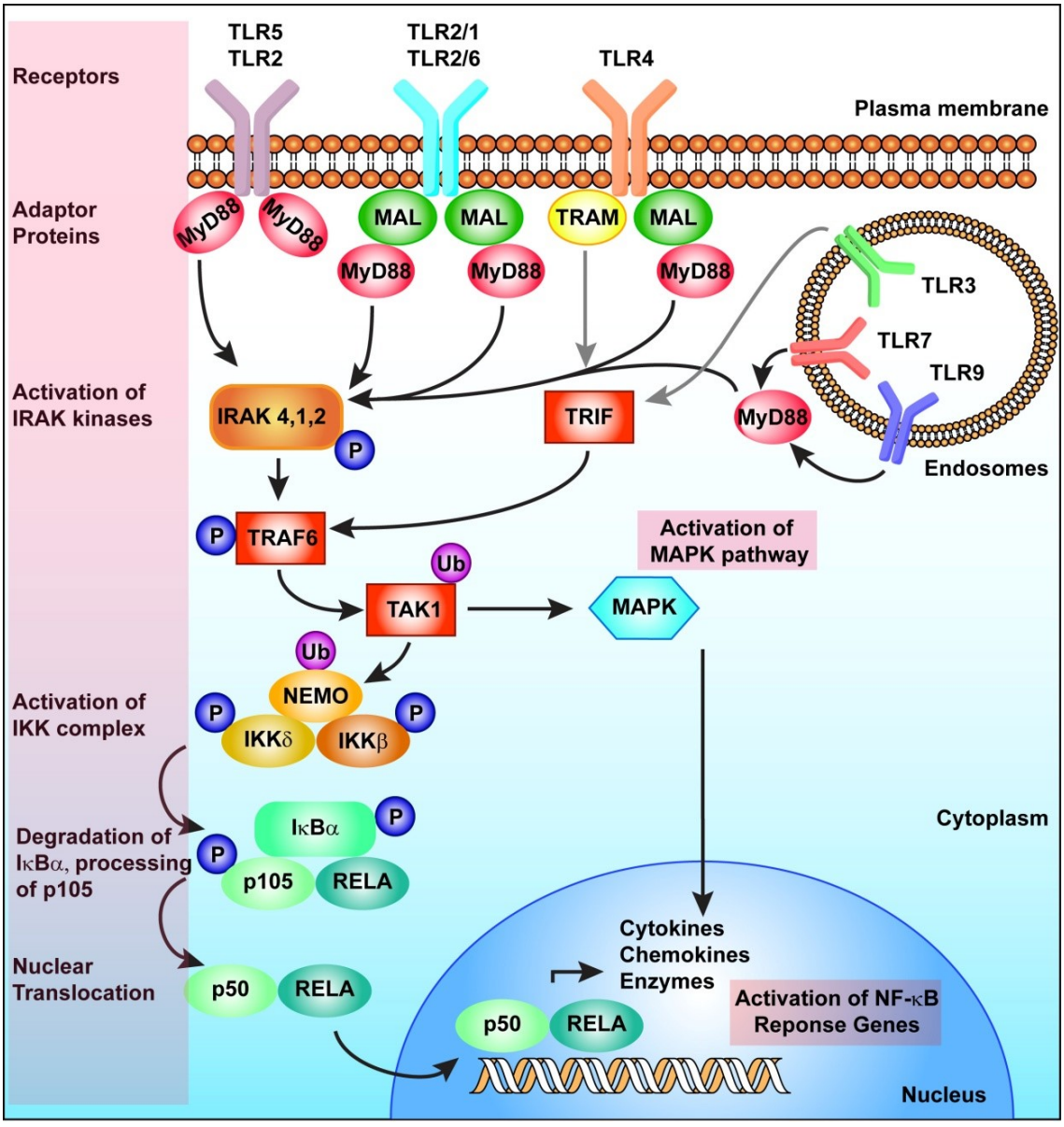

Figure 1 – Simplified overview of the TRAF6-dependent TLR signaling pathway. PAMPs activate the TLR signaling pathway. Most TLRs signal through the adaptor protein MyD88, while TLR3 recruits TRIF. TLR4 can signal through both MyD88 and TRIF and needs the additional adaptor protein TRAM in the latter case. TRAF6 becomes activated either by IRAK proteins or by TRIF and recruits TAK1, which activates MAP kinase and phosphorylates the IKK complex. Subsequent degradation of inhibitory IκB proteins releases NF-κB molecules, which enter the nucleus as homo-o heterodimers and activate the transcription of NF-κB response genes like cytokines and chemokines. Image by Sofiya Fedosyuk (Dissertation 2014).

1.2 Vaccinia virus

1.2.1 Reasons for vaccinia virus research

Even though the smallpox disease has been declared eradicated in 1980 by the WHO, vaccinia virus remains a subject of ongoing research for a variety of reasons.

First, as reproductive variola virus is still reposited in two institutes worldwide to the present day, concerns have been raised about the possibility of its misuse in bioterrorist attacks. Since the last vaccination against smallpox took place in 1978, people of younger generations all over the world would be highly susceptible to a reintroduction of this disease into society (Mayr, 2003). Furthermore, due to its high genetic similarity with variola virus, monkeypox virus (MPXV) can cause smallpox-like symptoms in humans and continued to lead to minor numbers of infections in African countries after the official eradication of smallpox (Nalca et al., 2005). MPXV, as well as other closely related viruses from the orthopoxvirus genus, like cowpox virus, camelpox and mousepox virus, have all been mentioned as further possible bioterrorism agents (Mayr, 2003). VACV strains stockpiled by the WHO to mass-immunize people in case of a reintroduction of a poxviral disease vary between countries and show differences in their potential to cause post-vaccination complications like encephalitis, and previous estimations of the number of deaths associated with vaccination may have been low (Kretzschmar et al., 2006). It is therefore necessary to search for novel, attenuated strains of VACV that would present safer options for vaccination.

Moreover, because of its capability to express foreign DNA inserted into its genome and because it is, in contrast to many other viral vectors, not oncogenic, recombinant VACV has been proposed as a vector for other live vaccines (Panicali and Paoletti, 1982). Insertion of the coding sequences of three different viral proteins into the genome of VACV and subsequent inoculation of these recombinant viruses into rabbits led to the animals producing antibodies against all three proteins (Perkus et al., 1985). Further characteristics of VACV that make it a promising tool for administering live vaccines include its cytoplasmic replication, broad host range, efficiency of transcribing inserted foreign DNA, lack of viral splicing machinery, relative vaccination safety, ease of administering the vaccine and its stability during storage (Hruby, 1990). Even though no VACV-mediated vaccine for use in humans has been approved to date, the potential of VACV for the immunization against various pathogens has long been acknowledged (Moss, 1991; Henderson and Moss, 1999). Multiple animal vaccines have been developed using VACV as a vector, including vaccines against vesicular stomatitis virus and rinderpest in cattle, pseudorabies in swine and influenza in chicken (reviewed in Henderson and Moss, 1999). Most notably perhaps is the eradication of fox rabies from Europe during the last three decades for

which, among other mechanisms of animal vaccination, a recombinant VACV expressing the glycoprotein of rabies virus was used (Freuling et al., 2013; Blancou et al, 1986; Brochier et al., 1995).

Finally, VACV is being investigated as a potential anti-tumor agent. Both active and irradiation-inactivated vaccinia viruses have been shown to inhibit tumor formation in rats suffering from chloroleukemia (Zakay-Roness and Bernkopf, 1964) and its oncolytic ability has long been recognized (Thorne et al., 2005). Deletion of various VACV genes can be employed to restrict its replication to neoplastic cells, and the expression of anti-tumor antigens as for example granulocyte–macrophage colony-stimulating factor in recombinant VACV has proven to confer antitumoral immunity (Goldufsky et al., 2013; Kirn and Thorne, 2009). Recently, the vaccinia virus Lister strain (L-IVP) has been shown to selectively target tumor cells both in vitro and in a mouse model and to decrease tumor size both by direct cell lysis and by arresting mitosis in malignant cells (Zonov et al., 2016). Overall, VACV is a promising anti-cancer agent because of its strong lytic nature concerning replicating cells and the ease of using it as a vector for introducing anti-tumor antigens into the afflicted tissues.

1.2.2 Vaccinia virus taxonomy

VACV is classified as an orthopoxvirus together with nine other closely related viruses, like VARV and MPXV. Even though it has been used in the WHO's global smallpox eradication campaign and studied extensively for the reasons mentioned in the previous chapter, the origin of VACV remains uncertain. All known strains of cowpox virus (CPXV), the virus originally used in vaccinations by Edward Jenner, show clear differences to the genome of VACV (Qin et al., 2015). A close phylogenetic familiarity with horsepox virus (HSPV) has been found, proposing a relatively recent common ancestor of HSPV and VACV (Tulman et al., 2006).

During the worldwide smallpox eradication campaign, multiple different strains of VACV have been used (Jacobs et al., 2009). As early vaccination procedures have been carried out in many countries without international standardization, VACV strains used in different parts of the world exhibited different biological properties and early strains were often named after the region that they were used in (Sánchez-Sampedro et al., 2015; Fenner et al., 1988; Jacobs et al., 2009).

1.2.3 Vaccinia virus structure

VACV is one of the largest viruses known to replicate in humans and exhibits a complex morphology. As a member of the poxvirus family, it lacks helical or icosahedral symmetry typical for many other viral families (Condit et al., 2006). Instead, the virion particle is of a rounded rectangle shape of approximately 350x270 nm size (Dubochet et al., 1994). Fenner et al. subdivided the virion into four sections: The core, which consists of one or more inner membranes surrounding the viral DNA and associated proteins, the lateral bodies, the outer membrane, and the envelope (Fenner et al., 1989). Fig. 2 shows a cryo-electron micrograph cross-section through an intracellular mature virion (IMV) (adapted from Cyrklaff et al., 2005) and Fig. 3 shows a schematic comparison of a mature virion and an enveloped virion.

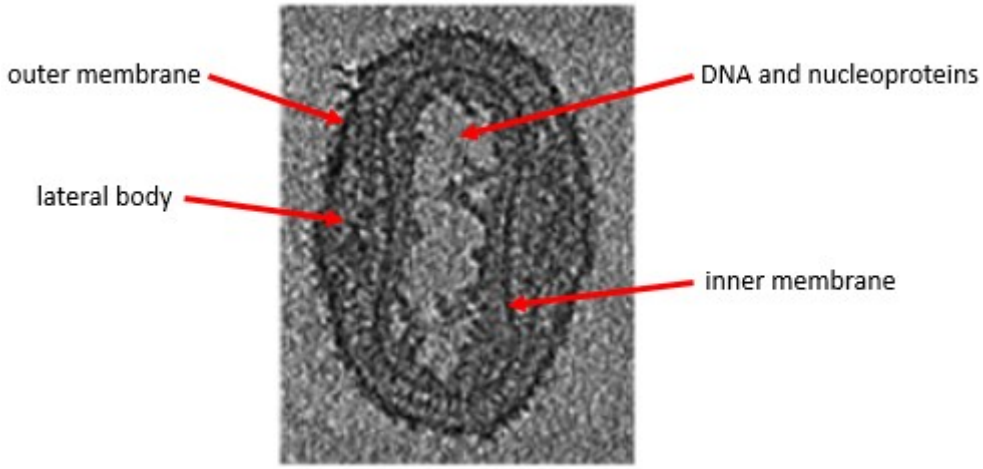

Figure 2 - Cryo-electron tomography of an IMV VACV particle. The inner and outer membrane are visible. The oval cavities between the membranes are the lateral bodies. DNA and nucleoproteins are contained within the inner membrane. No envelope is present on the IMV particle. Adapted from Cyrklaff et al., 2005.

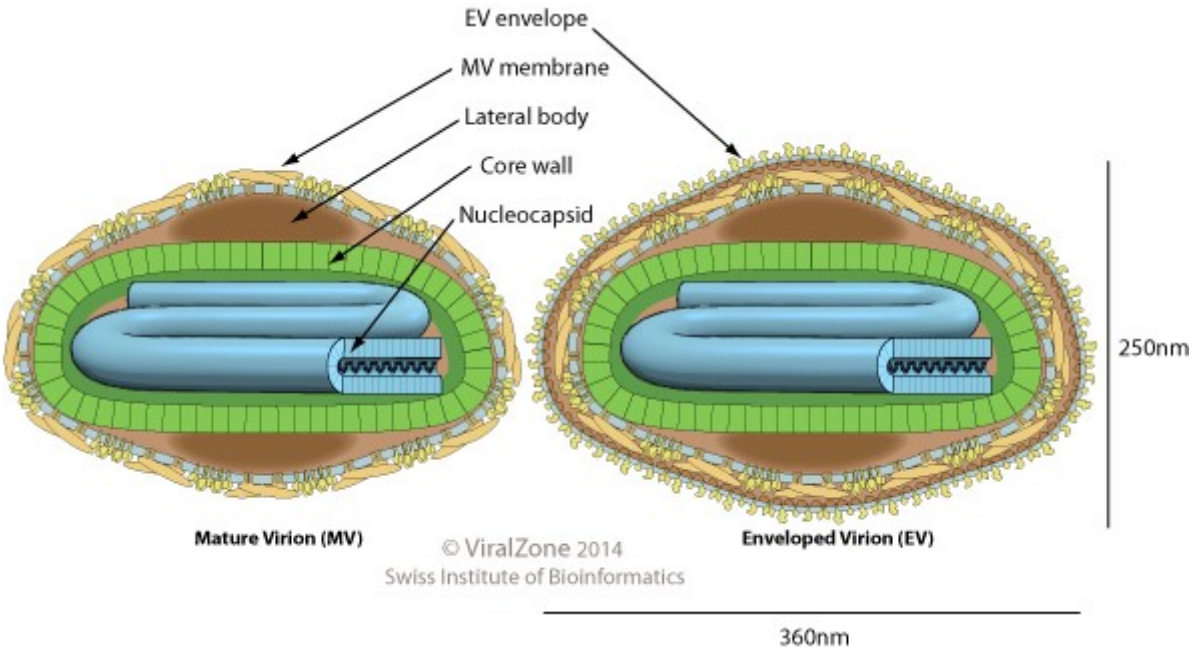

Figure 3 -Schematic cross-section of a mature intracellular virion and an enveloped extracellular virion. Image taken from http://viralzone.expasy.org

As can be seen in Fig. 2, there is no envelope present in IMVs. Indeed, intra- and extracellular VACV particles are antigenically different and extracellular virions possess an envelope, while no such structure is found in intracellular viral particles. This also explains why antisera targeting only intracellular virions cannot stop the spread of the virus in tissue culture (Appleyard et al., 1971). IMVs can form extracellular enveloped virions (EEVs). The IMVs are enveloped by an additional double membrane in the cytoplasm and transported to the periphery of the host cell, where the outermost membrane of the virion fuses with the plasma membrane, therefore releasing the EEV which is enveloped in one membrane more than the IMV (Payne and Kristenson, 1979; Morgan, 1976; Roper et al., 1996). The questions how the core particles acquire their membranes and how many membranes they contain remain very controversial topics. Some scientists claim that the membranes are derived from the endoplasmatic reticulum (Sodeik et al., 1993; Griffiths et al., 2001). However, others believe that the inner membrane is assembled *de novo* and only consists of one membrane (Dales and Mosbach, 1968; Hollinshead, 1999). Both IMVs and EEVs are infectious (Appleyard et al., 1971), although IMVs present the majority of viral progeny produced (Vanderplasschen et al., 1998).

The lateral bodies were found to consist of various proteins and dissociate from the core upon its release into the cytoplasm (Ichihashi et al., 1984). It has been speculated that VH1, a main component of the lateral bodies, subsequently functions to subvert the host's immune response at a point during the infection when no viral proteins have yet been expressed (Schmidt et al., 2013).

The genome of poxviruses consists of a linear, double-stranded DNA molecule approximately 191 kb in length (Goebel et al., 1990; Moss, 2013). It exhibits an inverted terminal repetition containing short

tandem repeats and AT-rich hairpin structures at both ends of each DNA strand (Moss, 2013; Wittek and Moss, 1980; Baroudy et al., 1982). While the terminal regions of the DNA which vary in length contain genes associated with host range, virulence and immunomodulation and the inverted terminal repeats vary in length from 0.65 to 12 kb between different orthopoxviruses, the central region is more conserved and contains genes crucial for transcription, DNA replication, enzymes and structural proteins (Fig. 4) (Smith and McFadden, 2002).

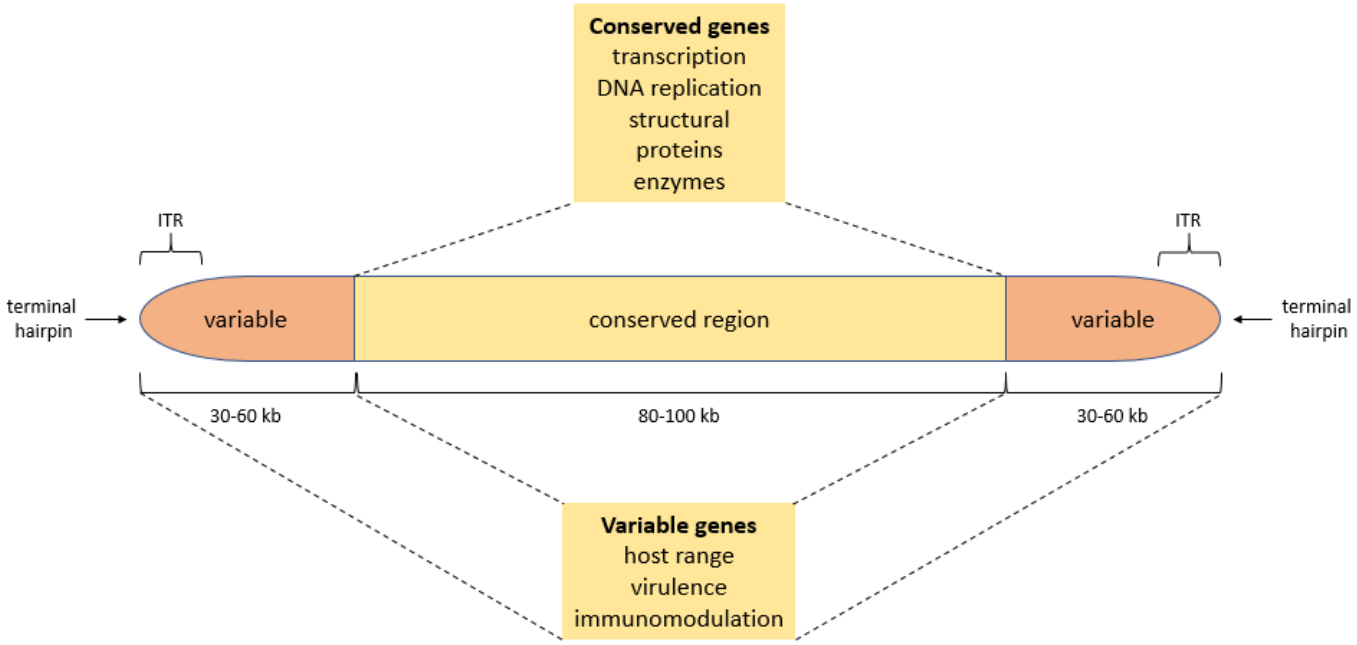

Figure 4 – Schematic drawing of the poxvirus genome. The central region is conserved and contains genes necessary for viral replication and assembly. The lateral regions vary in length between different poxvirus species and carry the genes involved in the modulation of the host's immune response. Inverted terminal repetitions and terminal hairpins are located at both ends of the DNA molecule. Adapted from Smith and McFadden, 2002.

1.2.4 Vaccinia virus life cycle

1.2.4.1 Host cell entry

Although many studies have investigated possible mechanisms of attachment and entry of VACV into the host cell, these processes have remained incompletely understood. VACV has two infectious virion states, the IMV and the EEV, which both are able to infect host cells, even though they use different cellular receptors. This peculiarity could be advantageous for the virus by broadening the cell, tissue or host tropism or by facilitating transmission (Vanderplasschen and Smith, 1997). While EEVs are created by fusion of double-membrane wrapped intracellular virions with the plasma membrane, IMVs are released from the host cell upon lytic rupture (Locker et al., 2000).

Different ways of cell entry have been proposed for VACV. While earlier studies have reported that virions enter the host cell by fusion with the plasma membrane (Armstrong et al., 1973; Chang and Metz, 1976; Doms et al., 1990), it has been shown more recently that a majority of VACV particles enters the cell by an endosomal pathway dependent on low pH (Townsley et al., 2006; Townsley and Moss, 2007). Another study reported that the binding of IMVs to cells triggers an intracellular signaling cascade involving rac1, rhoA, ezrin and tyrosine as well as protein kinase C phosphorylation, which leads to the formation of actin and ezrin containing membrane protrusions and subsequent uptake of the IMVs (Locker et al., 2000). It has been speculated that the ability of VACV to infect hosts cells via different routes could be a result of extensive cell culture passaging (Moss, 2012), or another adaptation of the virus to broaden its host cell range.

In a study focusing on the endocytotic uptake of VACV, virus particles were observed to move along filopodia to reach the host cells' surface, where they induce the formation of membrane blebs prior to cell entry by micropinocytosis (Mercer and Helenius, 2008). The process of membrane blebbing and the uptake of virions is dependent on PAK1 (Mercer and Helenius, 2008), a kinase crucial for cell motility and macropinocytosis (Dharmawardhane et al., 2000).

At present, the four viral proteins D8, H3, A26 and A27 have been shown to mediate attachment of the viral IMV particles to the host cell (Moss, 2012). D8 was shown to be a transmembrane protein that is synthesized late during infection (Niles and Seto, 1988). It features a carbonic anhydrase fold that can bind to the glycosaminoglycan chondroitin sulfate on the cellular surface (Matho et al., 2012). H3 is a highly conserved poxviral transmembrane protein with a glycosyltransferase fold that binds to UDP-glucose and the glycosaminoglycan heparan sulfate which is highly expressed on the cellular surface (Singh et al., 2016). A26 and A27 form a complex that is anchored to the IMV membrane via the transmembrane protein A17 (Howard et al., 2008; Wang et al., 2014). While A26 was proposed to facilitate IMV entry by binding to laminin (Chiu et al., 2007), A27 has been named as another possible anchor protein to the cellular membrane because of its ability to bind to heparan sulfate (Chung et al., 1998). However, while binding of IMVs to glycosaminoglycans appears to be a factor in IMV attachment, it seems to be cell-type specific and not a prerequisite for IMV entry into the cells (Carter et al., 2005). Furthermore, none of these proteins proved to be essential for IMV attachment or infectivity (Niles and Seto, 1988; Da Fonseca et al., 2000; Chang et al., 2010; Ward 2005). Additionally, to the study of possible proteins mediating attachment and cell entry, contradictory data exists about a possible role of the lipid phosphatidylserine in the uptake of VACV particles (summarized in Moss, 2012).

Further complication of the dissection of entry pathways of VACV stems from the fact that the mechanisms of VACV entry vary depending on the host cell (Whitbeck et al., 2009) and that different strains of VACV exhibit different mechanisms of micropinocytosis (Mercer et al., 2010).

1.2.4.2 Transcription

Poxviruses are one of the few DNA viruses that replicate in the cytoplasm of the host cell, as opposed to the nucleus (Minnigan and Moyer, 1985), which implicates that they must encode their own proteins for successful replication. Such enzymes include viral DNA ligase (Sambrook and Shatkin, 1969), DNA-dependent RNA polymerase (Kates and McAuslan, 1967) and DNA polymerase (Jones and Moss, 1984; Traktman et al., 1984). VACV RNA polymerase was described early as a high-molecular weight protein complex that was obtained by glycerol gradient sedimentation and was capable of accurate transcription initiation and termination (Broyles and Moss, 1987). Following those first purifications, nine subunits of the viral RNA polymerase were identified (reviewed in Broyles, 2003). Soon after the entry into the host cell, the outer membrane is degraded by cellular enzymes, leaving the viral core containing the DNA and nucleoproteins intact (Fenner et al., 1989). Subsequently, the viral DNA-dependent RNA polymerase synthesizes early poxviral messenger RNAs, which leave the core particle (Kates and McAuslan, 1967). From these early mRNAs, a protease with trypsin-like activity is produced which subsequently releases the poxviral DNA from the core particle into the cytoplasm (Pedley and Cooper, 1987). After uncoating of the viral DNA, mRNA synthesis is detectable quickly in the cytoplasm of the host cell and reaches its maximal synthesis rate approximately four hours after infection (Joklik, 1966). VACV mRNAs are capped at their 5'-terminus with either 2'-O-methyladenosine or 2'-O-methylguanosine (Wei and Moss, 1975). The capping enzyme encoded by VACV is a two-subunit protein that is approximately 118 kDa in size (Morgan et al., 1984) and was later found to be the same protein that also mediates poly-A-tail formation on the viral mRNAs (Schnierle et al., 1992). The transcription and replication of the viral DNA occurs in cytoplasmic foci termed virosomes (Cairns, 1960), which appear approximately two hours after infection and consist of dense fibrous material (Dales and Siminovitch, 1961). These virosomes, also termed factories, resemble interphase nuclei or chromosomes (Dales, 1963) and become enwrapped in endoplasmatic reticulum membranes approximately three hours after infection. These membranes disassemble again as immature precursor virions are produced in the late phase of transcription (Tolonen et al., 2001). The transcription of certain sets of VACV genes is strictly regulated in time. While genes encoding proteins for DNA replication, nucleotide biosynthesis and intermediate gene transcription are transcribed early during infection, genes for virion morphogenesis and assembly are transcribed during later phases (reviewed in Broyles, 2003). Specific promoter regions on the DNA of vaccinia virus have been

identified for early, intermediate and late gene transcription factors (Davison and Moss, 1989a; Baldick et al., 1992; Davison and Moss, 1989b). The transcription factor VETF consists of two subunits of approximately the same size and was shown to be a general promoter of early gene transcription, while itself being expressed only prior to packaging into virions (Broyles et al., 1988; Gershon and Moss, 1990). Therefore, VACV is not dependent on the host cell's machinery for the synthesis of early proteins. Expression of intermediate transcription factors (VITFs) begins immediately after DNA replication, but is not dependent on *de novo* protein synthesis, suggesting that VITFs are already present in the viral particle upon infection, but repressed until the DNA has been replicated. Intermediate genes encode for late transcription factors, thus making *de novo* protein synthesis as well as DNA replication essential for the activation of late genes (Vos and Stunnenberg, 1988; Keck et al., 1990).

1.2.4.3 Replication

VACV DNA replication, as well as viral RNA and protein synthesis and virion assembly, takes part in the factories in the cytoplasm (Katsafanas and Moss, 2007). DNA replication ensues approximately two hours after infection (Fenner et al., 1989). As stated above, this process leads to derepression of intermediate transcription factor activation. DNA replication is, alongside *de novo* protein synthesis, essential for the activation of late transcription (Vos and Stunnenberg, 1988).

VACV DNA polymerase is a polypeptide with a molecular size of approximately 115kDa that has both polymerase and 3'-5' exonuclease activity (Challberg and Englund, 1979). Further factors for the correct function of viral DNA polymerase have been identified: D4R is a viral uracil-DNA glycosylase whose ability to excise uracil from DNA is essential for virus viability (Stuart et al., 1993; Ellison et al., 1996). D5 is a nucleotide triphosphatase (Evans et al., 1995) which forms oligomers to catalyze ATP binding and hydrolysis (Boyle et al., 2007) and was also shown to have DNA primase activity (De Silva et al., 2007). A20R, a protein that binds to both D4 and D5 (McCraith et al., 2000), bridges D4 to the polymerase (Boyle et al., 2011) and also interacts with D5 (Ishii and Moss, 2001).

The exact mechanism of VACV DNA replication has been a matter of longstanding debate. As the two DNA strands of VACV are linked by terminal hairpins of complementary sequence (Baroudy et al., 1982), newly replicated DNA is present as concatamers (Moyer and Graves, 1981), which are afterwards separated by A22R, a Holliday junction resolvase (Garcia and Moss 2001).

It has further been found that various circular plasmids transfected into cells infected with VACV are replicated in the cytoplasm, indicating that no specific site of origin is necessary for DNA replication

carried out by VACV (DeLange and McFadden, 1986). However, a recent publication employing directional deep sequencing claimed that DNA replication of the VACV genome starts as a replication fork located at a terminal hairpin and that a main start site of replication may lie 35 nucleotides away from the hairpin apex. This study also implied the contribution of RNA-primed Okazaki fragments to VACV replication (Senkevich et al., 2015). Further studies will be necessary to elucidate the mode of VACV DNA replication in more detail.

1.2.4.4 Maturation and release

The first step of intracellular virus maturation is the formation of crescent-shaped membranes around the virus factories (Risco et al., 2002). While the first study proposed that these membranes are formed *de novo* (Dales and Mosbach, 1968), more recent studies concluded that they must be derived from the endoplasmatic reticulum (reviewed in Liu et al., 2014). These crescent membranes engulf viral material to form immature virions (IVs) (Condit et al., 2006). Additionally, so far nine genes have been identified to encode for proteins that play essential roles in crescent membrane formation, including the scaffold protein D13, the structural components A14 and A17, as well as regulatory proteins L2, A30.5, A11, A6, H7 and F10 (reviewed in Liu et al., 2014). A14 and A17 have been shown to be associated with the membranes of crescents, IVs and IMVs and co-immunoprecipitate with each other (Traktman et al., 2000; Rodríguez et al.; 1993; Rodríguez et al.; 1997). However, whether A14 and A17 truly bind to each other remains unknown, as binding experiments between their subregions did not show any interactions (Unger et al., 2013). The membrane(s) surrounding the IVs are coated in a honeycomb-shaped protein lattice composed of trimers of the D13 protein that disappears during the transition from IVs to IMVs and is replaced by a thicker, but less ordered protein coat (Heuser, 2005; Szajner et al., 2005). A17 and D13 interact with each other via residues 16 to 38 of A17, as binding between the two proteins was lost when this part of A17 was removed. Furthermore, membrane crescents are not formed in cells infected with VACV that expresses only an N-terminally truncated variant of A17. Crescents do form when a C-terminal truncation of A17 is expressed, however, in those cases no complete IV or IMV formation occurs, suggesting that A17-D13 interaction is crucial for crescent formation and that the C-terminus of A17 plays an important role in later stages of virion morphogenesis (Bisht et al., 2009). The VACV protease I7 cleaves A17 near its N- and C-terminus (Ansarah-Sobrinho and Moss, 2004), and this cleavage is responsible for the removal of D13 from the virions, which is required for successful IV to IMV transformation (Bisht et al., 2009; Unger et al., 2013).

How the IMV particle becomes enwrapped in membranes prior to release from the cell is still a matter of debate. Studies have suggested that these membranes stem from the trans-Golgi network (Schmelz

et al., 1994) or the endosomes (Tooze et al., 1993). These virions are subsequently expelled from the cell via exocytosis or upon cell lysis (Smith and Law, 2004). A subset of IMVs are enwrapped in one additional membrane from the trans-Golgi network to form enveloped virions (EVs). Those virions can then fuse with the plasma membrane and therefore exit the cell with one additional membrane layer compared to IMVs (Liu et al., 2014).

A visual summary of the VACV life cycle comprising infection, transcription, replication, packaging and release from the host cell is given in Fig. 5.

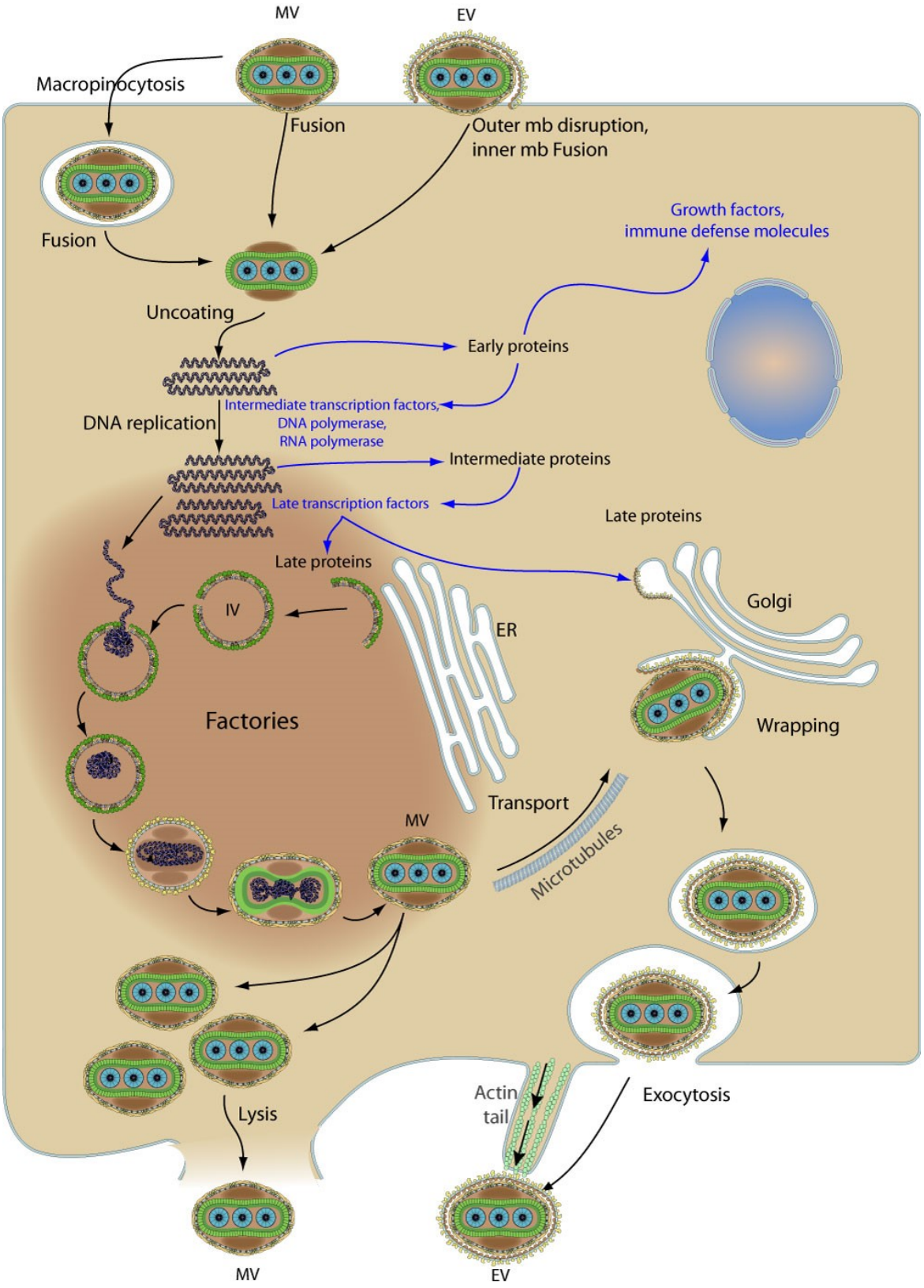

Figure 5 – Schematic overview of the VACV life cycle. Mature virions (MV) or extracellular mature virions (EV) enter the cell by macropinocytosis or membrane fusion and become uncoated and DNA replication and transcription of early proteins ensues. Many early proteins function to interfere with the host's immune system to ensure successful replication of the virus. DNA replication and transcription take place in virosomes, also called factories. Late genes code for structural proteins involved in packaging of the virus. The endoplasmatic reticulum (ER) forms crescent-shaped membrane structures that engulf viral material to form Immature virions (IVs) which subsequently mature. MVs can leave the cell through lysis, or they might be enwrapped by membranes of the Golgi or the endosomes and leave the cell as EV through exocytosis. Image from http://viralzone.expasy.org

1.2.5 Vaccinia virus proteins involved in immune evasion

To ensure successful replication, viruses have evolved various strategies to escape or impede the host's immune system. VACV exhibits an especially large arsenal of proteins that function to subvert the immune defense in various ways, both intra- and extracellularly. Notably, VACV expresses proteins that impede the function of the complement system, block the induction or inhibit the function of interferons, interfere with NF-κB activation, attenuate the effects of chemokines and cytokines like tumor necrosis factor (TNF) or interleukins or subvert apoptosis (Smith et al., 2013; Bahar et al., 2011; Seet et al., 2003). In this chapter, I will give a brief overview of the VACV proteins that specifically target the TLR pathway to inhibit the activation of NF-κB or INF-responsive genes.

It has long been known that during evolution, poxviruses took up genetic material from their hosts that became incorporated into the viral genome and underwent countless adaptational mutations (Hughes and Friedman, 2005; Shackelton and Holmes, 2004; Brady and Bowie, 2014). The structure of proteins in more conserved than their amino acid function. Thus, poxviruses express a variety of proteins that are structurally very similar to proteins found in their hosts, but show no apparent sequence similarity among themselves or to the host's ancestral protein (Franklin and Khan, 2013). An example of a group of such viral proteins are those that possess a Bcl-2 like fold, a structure that is commonly found in mammalian regulators of apoptosis, such as for example Bak and Bax (Franklin and Khan, 2013). VACV expresses a variety of proteins that are structurally very similar to these mammalian proteins, but do not play a role in apoptosis. Rather, they have evolved to impair the host's immune function, for example by inhibiting the activation of NF-κB either directly or by interfering with various steps in the TLR signaling pathway. Proteins of this group include B14, K7, A46, A52 and N1 (Graham et al., 2008; Brady and Bowie, 2014; Franklin and Khan, 2013). N1 has been reported to possess anti-inflammatory properties and to interact with cellular proteins involved in apoptosis, however, contradictory information exists concerning its binding to proteins of the apoptotic pathway (Franklin and Khan, 2013). Other proteins involved in immune suppression which have been predicted to exhibit a Bcl-2-like fold include N2, C1, C6 and C16/B22 (Franklin and Khan, 2013).

B14 is a 17kDa protein that contributes to virulence by inhibiting NF-κB activation from multiple pathways. It binds to the IKK complex via IKKβ and inhibits phosphorylation of IKKβ in a region called the activation loop. This in turn interferes with the phosphorylation of IκBα and therefore with the activation of NF-κB (Chen et al., 2006; Chen et al., 2008). Similarly, C4, a 37kDa protein that contributes to VACV virulence, inhibits NF-κB activation at or downstream of the IKK complex (Ember et al., 2012). Another VACV protein belonging to the Bcl-2-like family is K7 (Kalverda et al., 2009). It was reported to inhibit NF-κB activation through TLR3, TLR4 and IL-1 signaling as well as IRF3 and IRF7 activation

through TRIF-dependent signaling. It exerts this function by binding to IRAK2 and TRAF6, as well as to the DEAD box containing RNA helicase DDX3, which was found to interact with TBK1 and to be a positive regulator of TBK1/IKKε-mediated IRF3 and IRF7 activation (Schröder et al., 2008; Soulat et al., 2008). N1 was originally reported to inhibit signaling to NF-κB by IL-1β, TNFα, and the receptors TLR2, TLR3 and TLR4 and to associate with both TBK1 and the IKK complex (DiPerna et al., 2004). However, later studies found no ability to inhibit TNFα signaling or to bind IKK, rather suggesting that N1 would function at the level of TRAF6 (Graham et al., 2008; Chen et al., 2008). More research will therefore be necessary to elucidate the ways by which N1 exerts its anti-inflammatory function. A46 inhibits signaling of a variety of TLRs by binding to the adaptor proteins MyD88, Mal, TRIF and TRAM and to TLR4 itself (Stack et al., 2005; Brady and Bowie, 2014). Finally, A52 was shown to interfere with pathways leading to the activation of NF-κB from various TLRs by binding to TRAF6 and inhibiting TRAF6-TAB1 complex formation. Moreover, the binding of A52 to TRAF6 leads to the activation of p38 MAPK, which upregulates the production of the anti-inflammatory cytokine IL-10 (Maloney et al., 2005). Furthermore, A52 binds to the death domain of IRAK2 which also leads to a reduction of TLR-signaling-mediated NF-κB activation (Harte et al., 2003).

Other VACV proteins involved in the suppression of NF-κB which do not show the Bcl-2 like fold include A49, which mimics the molecular structure of phosphorylated IκBα and prevents IκBα ubiquitylation by β-TrCP, K1, a protein exhibiting ankyrin-like repeats that functions to prevent IκBα degradation, and E3, which contains a Z-DNA/RNA motif and blocks the activation of TLR7 (reviewed in Brady and Bowie, 2014).

In the following chapter, I will describe in more detail what is known to date about the structure and function of A46, the viral protein of interest in this thesis.

1.2.5.6 A46

As mentioned above, the VACV protein A46 has been reported to interact with the mammalian adaptor proteins MyD88, Mal, TRIF and TRAM as well as with TLR4 itself (Stack et al., 2005). The same study also found the protein to be expressed early during infection and contribute to VACV virulence in *in vivo* mouse models. A46 was originally described by Bowie et al. as an inhibitor of IL-1-mediated NF-κB activation and proposed to have a TIR domain to interact with its mammalian targets (Bowie et al., 2000). However, a more recent report predicted that A46 would possess a Bcl-2-like fold (González and Esteban, 2010). This was later confirmed by solving the structure of residues 87-229 of the protein, which revealed that the C-terminus of A46 consists of seven α-helices adopting the Bcl-2-like fold (Fig. 6A) (Fedosyuk et al., 2014). The viral inhibitor peptide of TLR4 (VIPER), a motif consisting of amino acid

residues 88-98 of A46, was reported to specifically bind to TRAM and Mal, but not to MyD88 or TRIF, and to inhibit TLR4 signaling (Lysakova-Devine et al., 2010). The authors speculated that since VIPER is located in an electropositive region on the surface of A46, it could interact with the binding sites of Mal and TRAM with TLR4, which are electronegative. This assumption was consolidated by the finding that a K88A mutation of A46 strongly reduced the interaction of the viral protein with Mal (Kim et al., 2014). Another study found that A46 lacking a functional VIPER region lost its ability to inhibit the TLR4 pathway, but left other TLRs unaffected (Stack and Bowie, 2012). This mutant protein also failed to bind to TRAM, but retained its ability to interact with Mal, indicating that A46 uses different interfaces to bind these two adaptor proteins. The same study identified a proline residue in a region called the BB loop of the TIR-domain of TLR4 as well as the adaptor proteins MyD88, Mal, TRIF and TRAM to be necessary for binding A46, and found that A46 inhibited receptor-adaptor interactions rather than receptor dimerization or adaptor-adaptor interactions. However, a complete model of how A46 interacts with its mammalian targets is still not available.

By employing size exclusion chromatography coupled to multi-angle laser light scattering analysis, full-length A46 was shown to be a tetramer, whereas A46 lacking the 86 N-terminal residues behaved as a dimer. This suggests that the N-terminus of A46 functions to hold together two dimers of the viral protein (Fedosyuk et al., 2014). Recently, the crystal structure of the A46 N-terminus comprising residues 1-83 has been solved. The N-terminus exhibits an all-β-sheet fold and assembles with another N-terminus to form a β-sheet sandwich that can accommodate fatty acids in its hydrophobic cavity (Fig. 6 B+C). Two such dimers assemble into a tetrameric structure with the dimers rotated approximately 90°C relative to each other, supporting the aforementioned hypothesis that the N-terminus of A46 is the mediator of its tetrameric nature (Fedosyuk et al., 2016). The presence of a molecule of myristic acid in the crystal is particularly interesting as it could present a novel way of interaction between A46 and TRAM. Since TRAM is myristoylated on its N-terminus in mammalian cells and this modification is necessary to locate it to the cellular membrane (Rowe et al., 2006), it can be speculated that the N-terminus of A46 binds to the myristic acid present on TRAM via its hydrophobic cavity, therefore removing TRAM from the cellular membrane and disrupting its function.

Fig. 7 shows a schematic model of the A46 tetramer and a possible way how it could simultaneously bind to various adaptor proteins of the TLR signaling pathway.

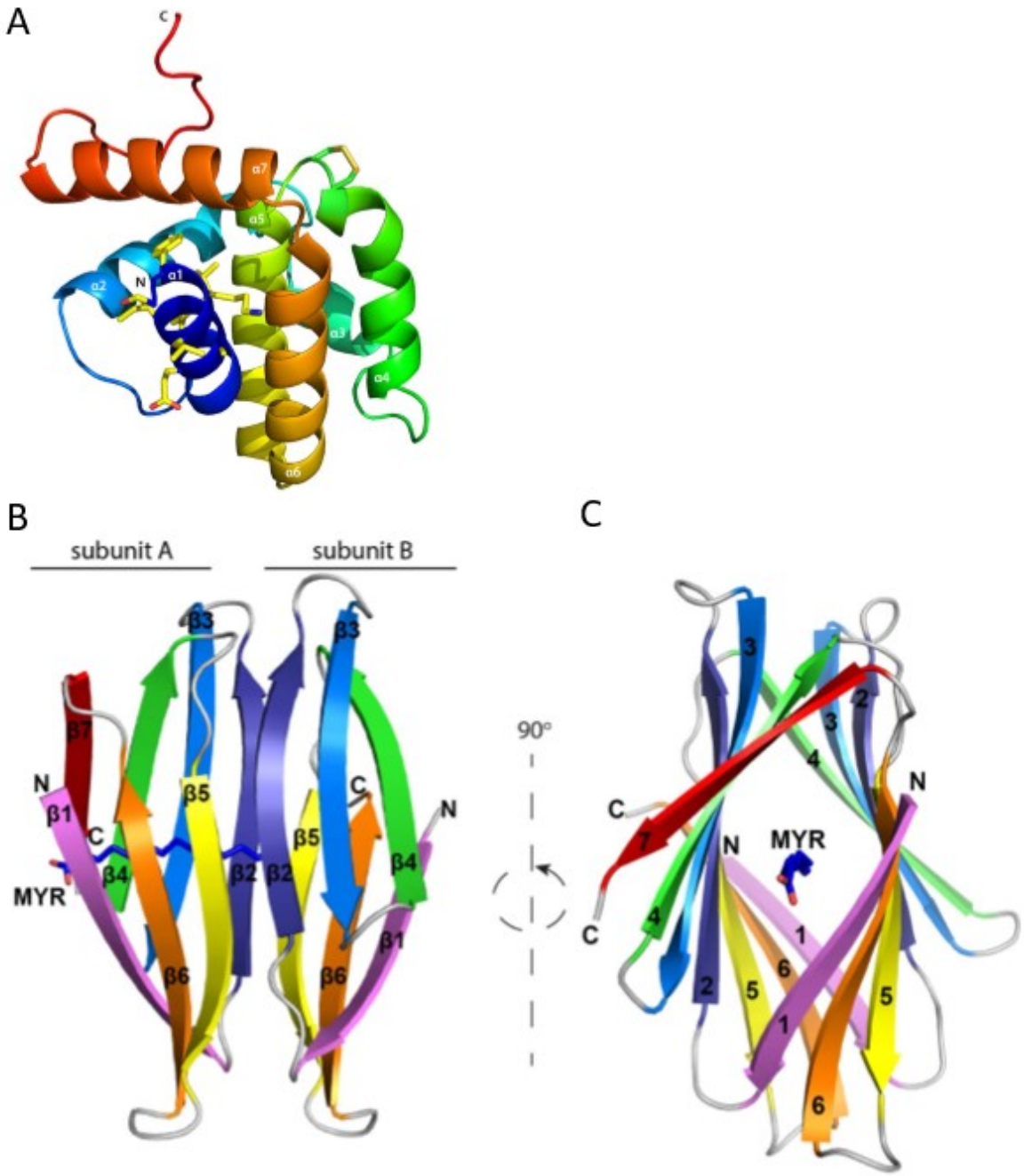

Figure 5 – Crystal structures of the A46 C- and N-terminal domain. ***(A)*** *Crystal structure of the C-terminal domain, which exhibits a Bcl-2-like fold. The central helix α5 is surrounded by six more helices. Image by Fedosyuk et al., 2014.* ***(B)*** *Side view of the β-sheet sandwich formed by the assembly of two A46 N-termini. Each subunit resembles one N-terminus. A molecule of myristic acid can fit into the hydrophobic cavity of the β-sandwich. Image by Fedosyuk et al., 2016.* ***(C)*** *The β-sandwich rotated by 90°. The polar head group of the myristic acid faces the solvent, while the hydrophobic tail is hidden in the viral protein. Image from Fedosyuk et al., 2016.*

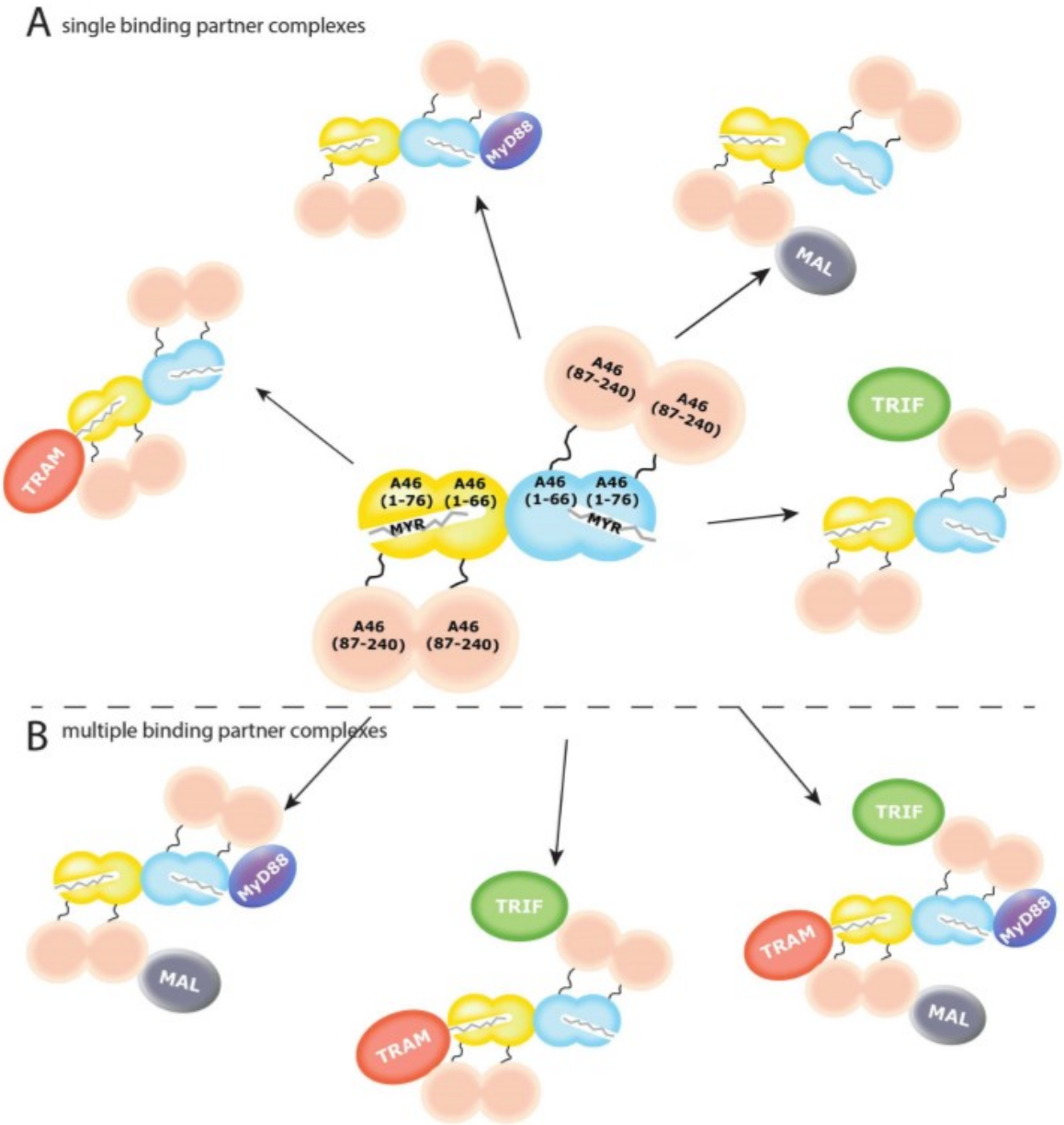

Figure 6 – Schematic drawing of a model of the A46 tetramer and how it could bind to various adaptor proteins of the TLR signaling pathway. Two A46 dimers are linked together via the B subunits of their N-termini. The hydrophobic cavity formed by the β-sandwich of either dimer can accommodate fatty acids like myristic acid. This tetrameric assembly would allow A46 to interact with multiple adaptor proteins simultaneously. Image from Fedosyuk et al., 2016.

1.3 Aim of Study

As has been described above, vaccinia virus protein A46 binds to various mammalian immune adaptor proteins involved in the TLR signaling pathway, therefore sequestering the host's immune response. One goal of this thesis was to elucidate the ability of A46 to form a complex with the TIR-domain of TRIF as well as with the human immuno-adaptor TRAM. We aimed to establish protocols for the expression and purification of both TIR-TRIF and TRAM. Furthermore, we investigated a potential complex formation between A46 and TRAM by co-expression and purification of both proteins and in *in vitro* pulldown experiments with the purified proteins.

The N-terminus of A46 was shown to bind myristic acid (Fedosyuk et al., 2016). We tried to express and purify five point mutants of the A46 N-terminus to determine whether these mutations influenced the ability of the viral protein to bind this fatty acid.

Furthermore, since TRAM is myristoylated in vivo, and this myristoylation is necessary to anchor TRAM to the cellular membrane and for the correct function of TRAM in the TLR signaling pathway (Rowe et al., 2006), it is possible that A46 could bind to the myristate of TRAM to delocalize it from the membrane and thus disrupt its function. The final aim of this thesis therefore was to investigate whether A46 has an effect on the subcellular localization of TRAM in mammalian cells. To this end, we performed subcellular fractionation on HEK293T HiExp cells that were transfected with both proteins and monitored their localization within the cells by Western Blotting. We also performed this set of experiments with full-length A46 as well as its N- and C-termini alone to gain a better understanding of their possible functions concerning localization and action in the host cell.

2. Materials and Methods

2.1 Buffers and solutions

The following list comprises buffers and solutions frequently used throughout the duration of this thesis. Buffers only used in one test expression are listed alongside the respective expressions in chapters 3.3 and 3.5.

LB medium:

25g Luria Bertani Broth per 1L of dH_2O, autoclaved

2x YT medium:

16g tryptone, 10g yeast extract, 5g NaCl per 1L of dH_2O, adjusted pH to 7.0 with NaCl, autoclaved

RF1:

100mM KCl, 50mM MnCl2, 30mM potassium acetate, 10mM CaCl2, 15% (w/v) glycerol, adjusted to pH 5.8 with HCl, sterile filtered

RF2:

10mM 3-morpholinopropane-1-sulfonic acid, 10mM KCl, 75mM CaCl2, 15% (w/v) glycerol, adjusted pH to 6.8 with KOH, sterile filtered

1X TAE buffer: 40mM Tris pH 7.6, 20mM acetic acid, 1mM EDTA

10x SDS running buffer:

25mM Tris, 192mM glycine, 0.1% SDS in dH_2O

Coomassie staining solution:

0.4% Coomassie brilliant blue, 40% C2H5OH in dH_2O

Transfer buffer:

25mM Tris, 192mM glycine, 20% CH2OH in dH_2O

1x PBS:

1.4mM KH2PO4, 2.7mM KCl, 4.3mM Na2HPO4, 137mM NaCl

1x PBST:

0.1% Tween20 in PBS

1x TBS:

50mM Tris, 150mM NaCl, adjusted pH to 7.5 with HCl

1x TBST:

0.1% Tween20 in TBS

Blocking solution:

20mg Tropix® I-BLOCK™(applied Biosystems) per 10ml of PBST

Stripping buffer:

15g glycine, 1g SDS, 10ml Tween20 per 1L of dH_2O, adjusted pH to 2.2 with HCl

2x SDS sample buffer:

20% glycerol, 10% β-mercaptoethanol, 6% SDS, 125mM Tris, 0.01% bromphenol blue in dH_2O, adjusted pH to 6.8 with HCl

5x SDS sample buffer:

50% glycerol, 25% β-mercaptoethanol, 15% SDS, 310mM Tris, 0.025% bromphenol blue in dH_2O, adjusted pH to 6.8 with HCl

Fractionation buffer:

20mM Tris/HCl pH 7.5, 10mM MgCl2, 1mM EDTA, 250µM sucrose, 200µM PMSF; sterile filtered; added 25x protease inhibitors directly before use (Rowe et al., 2006)

Nuclear lysis (NL) buffer:

50mM Tris/HCl pH 8.0, 150mM NaCl, 1% NP-40, 0.5% sodium deoxycholate, 0,1% SDS, sterile filtered, added protease inhibitors directly before use (Yu et al., 2013)

A46 N-term. lysis buffer:

20mM Tris/HCl pH 8.5, 100mM NaCl, 25mM imidazole, 5% glycerol, 10mM β-mercaptoethanol

A46 N-term. elution buffer:

20mM Tris/HCL pH 8.5, 300mM NaCl, 200mM imidazole, 15mM β-mercaptoethanol

A46 N-term. dialysis buffer

1: 20mM Tris/HCl pH 8.5, 150mM NaCl, 10mM imidazole, 15mM β-mercaptoethanol

A46 N-term. dialysis buffer 2:

20mM Tris/HCl pH 8.5, 2mM DTT

A46 N-term. FPLC buffer:

20mM Tris/HCl pH 8.5, 10mM DTT

A46 FL lysis buffer:

20mM Tris/HCL pH 8.5, 100mM NaCl, 10mM β-mercaptoethanol, 5% glycerol

A46 FL elution buffer:

20mM Tris/HCl pH 8.5, 100mM NaCl, 10mM β-mercaptoethanol, 5% glycerol, 250mM imidazole

A46 FL dialysis buffer 1:

20mM Tris/HCl pH 8.0, 200mM NaCl, 15mM β-mercaptoethanol

A46 FL dialysis buffer 2:

20mM Tris/HCl pH 8.5, 10mM DTT

TRAM lysis buffer:

50mM Tris/HCl pH 8.0, 500mM NaCl, 20mM imidazole, 10mM β-mercaptoethanol

TRAM elution buffer:

50mM Tris/HCl pH 8.0, 500mM NaCl, 10mM β-mercaptoethanol, 250mM imidazole

TRAM dialysis buffer:

50mM Tris/HCl pH 8.0, 500mM NaCl, 10mM β-mercaptoethanol

TRAM trial buffer:
20mM Tris pH 8.5, 100mM NaCl, 25mM imidazole, 10mM BME, 5% glycerol

2.2 Plasmids

The empty pET-11d, pET-29a, pCAGGS and pET-TRX1 vectors were kindly provided by Sofiya Fedosyuk. The pET-11d vectors containing the sequences of TRAM-TEV-His_{10} or His_{10}-TEV-TIR/TRIF between the cleavage sites of NcoI and BamHI were ordered from GenScript (www.genscript.com). For the preparation of the N-terminal mutants of A46, a pET-TRX1 vector with the EYFP sequence exchanged for the sequence of the N-terminal domain of A46 was used. This vector was as well provided by Sofiya Fedosyuk. For the expression of full-length A46, the pSF21 vector which had previously been designed by Sofiya Fedosyuk was used. It is based on the MalpET vector and encodes for MBP followed by a His_{10}-tag, the TEV cleavage site and the full-length A46 preceded by four additional amino acids (GSQQ). All plasmid maps without inserts are depicted in Fig. 8.

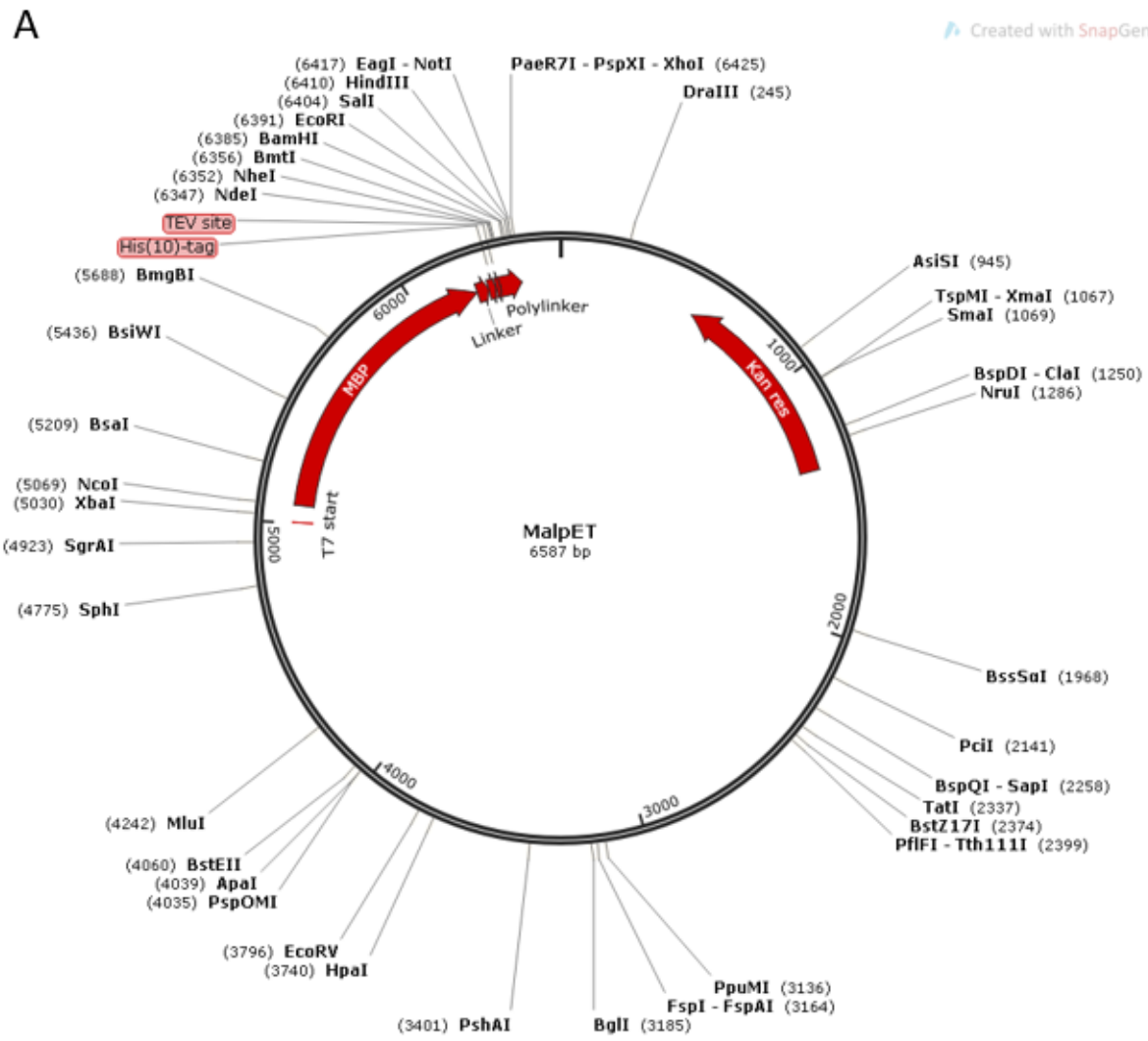

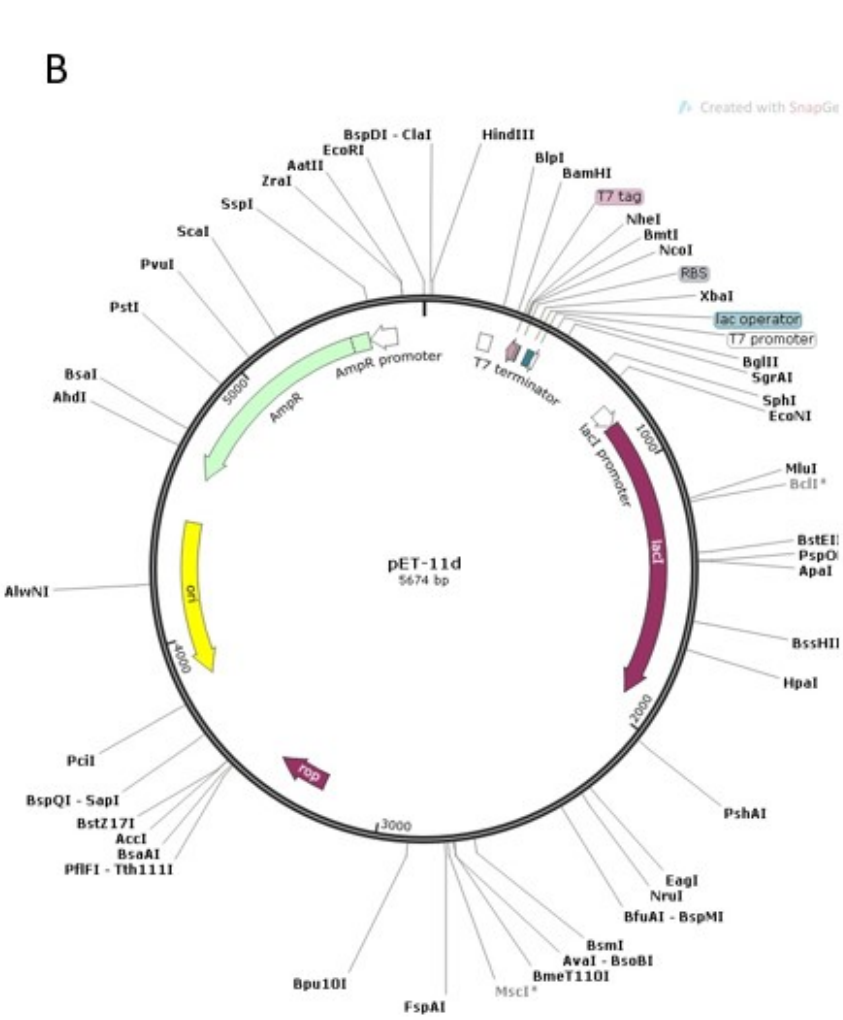
B
Created with SnapGe
pET-11d
5674 bp
BspDI - ClaI
EcoRI
HindIII
AatII
BlpI
ZraI
BamHI
SspI
T7 tag
ScaI
NheI
BmtI
PvuI
NcoI
RBS
PstI
XbaI
lac operator
T7 promoter
BsaI
BglII
AhdI
SgrAI
SphI
EcoNI
MluI
BclI*
BstEII
PspO
ApaI
AlwNI
BssHII
HpaI
PciI
PshAI
BspQI - SapI
BstZ17I
AccI
BsaAI
PflFI - Tth111I
EagI
NruI
BfuAI - BspMI
BsmI
AvaI - BsoBI
BmeT110I
MscI*
Bpu10I
FspAI
AmpR promoter
T7 terminator
lacI promoter
AmpR
ori
rop
lacI
5000
1000
2000
3000
4000

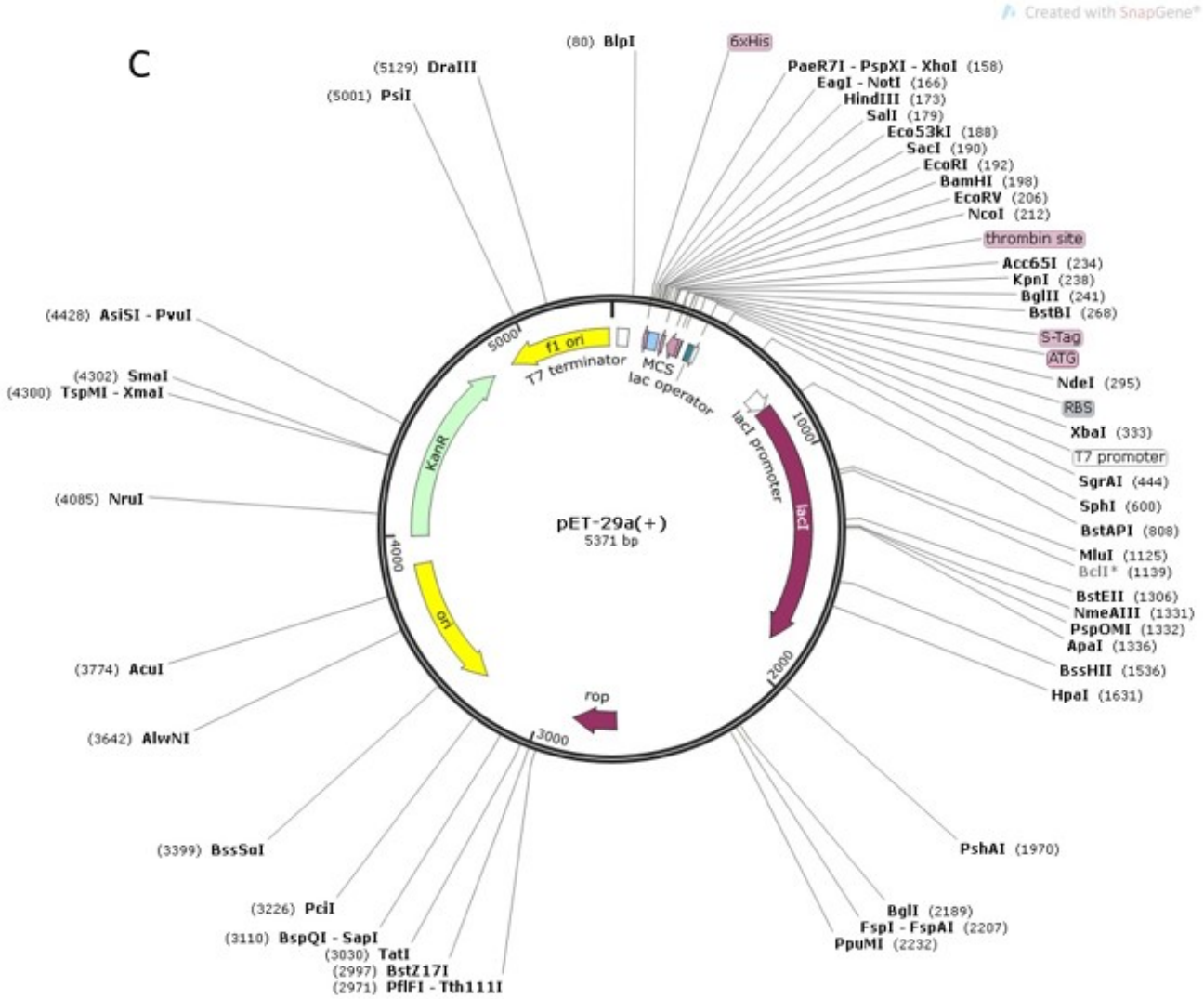
C
Created with SnapGene®
pET-29a(+)
5371 bp
(80) BlpI
6xHis
(5129) DraIII
PaeR7I - PspXI - XhoI (158)
(5001) PsiI
EagI - NotI (166)
HindIII (173)
SalI (179)
Eco53kI (188)
SacI (190)
EcoRI (192)
BamHI (198)
EcoRV (206)
NcoI (212)
thrombin site
Acc65I (234)
KpnI (238)
BglII (241)
BstBI (268)
S-Tag
ATG
NdeI (295)
RBS
XbaI (333)
T7 promoter
SgrAI (444)
SphI (600)
BstAPI (808)
MluI (1125)
BclI* (1139)
BstEII (1306)
NmeAIII (1331)
PspOMI (1332)
ApaI (1336)
BssHII (1536)
HpaI (1631)
PshAI (1970)
BglI (2189)
FspI - FspAI (2207)
PpuMI (2232)
(4428) AsiSI - PvuI
(4302) SmaI
(4300) TspMI - XmaI
(4085) NruI
(3774) AcuI
(3642) AlwNI
(3399) BssSaI
(3226) PciI
(3110) BspQI - SapI
(3030) TatI
(2997) BstZ17I
(2971) PflFI - Tth111I
f1 ori
T7 terminator
MCS
lac operator
lacI promoter
KanR
ori
rop
lacI
5000
1000
2000
3000
4000

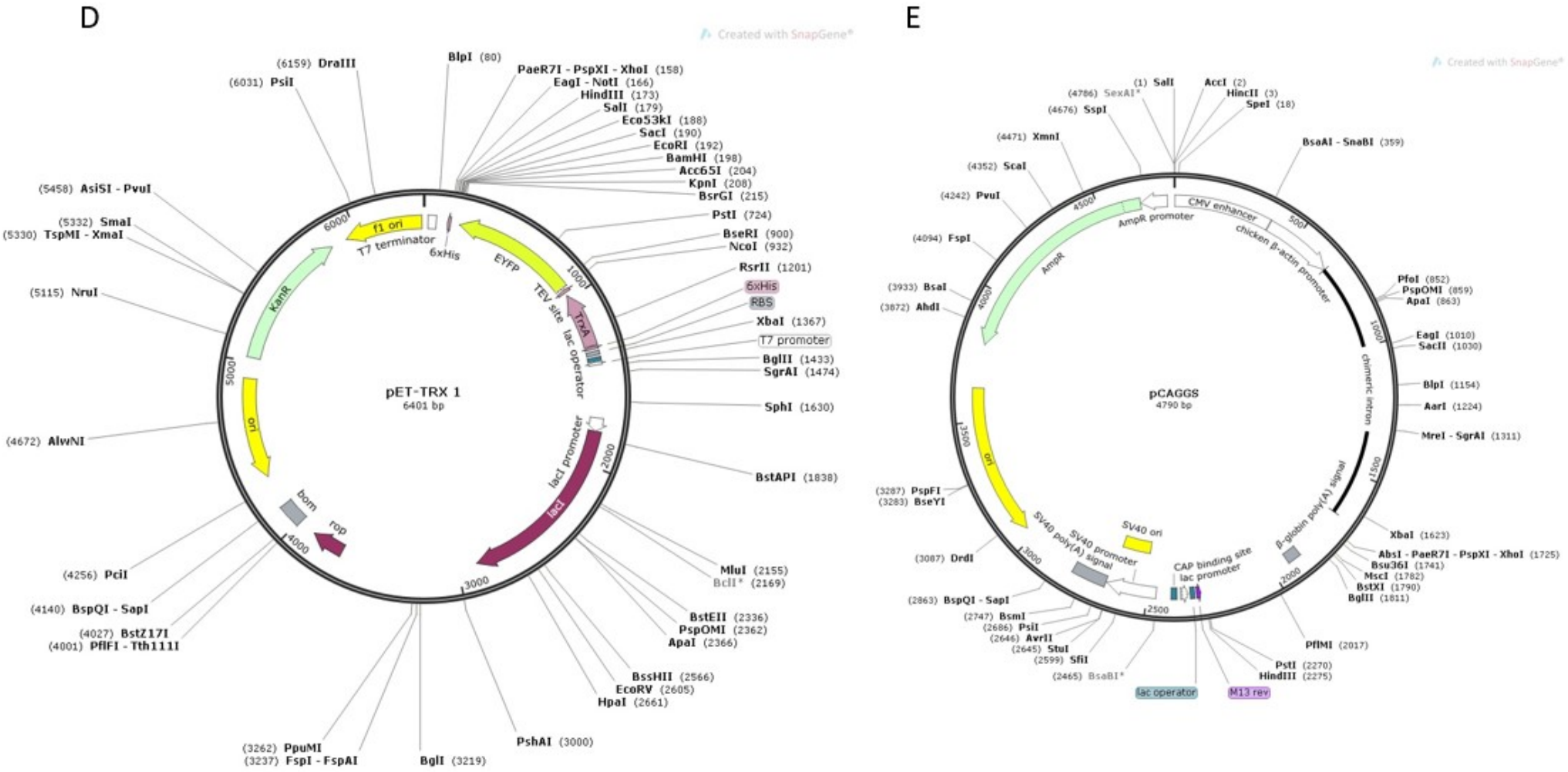

Figure 7 - Maps of four plasmids used in this work. ***(A)*** *Plasmid map of MalpET* ***(B)*** *Plasmid map of pET-11d* ***(C)*** *Plasmid map of pET-29a* ***(D)*** *Plamsid map of pET-TRX1. The sequence of EYFP was exchanged for the sequences of the different N-terminal mutants of the A46 protein.* ***(E)*** *Plasmid map of pCAGGS.*
Vector maps were created with the SnapGene Viewer program.

2.3 DNA methods

2.3.1 Competent *E. Coli* cells

70µl aliquots of *E. Coli* Top10, BL21 or B834 cells were inoculated into 3ml of 2xTY medium and grown overnight at 37°C, 210 rpm. The next morning, these overnight cultures were used to inoculate 100ml of 2xTY medium and the cells were grown until the OD_{600} reached a value of 0.45 – 0.55. At this point, the cultures were cooled on ice for 15 minutes and the cells were collected by centrifugation at 2500 rpm on 4°C for 15 minutes. The supernatant was discarded and the pellet was carefully resuspended in 33ml of ice cold RF1 buffer. Subsequently, the suspension was incubated on ice for 15 minutes and the cells were collected by centrifugation as described before. The supernatant was removed and the cells were carefully resuspended in 5ml of ice cold RF2 buffer. The competent cells were aliquoted into eppendorf tubes which had been precooled on -20°C and the aliquots were snap frozen in liquid nitrogen and subsequently stored on -80°C.

2.3.2 Transformation

100µl of competent *E. coli* cells were thawed on ice for 5 minutes and 1µl of plasmid DNA or 10µl of DNA from ligations or PCR reactions were added. Cells were incubated on ice for 15 minutes before being subjected to a 42°C heat shock for 45 seconds. Subsequently, 500µl of antibiotic-free LB medium were added and cells were revived on 37°C for 60 minutes. The cells were then either inoculated into LB containing the respective antibiotic and grown overnight at 37°C, 210 rpm or plated out on agar plates containing the respective antibiotic and grown overnight at 37°C.

2.3.3 DNA Minipreparation

Single *E. Coli* colonies were picked from agar plates and inoculated into 5ml of LB containing the respective antibiotics. Cultures were grown overnight at 37°C and 210 rpm. The next morning, cells were collected by centrifugation at 5000 rpm for 5 minutes and the supernatant was discarded. Plasmid DNA was extracted from the pelleted cells and purified using the Wizard® Plus SV Minipreps DNA Purification System from Promega according to the manufacturer‘s manual. In the last step, the plasmid DNA was eluted with 40µl dH_2O. Concentration was measured on a Nanodrop ND-1000 Spectrophotometer and the samples were frozen on -20°C for storage.

2.3.4 DNA Midipreparation

Single *E. Coli* colonies were picked from agar plates and inoculated into either 100ml or 150ml of LB containing the respective antibiotics. The cultures were grown overnight at 37°C, 210 rpm and cells were pelleted the next morning by centrifugation at 4000 rpm for 10 minutes. The supernatant was discarded and the cell pellet was used to extract plasmid DNA using the PureYieldTM Plasmid Midiprep System from Promega according to the manufacturer's manual. In the final step, DNA was eluted with 400µl of dH_2O. Concentration was measured with a Nanodrop ND-1000 Spectrophotometer and the samples were frozen on -20°C for storage.

2.3.5 Polymerase chain reaction (PCR)

Polymerase chain reactions were employed to either introduce point mutations into plasmid sequences or to amplify desired fragments from vectors for subsequent ligation into other plasmids. All PCRs were carried out on a Mastercycler®gradient (Eppendorf) with the standard program given below. Depending on whether a fragment or a whole vector should be amplified, we varied the elongation time of the program and the total reaction volume. In the case of fragment amplification, we used a one minute elongation time and three reactions of 50µl, whereas for whole vector amplification, we set an elongation time of five minutes and carried out the reaction with one tube of 50µl.

Amounts of reagents for one PCR reaction	
plasmid DNA	0.5-1µl
primer 1	0.5µl
primer 2	0.5µl
2mM dNTPs	5µl
Q5 reaction buffer	10µl
Q5 polymerase	0.5µl
dH_2O	32.5µl
total volume	50µl

PCR parameters		
98°C	10’	
98°C	30’’	25 cycles
50°C	30’’	
72°C	1’ or 5’	
72°C	10’	
4°C	hold	

2.3.6 PCR of colonies

Single *E. coli* colonies from transformations with ligation products were picked and resuspended in 10µl of dH_2O. 1µl of these suspensions was used in the following PCR along with two primers that would amplify the potentially ligated desired sequence from the plasmid DNA in the cells. 0.5µl of an uncut vector containing the right sequence was used as a control in all experiments and subjected to the same PCR as all samples in question. Afterwards, 13µl of all samples were run on an 1% agarose gel and suspensions which showed a band of the same size as the amplified fragment of the control vector were inoculated for minipreps.

Amounts of reagents for one colony PCR reaction

Cell suspension	1µl
primer 1	0.25µl
primer 2	0.25µl
OneTaq®2xMM	12.5µl
dH_2O	11µl
Total volume	25µl

Colony PCR parameters

95°C	5’	
95°C	30’’	25 cycles
53°C	30’’	
72°C	1’	
72°C	1’	
4°C	hold	

2.3.7 Restriction digest and DpnI-mediated digest of methylated DNA

DNA fragments amplified by PCR and vectors which were needed as backbone in subsequent ligations were both cut with two restriction enzymes each to allow ligation afterwards. All restriction enzymes were purchased from NEB. They cut the DNA at specific restriction sites and thereby create short, single-stranded overhangs which can then be annealed to and ligated with complementary single-stranded overhangs of another DNA piece. For DNA inserts amplified by PCR, 0.5µl of each restriction enzyme was added per 50µl of PCR reaction product. For whole vectors, 2µl of each restriction enzyme were added per 45µl of vector DNA. The digests were carried out at 37°C for at least 1.5 hours. Table 1 shows all restriction enzymes used in this thesis and their respective restriction sites.

Table 1 - restriction enzymes used in this thesis and their respective restriction sites in the 5' --> 3' direction. The restriction site is marked with a "ˇ".

Restriction enzyme	Restriction site 5’ → 3’
***Nco*I**	CˇCATGG
***Bam*HI**	GˇGATCC
***Nde*I**	CAˇTATG
***EcoR*I**	GˇAATTC
***Xho*I**	CˇTCGAG

For the specific degradation of methylated DNA, the enzyme DpnI (NEB) was used. DpnI degrades methylated but not non-methylated DNA. Since plasmids produced by *E. coli* have these modifications but DNA synthesized during a PCR does not, DpnI can be added to a PCR product to specifically degrade the template DNA. 1.5µl DpnI were added to PCR products and the digest was carried out at 37°C for either 3-5 hours or overnight.

2.3.8 Dephosphorylation of cut vector backbone DNA

To prevent religation of vector backbone DNA after cutting it with restriction enzymes, 1.5µl of Calf Intestinal Alkaline Phosphatase (CIP; purchased from NEB) was added per 45µl of cut vector backbone. CIP is an enzyme that dephosphorylates the 5' end of DNA and thereby prevents the cut vector to religate even if the overlapping ends are complementary to each other.

2.3.9 Agarose gel electrophoresis

For analytical gel electrophoresis, either 35ml or 80ml of 0,5x TBE buffer containing 1-1,5% agarose was used. For DNA purification agarose gels, 35ml of 0,5x TAE buffer containing 0,7% agarose was used. The solution was heated up in a microwave to dissolve the agarose and cooled down on room temperature for a couple of minutes before pouring it into polymerization chambers. The gels were polymerized for at least 30 minutes before the start of the electrophoresis. Gels were run in 0,5x TAE buffer at 120V for 10-20 minutes and subsequently the DNA was stained in a water bath containing 0,01% ethidium bromide for 15 minutes before visualization on a UV-illuminator. GeneRuler™DNA Ladder Mix from Fermentas was used as marker and 6x Loading Dye from Fermentas was used to run the samples on the gels.

2.3.10 DNA gel extraction and cleanup

In the case of DNA gel extraction, the bands of interest were cut out from the agarose gel using a scalpel and transferred to a 1.5ml Eppendorf tube. In the case of PCR products that were not run on an agarose gel, the samples were directly used in the cleanup step without further treatment. The DNA was extracted from the samples and cleaned up using either the Wizard® SV Gel and PCR Clean-Up System from Promega or the Monarch TM PCR & DNA Cleanup Kit (5ug) from NEB according to the respective manufacturer's protocol. DNA was eluted with 8-50µl of dH_2O depending on which kit was used and the length of the DNA. The obtained samples were frozen on -20°C for storage.

2.3.11 Ligation

All ligations were carried out in a total volume of 10µl. Approximately 250ng of plasmid backbone DNA cut with the respective restriction enzymes were mixed with similarly cut insert DNA in a ratio of 1:5. The online tool NEBioCalculator was used to calculate how much insert DNA sample had to be used to reach this ratio. 1µl of 10x Buffer for T4 DNA Ligase and 0.5µl of T4 DNA ligase from NEB were added and the total volume of the reaction mix was adjusted to 10µl with ultrapure H_2O. The samples were kept on 4° either for one hour or overnight and subsequently transformed into Top10 *E. coli* cells.

2.3.12 Introducing point mutations into ptrx-A46 (1-83)

To express the mutants of the N-terminus of A46, we first needed to obtain the plasmids encoding for these mutant proteins. To do so, we employed site-directed mutagenesis on the ptrx-A46 (1-83) plasmid by PCR. In this approach, primers complementary to the original sequence but with one altered codon at the desired mutation site are used. 0.5µl ptrx-A46 (1-83) plasmid were used as template per PCR and the reaction was carried out in a total volume of 50µl per desired mutant plasmid.

The PCR products were cleaned up with the Promega Wizard® SV Gel and PCR Clean-Up System and incubated for 3-5 hours on 37°C with DpnI. After the digest, the sample was cleaned up again as before and eluted in 50 µl. 10µl of the product were used to transform *E. coli* Top10 cells and the transformed cells were plated out on kanamycin containing agar plates. Single colonies from these plates were inoculated into 5ml of LB with 50mg/ml kanamycin and grown overnight at 37°C, 210 rpm. The next

morning, minipreps were made of the resulting colonies. Obtained plasmids were sent to Microsynth AG for sequencing to check for plasmids containing the desired mutations.

F3D_F	GCAAATGGCGGATGATATATCAG
F3D_R	CTGATATATCATCCGCCATTTGC
H36L_F	GTTAATGATACACTCTACACTGTCG
H36L_R	CGACAGTGTAGAGTGTATCATTAAC
Y37A_F	GATACACACGCCACTGTCGA
Y37A_R	TCGACAGTGGCGTGTGTATC
Y37W_F	GATACACACTGGACTGTCGAATTTG
Y37W_R	CAAATTCGACAGTCCAGTGTGTATC
I72A_F	GAAACTAATGCTGGTTGCGCGG
I72A_R	CCGCGCAACCAGCATTAGTTTC

2.3.13 Creating a C-terminally deleted version of TRAM

To obtain the TRAMΔ5-TEV-His_6 sequence, we employed three PCRs with a volume of 50µl each with the primers TIM2224 and TIM2226. 1µl of pET11d TRAM-TEV-His_{10} was used as a template per sample and 30 cycles were run with an elongation time of one minute. The products were digested for 5 hours with DpnI on 37°C and subsequently cleaned up with the Promega Wizard® SV Gel and PCR Clean-Up System and the DNA was eluted in 50µl ultrapure H_2O per sample. Subsequently, the samples were pooled, mixed with NcoI, BamHI and DpnI and set to digest for 1.5 hours on 37°C. The sample was subsequently purified on the Monarch TM PCR & DNA Cleanup Kit (5ug) from NEB, eluted in 20µl and run on a 0.7% agarose gel. The visible band was cut out and extracted from the gel using the Monarch® DNA Gel Extraction Kit from NEB. The DNA was eluted in 8µl ultrapure H_2O. The fragment obtained in this way was used in a ligation with a dephosphorylated pET-11d vector backbone that had been cut with the restriction enzymes NcoI and BamHI. This cut backbone DNA was kindly provided by Sofiya Fedosyuk. The ligation was carried out for 2 hours on room temperature and the whole sample was used to transform *E. coli* Top10 cells that were subsequently plated on ampicillin containing agar plates. One resulting colony was inoculated into 5ml of LB with 100mg/ml ampicillin and grown overnight at 37°C, 210 rpm. A DNA miniprep was made from the culture and the obtained plasmid was sent to Microsynth AG for sequencing, which confirmed that the correct sequence had been obtained.

TIM2224	CGCAAGCCATGGGTATCGGTAAAAGCAAAATC
TIM2226	GCCCGGATCCTTAGTGGTGGTGATGATGGTGACCCTGGAAATACAGATTCTCCTGCACCATGTTAC

2.3.14 Creating trx-TIR/TRIF and trx-TIR/TRIF (396-545)

A DNA fragment encoding for the sequence of TIR/TRIF flanked by the restriction sites for NcoI and BamHI was obtained by PCR with the primers TIM2217 and TIM2218 following the standard program with 1 minute elongation time. The pET-11d vector containing the His_{10}-TEV-TIR/TRIF sequence was used as a template and the reaction was carried out in three tubes of 50µl each. The products were pooled, cleaned up on the Promega Wizard® SV Gel and PCR Clean-Up System and eluted in 50µl ultrapure H_2O. The sample was subsequently mixed with 37µl dH_2O, 10µl CutSmart buffer and 1.5µl of each of the restriction enzymes NcoI and BamHI and digested at 37°C overnight. The next morning, the sample was purified using the Promega Wizard® SV Gel and PCR Clean-Up System and eluted in 20µl. A ligation was set with a dephosphorylated pET-TRX1 vector backbone that had previously been cut with NcoI and BamHI and was kindly provided by Sofiya Fedosyuk. The ligation was carried out at 4°C overnight and the whole product was transformed into *E. coli* Top10 cells. The bacteria were plated out on a kanamycin containing agar plate, colonies were inoculated into 5ml of LB with 50mg/ml kanamycin and grown overnight at 37°C, 210 rpm for minipreps the next morning. Obtained plasmids were sent to Microsynth AG for sequencing. This confirmed that we had obtained a pET-TRX1 plasmid carrying the sequence of TIR/TRIF.

To obtain the N-terminally truncated version TIR/TRIF (396-545), a PCR was carried out using the primers TIM2255 and TIM2218 as well as the pET11d vector containing the sequence of His_{10}-TEV-TIR/TRIF as a template. The reaction was again carried out in three tubes of 50µl each using the standard program with 1 minute elongation time. The products were cleaned up and cut with the same restriction enzymes as described before. They were ligated overnight at 4°C into a dephosphorylated pET-TRX1 vector backbone that had previously been cut with NcoI and BamHI. As described before, the product was transformed into *E. coli* Top10 cells and a PCR of colonies was employed to check for correct size inserts. The desired plasmid was obtained by making minipreps of promising colonies and the correct sequence was confirmed by sending the samples to Microsynth for sequencing.

TIM2217 CGCAAGCCATGGAGAGCAGCAGCGAGCAG

TIM2218 GCCCGGATCCTTAGTCCTGTTCTTTACGC

TIM2255 CGCAAGCCATGGCACATCACCATCACCATCACGAAAACCTGTATTTTCAGGGAAATTTCGTTATCCTGC

2.3.15 Creating a C-terminally myc-tagged A46 (1-240)

To create a C-teminally myc-tagged version of A46 (1-240), we performed a PCR with the primers TIM 1814 and TIM2281 using 1.5µl of the plasmid pSF21 as a template per reaction. The PCR was carried out in 3 samples with a total volume of 50µl each. The products were pooled, cleaned up with the Promega Wizard® SV Gel and PCR Clean-Up System and eluted in 50µl. The sample was subsequently digested with 1.5µl of DpnI, NdeI and BamHI respectively for 4 hours on 37°C and purified again as described before and eluted in 50µl ultrapure H_2O to obtain the insert DNA.

Two digests of the pET-29a vector were set up, each with 45µl pET-29a plasmid, 86µl dH_2O, 15µl CutSmart buffer and 2µl of both NdeI and BamHI. The digest was carried out on 37°C for 1.5 hours, then 1.5µl of CIP was added to each sample and the samples were incubated on 37°C for 30 minutes more. They were purified with the Monarch TM PCR & DNA Cleanup Kit (5ug) and eluted in 20µl each before being run on a 0.7% agarose gel. The bands were cut out and the DNA was extracted with the Monarch® DNA Gel Extraction Kit from NEB. DNA was eluted in 10µl ultrapure H_2O each and the elutions were pooled together to obtain the cut vector backbone sample. Both insert and backbone were then used in a ligation reaction. The ligation was carried out for approximately 72 hours on 4°C and the whole reaction product was transformed into *E. coli* Top10 cells which were plated out on kanamycin containing agar plates. The resulting colonies were analyzed by a PCR of colonies the next morning in which the pSF21 plasmid was used as a positive control. Promising clones were set up for minipreps and the obtained plasmids were sent to Microsynth AG for sequencing. The results confirmed that we had obtained the C-terminally myc-tagged A46 (1-240) in the pET-29a vector.

TIM1814 CCCCCATATGGCGTTTGATATATCAG

TIM2281 CAAGGGATCCTTACAGATCCTCTTCAGAGATGAGTTTCTGCTCTACATCCGTTTCCCTG

2.3.16 Introduction of the sequence of FLAG-tagged TRAM into the pCAGGS vector

To be able to carry out co-transfection experiments with TRAM and A46 in mammalian cells, we first had to introduce the sequence of TRAM into a vector suitable for expression in mammalian cells. Furthermore, the protein had to be fused to a tag which could later be detected by Western blotting. The sequence of full-length TRAM with a C-terminal FLAG-tag was ordered from Addgene and provided in the pEF-Bos vector. This plasmid was used as a template in a PCR reaction of three times 50µl with the primers TIM2258 and TIM2260 under standard conditions with an elongation time of one minute to create a fragment of the desired TRAM-FLAG sequence flanked by the restriction sites of EcoRI and XhoI. The products were pooled and cleaned up as described before and digested overnight at 37°C with the restriction enzymes EcoRI and XhoI as well as with DpnI. The sample was cleaned up again using the Promega Wizard® SV Gel and PCR Clean-Up System and eluted in 25µl ultrapure H_2O. The ligation was set up with a DNA backbone of the pCAGGS vector that had previously been cut with the same restriction enzymes and dephosphorylated with CIP. The ligation was carried out for approximately four hours on 4°C and subsequently the whole sample was used for transformation of *E. coli* Top10 cells. PCR of colonies and minipreps were made as described before to obtain the pCAGGS vector with the desired TRAM-FLAG insert.

TIM2258 GCCCGAATTCCGAGAATGGGTATCGGGAAGTCTAA
TIM2260 CCGCTCGAGTCAGTGGTGGTGGTGGTGGTGCTTGTC

2.4 Protein methods

2.4.1 Overnight pre-cultures

Transformed *E. coli* cells were either picked as single colonies from agar plates or directly taken after transformation as liquid samples and inoculated into 40ml fresh LB medium containing the respective antibiotics. Cultures were grown in 100ml flasks overnight at 37°C and 210 rpm.

2.4.2 Protein overexpression

Expressions were carried out in 2L of fresh LB medium in 5L flasks. 10-20ml of overnight precultures were inoculated per 2L of expression medium containing the respective antibiotics. Cells were grown at 37°C, 170 rpm until an OD_{600} of approximately 0.6. At this point, protein expression was induced

with IPTG and the expression was continued on 170 rpm either for 4-5 hours on 23°C or overnight at 16°C depending on the construct. Cells were harvested by centrifugation at 5000 rpm for 10 minutes, resuspended in 20ml of the respective lysis buffers and stored on -80°C (see chapters 2.1, 3.3 and 3.5). Table 2 shows the expression conditions for four important proteins that were investigated in this thesis. Further purification trials and the corresponding conditions are mentioned in chapters 3.3 and 3.5.

Table 2 - Expression conditions for the constructs most frequently expressed during the duration of the thesis

Construct	IPTG concentration (mM)	Antibiotics in culture medium	Expression conditions	Cold shock before induction
A46 N-terminal mutants	0.25	50mg/L kanamycin	4h, 23°C	No
MBP-His10-TEV-N4-A46 (1-240)	0.25	50mg/L kanamycin	5h, 23°C	no
Trx-TEV-TIR/TRIF (396-545)	0.25	50mg/L kanamycin	overnight, 16°C	Yes
TRAMΔ5-TEV-His6	0.25	100mg/L ampicillin	overnight, 16°C	yes

2.4.3 Cell lysis

The *E. coli* cell suspensions were thawed on room temperature and 100µl of 2mg/ml DNase were added per sample. The cells were broken open by six passages through an Emulsiflex-C3 homogenizer (Avestin) at 10000 psi and 4°C. The lysed cells were centrifuged at 18000 rpm on 4°C for 30 minutes to separate the soluble and insoluble fractions. The supernatants were filtered through a 0.45µm pore size filter to remove rests of cell debris and the cleared lysates were subsequently used in on-batch His-affinity chromatography.

2.4.4 SDS gel electrophoresis

SDS gels were used to analyze fractions of both on-batch His affinity chromatographies and size exclusion chromatographies as well as for analysis of proteins by Western blotting. The gels were self-cast using Mini-PROTEAN®chambers from Bio-Rad. SDS gels with 1.5mm spacers were used for all

mammalian subcellular fractionation experiments. Gels with 0.75mm spacers were used in all other cases (table 3).

Protein samples were mixed with 2x or 5x SDS sample buffer, heated on 95°C for approximately 10 minutes and then loaded on the SDS gels (see table 3). Gels were run at 300V for 30 minutes, stained with Coomassie Brilliant Blue solution for roughly five minutes and subsequently destained in tap water until protein bands became clearly visible. Precision Plus Protein™ All Blue Prestained Protein Standards from Bio-Rad was used as a marker.

Table 3 - Reagent volumes for one respective hand-cast SDS gel

	0,75mm spacer		1,5mm spacer	
	Stacking gel 4%	**Separation gel 15%**	**Stacking gel 4%**	**Separation gel 15%**
30% Acrylamide/Bis	330µl	2.5ml	693µl	5.25ml
0.5M Tris-HCl pH 6.8, 0.4% SDS	630µl	-	1.32ml	-
1.5M Tris-HCl pH 8.8, 0.4% SDS	-	1.25ml	-	2.63ml
dH_2O	1.5ml	1.22ml	3.15ml	2.55ml
10% APS	12.5µl	25µl	26.25µl	52.5µl
TEMED	2.5µl	2.5µl	5.25µl	5.25µl

2.4.5 On-batch His-trap affinity chromatography

Cleared *E. coli* cell lysates were loaded on either 1ml or 5ml of Nickel Chelating Resin (GBiosciences) that had been pre-equilibrated with the respective lysis buffer. The samples were passed through the column by gravity flow, the flowthrough was collected on ice and the column was washed with 10x the bed volume of lysis buffer. Bound proteins were eluted in 5-7ml of the respective elution buffer. The column was washed with 1 bed volume of 1M imidazole and 6 bed volumes of dH_2O and stored in 20% ethanol on 4°C for reuse. Samples obtained during the purification were loaded on SDS gels for analysis.

2.4.6 Dialysis

After on-batch His-affinity chromatography, the eluted protein samples were transferred to a bag of SnakeSkin® dialysis tubing (Thermo Scientific) with a molecular weight cutoff of 10kDa. In cases where cleavage of the protein of interest by TEV protease was desired, 500µl of 2mg/ml TEV protease were added per sample. The bag was sealed with plastic clips on both sides. All dialyses were performed on 4°C against 3L of the respective dialysis buffers under constant rotation on a magnetic stirrer for 2-16 hours depending on the protein.

2.4.7 Protein concentration

Depending on the starting volume of the sample and the desired end volume, proteins were concentrated either in Centriprep®- 10K centrifugal units or in Amicon®Ultra-4 centrifugal filters (both from Merck). The concentration was carried out by centrifuging the samples at 4000 rpm and 4°C until the desired end volume was reached. The concentrated samples were either loaded on the ÄKTA pure machine for size exclusion chromatography or flash frozen in liquid nitrogen and stored on -80°C for later use.

2.4.8 Size exclusion chromatography

Size exclusion chromatographies were carried out on 4°C on an ÄKTA pure machine (GE lifesciences) using either a 16/60 Superdex 75, a 16/600 Superdex 200 or a 10/300 Superdex 200 column (GE lifesciences) depending on the protein that should be purified. All columns were permanently attached to the machine and stored in ultrapure water when not in use. Before each run, the column was washed with roughly two column volumes of the respective FPLC buffer until the conductivity and UV absorption were stable. The protein samples were either injected with a syringe into a sample loop in case the total sample volume was below 1 ml, or loaded onto the column using a sample pump in case the volume was close to 5 ml. In the latter case, the 16/600 Superdex 200 column was always used. The proteins were passed through the columns at a speed of 0.75 ml/min for the 16/60 Superdex 75 and the 10/300 Superdex 200 column and at 1.5 ml/min for the 16/600 Superdex 200 column. The maximum pressure applicable to each column was monitored by the machine and the sample flow was automatically slowed if the pressure of the solution exceeded the maximum threshold. The void volume was discarded and the fractions of interest were collected using a fraction collector. After each run, the columns were washed with two column volumes of ultrapure H_2O or until the conductivity

and UV absorption had reached zero. According to the UV absorption chromatograms recorded by the machine, fractions of interest that lied within UV absorption peaks were analyzed on SDS gels to check for proteins of the correct molecular size and to estimate the purity of the obtained protein sample. Fractions containing the purified protein of interest were subsequently concentrated as described above.

2.4.9 Purification protocols

2.4.9.1 Expression and purification of N-terminal mutants of A46

All five mutants of the A46 N-terminus were expressed and purified as described in detail by Fedosyuk et al. (Fedosyuk et al. 2016). Fractions collected during the different purification steps were loaded on SDS gels to check whether the proteins of interest could be obtained in a soluble and purified state.

2.4.9.2 Expression and purification of MBP-His_{10}-TEV-N4-A46 (1-240)

The protein was expressed from the pSF21 vector in BL21 *E. coli* cells. The cells were grown at 37°C and induced with 0.25mM IPTG when the OD_{600} reached a value of approximately 0.6. The expression was continued on 23°C for 5 hours, cells were harvested by centrifugation, resuspended in A46 FL lysis buffer and stored on -80°C. For purification, the suspensions were thawed, DNase was added and the cells were broken in a French press. The soluble fraction was obtained by centrifugation and purified by on-batch His-affinity chromatography on a column bed volume of 5ml of nickel chelating resin. The elution was dialyzed overnight at 4°C against A46 FL dialysis buffer 1 together with TEV protease to cleave off the MBP-His_{10}-tag. The next day, the dialyzed sample was again loaded on the His-affinity column to separate the tag and the protein of interest. Since A46 (1-240) should not be bound to the tag anymore and should therefore not be retained by the resin, the flowthrough (termed fth1) was collected and loaded three more times on the column to ensure an effective separation of the A46 protein from the tag and the TEV protease, which is also His-tagged. After these three passages through the column, the flowthrough (termed fth2) was dialyzed for at least three hours against A46 FL dialysis buffer 2, concentrated to a volume of less than 5ml and loaded on a HiLoad 16/600 Superdex 200 pg column for size exclusion using a sample pump. A46 FL dialysis buffer 2 was also used for the size exclusion chromatography. The fractions lying within UV absorption peaks were analyzed on an SDS page gel and the fractions containing the A46 (1-240) protein were concentrated to approximately

750µl and the concentration was measured on a Nanodrop. The sample was snap frozen in liquid nitrogen and stored on -80°C.

2.4.9.3 Expression and purification of His_6-trx-TEV-His_{10}-TEV-TIR/TRIF (396-545)

The construct was expressed in BL21 cells that had previously been transformed with the pG-Tf2 plasmid encoding for a chaperone to aid with solubilization of the target protein. The cells were grown at 37°C until an $OD6_{00}$ of approximately 0.6, then cold shocked on ice for 30 minutes and subsequently induced with 0.25mM IPTG. Protein expression was continued overnight at 16°C, 170 rpm. The cells were harvested by centrifugation, resuspended in a Tris-based buffer (50mM Tris pH 8.5, 10mM BME, 5% glycerol) and a HEPES-based buffer (50mM HEPES pH 8.0, 10mM BME, 5% glycerol) and frozen on -80°C until being processed further. For purification, the cells were thawed, DNase I was added and the cells were opened with a French press. After centrifugation to separate the soluble and insoluble phases, the supernatants were loaded on an on-batch His-affinity column with 1ml bed volume of nickel chelating resin. After the fractions collected during the purification were analyzed on an SDS gel, the elutions were pooled and dialyzed overnight against 50mM Tris pH 8.0, 10mM BME, 25mM imidazole together with TEV protease to cleave off the trx-tag. The dialyzed product was concentrated and further purified by size exclusion chromatography on a HiLoad 16/600 Superdex 200 pg column using a buffer with the same composition as the dialysis buffer. The fractions lying within UV absorption peaks were then run on an SDS gel to check for proteins of the correct molecular weight.

2.4.9.4 Expression and purification of TRAMΔ5-TEV-His_6

The construct was expressed in BL21 or B834 *E. coli* cells that were induced with 0.25mM IPTG and grown overnight at 16°C, 170 rpm. The cells were harvested by centrifugation and resuspended in TRAM lysis buffer (50mM Tris pH 8.0, 500mM NaCl, 20mM imidazole and 10mM BME) and frozen on -80°C for storage. For protein purification, the suspensions were thawed, DNase I was added and the cells were opened by passing them through a French press. After centrifugation to separate the soluble and insoluble phases, the lysate was purified on an on-batch His-trap and fractions of the purification were analyzed on an SDS gel as described above.

The sample obtained from the elution of the His-trap was dialyzed overnight at 4°C against TRAM dialysis buffer and further purified by size exclusion chromatography on a HiLoad 16/600 Superdex 200 pg column also using TRAM dialysis buffer. The fractions were run on an SDS gel to check for proteins

of the correct molecular weight and fractions containing the protein of interest were concentrated. The final concentration was measured on the Nanodrop and the sample was snap frozen in liquid nitrogen and stored on -80°C.

2.4.9.5 Coexpression and purification of TRAMΔ5-TEV-His_6 and A46 (1-240)-myc

E. coli BL21 and B834 that had been cotransformed with the pET-11d-TRAMΔ5-TEV-His_6 and pET-29a-A46 (1-240)-myc vectors were grown in LB medium containing 100mg/ml ampicillin and 50mg/ml kanamycin. Protein expression was induced with 0.5mM IPTG and cells were grown overnight at 25°C, 170 rpm. The cells were harvested by centrifugation, resuspended in a buffer containing 20mM HEPES pH 7.4, 150mM KCl, 20mM imidazole and 10mM β-mercaptoethanol and frozen on -80°C for storage. For the purification, the samples were thawed, 100µl of 2mg/ml DNase I was added and the cells were broken by six passages through a French press. The lysates were centrifuged to separate soluble and insoluble fractions and the cleared supernatants were purified by on-batch His-affinity chromatography. Fractions of the centrifugation steps were analyzed on an SDS gel.

For further purification, the elutions were pooled and dialyzed for 3½ hours against 3L of 20mM HEPES pH 7.4, 150mM KCl and 10mM β-mercaptoethanol. The sample was subsequently concentrated to a volume of 4ml and loaded on the HiLoad Superdex 16/600 200 column for size exclusion chromatography in the dialysis buffer. Fractions of interest were again analyzed on an SDS gel.

2.4.10 *In vitro* complex formation between TRAM and A46 (1-240)

30µg of purified TRAMΔ5-TEV-His_6 and 90µg of purified A46 (1-240) without tags were mixed together in different buffers in a total volume of 200µl and dialyzed on 4°C for 5 hours against 300ml of the respective buffer (see table 4) in Slide-A-Lyzer® Mini Dialysis Units (Thermo Scientific). The dialyzed sample was named the total fraction. After dialysis, 10µl of the total fraction were kept for analysis by SDS-PAGE and the rest of the sample was loaded onto 100µl bed volume of Nickel Chelating Resin (GBiosciences) in Mini-Spin™ chromatography columns (Bio-rad) that had been washed with dH_2O and pre-equilibrated with the respective dialysis buffers. The sample was passed through the column by spinning it in a tabletop centrifuge for approximately 2 seconds at 1000 rpm, to not let the column run dry. The flowthrough was collected and the column was washed four times with 500µl of the respective dialysis buffer with additional 20mM imidazole. The last washthrough (termed wth4) was collected separately and the proteins bound to the column were eluted with 100µl of the respective dialysis

buffers with 250mM imidazole. The fractions were loaded on an SDS gel along with the purified A46 and TRAMΔ5-TEV-His_6 proteins to analyze whether any A46 had co-eluted with TRAM.

Table 4 - Different buffers used in the in vitro pulldown experiments with purified TRAMΔ5-TEV-His_6 and A46 (1-240)

Buffer name	Buffer composition
Buffer I	50mM HEPES pH 7.4, 500mM NaCl, 5% glycerol, 10mM BME, 1mM MgCl2
Buffer II	50mM HEPES pH 7.4, 500mM KCl, 5% glycerol, 10mM BME, 1mM KCl
Buffer III	50mM Tris pH 8.0, 500mM NaCl, 5% glycerol, 10mM BME, 1mM MgCl2
BufferIV	50mM Tris pH 8.0, 500mM KCl, 5% glycerol, 10mM BME, 1mM MgCl2

2.4.11 Western Blot and membrane stripping

Proteins of interest fused with a His-, myc- or FLAG-tag were run on SDS gels as described before. For wet blotting, the gels were transferred to blotting chambers from Bio-Rad and covered with a PVDF membrane that had been activated by placing it in 100% methanol for five seconds. The chambers were filled with ice-cold transfer buffer and an additional cooling element was added to the chamber. Proteins were transferred to the membrane for 90 minutes at 400mA and room temperature or overnight at 40mA and 4°C under constant stirring on a magnetic stirrer. The membranes were blocked for 60 minutes in blocking solution (20mg of Tropix I-block in 10ml of PBST per membrane) to avoid unspecific binding of the antibodies to the membranes. The blocking solution was discarded and the membranes were incubated for one hour in 10ml of the respective antibodies diluted in PBST (see table 5). Subsequently, the membranes were washed three times for 8 minutes with PBST and the secondary antibody (rabbit anti-mouse, coupled to horseradish peroxidase, Jackson Immuno Research Laboratories) was added in a dilution of 1:10000 in PBST. After incubation for one hour, the membranes were washed again as before and the reporter reaction was induced using the SuperSignal® West Pico Chemoluminescent Substrate (Thermo Scientific). The signal was subsequently visualized by developing the films with an AGFA Curix6000 in a dark room. For very weak signals, one tenth of the photoreactant was replaced with SuperSignal® West Femto Chemoluminescent Substrate (Thermo Scientific) to be able to detect lower quantities of protein.

Table 5 - Dilutions and manufacturers of all primary antibodies used for Western Blotting

Primary antibody	Dilution in PBST	Manufacturer	Product number
Anti-His	1:3000	GE Healthcare	27-471001
Anti-myc	1:1000	Millipore	05-724
Anti-FLAG	1:1000	Sigma	F3165
Anti-ɣ-tubuline	1:5000	Sigma	T5326
Anti-α-calnexin	1:1000	BD Biosciences	610524

For stripping membranes, we followed the mild stripping protocol from abcam. In this protocol, the membrane is first incubated in fresh stripping buffer under constant shaking two times for ten minutes. The stripping buffer is then replaced by 1x PBS and the membrane is washed again two times for ten minutes. The 1x PBS is replaced by 1x TBST and the membrane is washed two times for five minutes. After stripping, the membranes were incubated for one hour in blocking solution before incubation with the respective primary antibodies.

2.4.12 BCA assay

To be able to compare total protein concentrations in different samples, the BCA assay was performed with the Pierce™BCA Protein Assay Kit (ThermoFisher) according to the manufacturer's manual. Samples were diluted 1:4 (5µl sample in 15µl dH_2O) before the reagent was added. Duplicates of every sample were analyzed on a Synergy H1 microplate reader (BioTek) at a wavelength of 600nm. The mean of all duplicates as well as the total mean of all means were calculated. A certain volume of the sample that had the value which was closest to the total mean was determined to be loaded on an SDS gel. The amounts of all other samples that were needed to reach the same amount of protein in all lanes on the gel was calculated by multiplying the previously defined volume with the quotient of the total mean value divided by the respective duplicate mean of each sample.

2.5 Mammalian cell methods

2.5.1 Cell culture

HiExp human embryonic kidney cells were cultured at 37°C, 5% CO_2 in 10cm dishes in Dulbecco's Modified Eagle Medium (life technologies™) with 10% heat-inactivated fetal calf serum and 1% Pen-Strep (lonza). Every four days, cells were split 1:20 into fresh DMEM medium for maintenance under a

tissue culture hood. For splitting, the old medium was removed from the plates and the cells were washed carefully with 3ml prewarmed 1xPBS. PBS was removed and 3ml of prewarmed 0.05% Trypsin-EDTA (life technologies™) were added to detach the cells from the dish. This reaction was facilitated by slightly tilting the dish until all cells had detached. The detached cells were resuspended in 7ml of fresh, prewarmed DMEM and split into new prewarmed DMEM in a ratio of 1:20 to a final volume of 10ml.

2.5.2 Transfection

Confluent HiExp human embryonic kidney cells were seeded in a ratio of 1:4 in 6-well plates in 2ml total volume per well and grown overnight at 37°C, 5% CO_2 to a density of approximately 80% confluency. Endotoxin-free DNA, Gibco® OptiMEM™ medium (Thermofisher) and TransIT®-LT1 transfection reagent (Mirus) were equilibrated to room temperature for 30 minutes and mixed in a tissue culture hood and incubated on room temperature for another 30 minutes. Per transfection of one well of a 6-well plate, 2µg total DNA, 150µl OptiMEM and 6µl of transfection reagent were mixed. Empty pET-11d or pFBDH vector DNA was used to adjust the total DNA amount per sample to 2µg. The DNA samples were subsequently pipetted carefully into each well of the 6-well plates and the cells were incubated on 37°C, 5% CO_2 for 48 hours. Afterwards, the medium was removed from the plates and the cells were frozen on -20°C until being processed further.

2.5.3 Subcellular fractionation

Cells were thawed and 250µl fractionation buffer containing protease inhibitors were added per well. The plates were shortly frozen on -80°C and thawed again to help break the cells. The cells were opened with 40 strokes of a Dounce homogenizer and pre-centrifuged on 1000 rpm, 4°C for 5 minutes to pellet the remaining unopened cells. The supernatants were centrifuged on 3000 rpm, 4°C for 5 minutes to pellet the nuclei. The pellets obtained from this step were resuspended in 400µl fractionation buffer containing protease inhibitors and centrifuged again for 10 minutes under the same conditions. The supernatants were discarded and the nuclei were resuspended in 100µl NL buffer plus protease inhibitors per sample and frozen on -20°C for storage. The supernatants containing the cytosol, mitochondria and cell membranes were centrifuged on 8000 rpm, 4°C for five minutes to pellet the mitochondria. The obtained pellets were centrifuged for 10 minutes under the same conditions and treated as the nuclei pellets before. The supernatants were centrifuged on 43.000 rpm, 4°C for one hour in an ultracentrifuge to separate the cytosol and membrane fractions. The cytosolic fractions

were frozen on -20°C for storage and the membrane pellets were resuspended in 400µl fractionation buffer containing protease inhibitors each and centrifuged for another hour under the same conditions. Subsequently, the supernatants were removed and the pellets containing the cellular membranes were resuspended in 70µl of NL buffer containing protease inhibitors and frozen on -20°C until being processed further. For analysis by Western blotting, the samples were thawed, 10µl of 2mg/ml DNase I were added per nuclear fraction sample to shear the DNA and the nuclear, mitochondrial and membrane fraction samples were sonicated three times for 10 minutes in a Bandelin Sonorex sonicator to homogenize the samples to be able to carry out the BCA assay with them.

3. Results

3.1 Purification of five mutants of the A46 N-terminus

To investigate the ability of the N-terminal, hydrophobic cavity of A46 to accommodate fatty acids and to identify possibly crucial residues for this protein-lipid interaction, we wanted to express and purify five mutants of the A46 N-terminus. The point mutations F3D, H36I, Y37A, Y37W and I72A were introduced into the ptrx-A46 (1-83) plasmid by PCR using the respective primers listed in materials and methods. These residues were chosen for mutation because they take on different conformations in either subunit of the N-terminal β-sandwich of A46, and except for H36, they all lie inside the hydrophobic cavity and therefore potentially stabilize the myristic acid there. The amino acid sequence of the His6-trx-TEV-A46 (1-83) construct with the sites of mutations highlighted is given below in Fig. 9.

MKHHHHHHPMSDKIIHLTDDSFDTDVLKADGAILVDFWAEWCGPCKMIAPILD
EIADEYQGKLTVAKLNIDQNPGTAPKYGIRGIPTLLLFKNGEVAATKVGALSKGQ
LKEFLDANLAGSGSGSENLYFQGAMAMAFDISVNASKTINALVYFSTQQNKLVI
RNEVNDTHYTVEFDRDKVVDTFISYNRHNDTIEIRGVLPEETNIGCAVNTPVSMT

MW = 23.95 kDa / pI = 5.39

Figure 8 - Amino acid sequence of the His_6-trx-TEV-A46 (1-83) construct that was used as a template to create the five mutant proteins. The TEV cleavage site is marked in blue, the sites of mutations are marked in orange. MW = molecular weight; pI = isoelectric point. MW and pI were obtained by entering the sequence into the Expasy ProtParam online tool.

The mutant proteins were expressed as described for the N-terminus of A46 in the paper of Fedosyuk et al. (Fedosyuk et al., 2016) and purified by on-batch His-affinity chromatography followed by dialysis with TEV protease (Fig. 10) and subsequent size-exclusion chromatography. Fig. 10 A and B are pictures of SDS gels of the fractions obtained from the first set of on-batch His-affinity chromatographies and show that all mutant proteins could be obtained in the elution fraction. Fig. 10 C and D show SDS gels of the samples after overnight dialysis with TEV protease and the following second set of on-batch His-affinity chromatographies. Almost all protein in the samples was successfully cleaved during the dialysis, creating the trx-tag fragment of approximately 14 kDa and the N-terminal A46 mutant proteins with a molecular weight of roughly 10 kDa. The remaining uncleaved protein as well as the cleaved trx-tag and TEV protease all have a His-tag and were therefore efficiently removed during the second set of on-batch His-affinity chromatography. The profiles obtained from the size-exclusion runs (data not shown) and the SDS gels of the fractions of interest showed that all mutant proteins had a comparable running behavior on the column and could be purified (Fig. 11 A-E). An SDS gel of the concentrated

samples (Fig. 11 F) indicated that we had successfully obtained all mutant proteins in a purified state after the final step of concentration. Mass spectrometry analysis of the samples by Terry K. Smith confirmed the identity of the mutant proteins and revealed differences in their ability to bind fatty acids like myristic acid. Most notably, all mutants except for the Y37A variant showed reduced amounts of bound lipids compared to the wild-type protein (Fedosyuk et al, 2016).

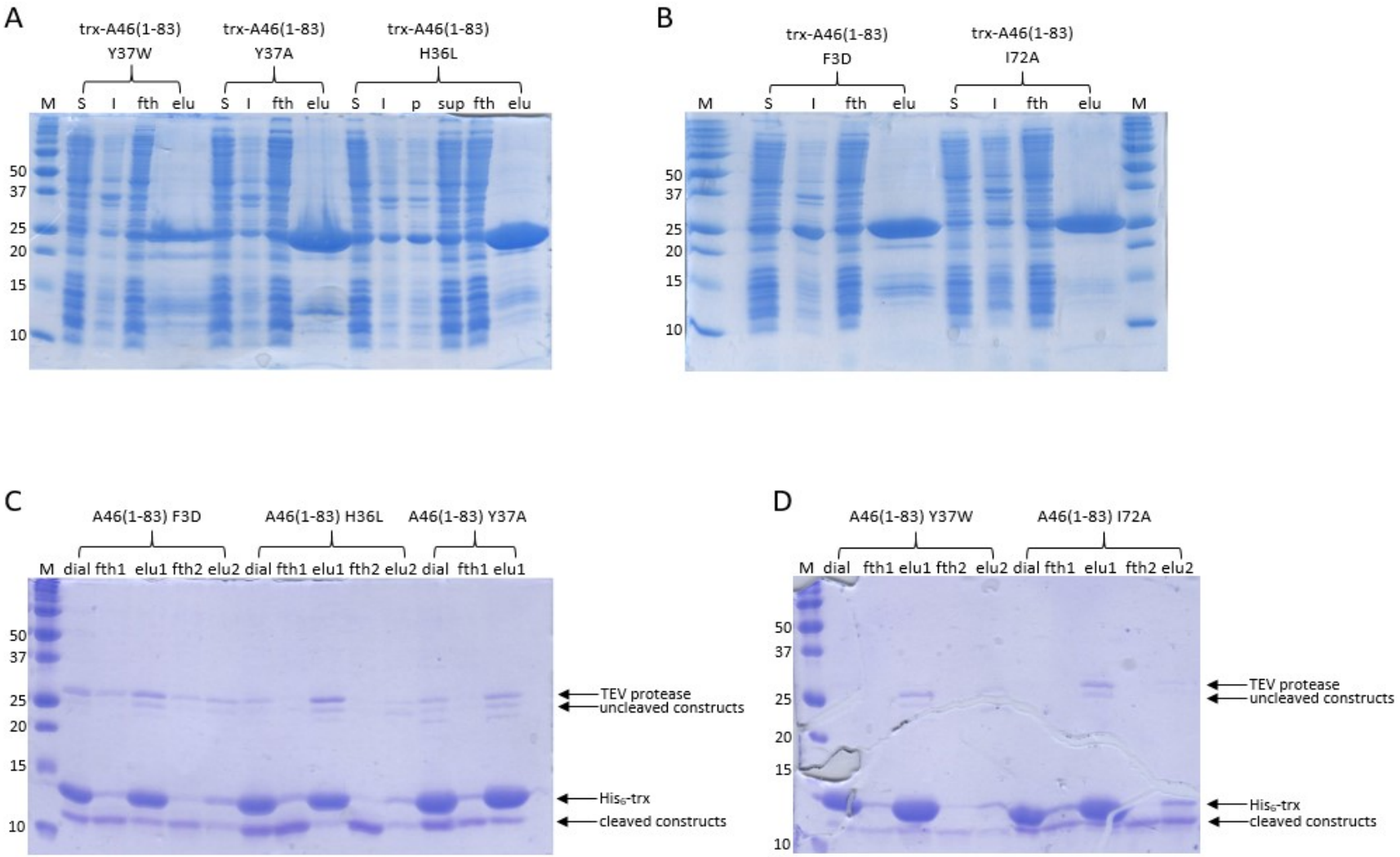

Figure 9 - SDS gels of the purification of all N-terminal constructs of A46 prior to size exclusion chromatography. ***(A+B)*** *Fractions of the first His-trap of the constructs* ***(C+D)*** *Fractions of the constructs after overnight dialysis with TEV protease and second His-trap to remove the trx-tag and the protease. Fth2 and elu2 of the Y37A protein were run on the gel in Fig. 4C. M = marker (4 µl); T = total (0.5 µl); S = soluble (0.5 µl); I = insoluble (0.5 µl), fth = flowthrough (0.5 µl), elu = elution (6.5 µl); dial = dialyzed sample (6.5 µl); fth1 = first flowthrough of the second His-trap (6.5 µl), elu1 = first elution of the second His-trap (6.5 µl); fth2 =second flowthrough of the second His-trap (6.5 µl); elu2 = second elution of the second His-trap (6.5 µl). fth2 and elu2 of the Y37A sample are shown in Fig. 3.*

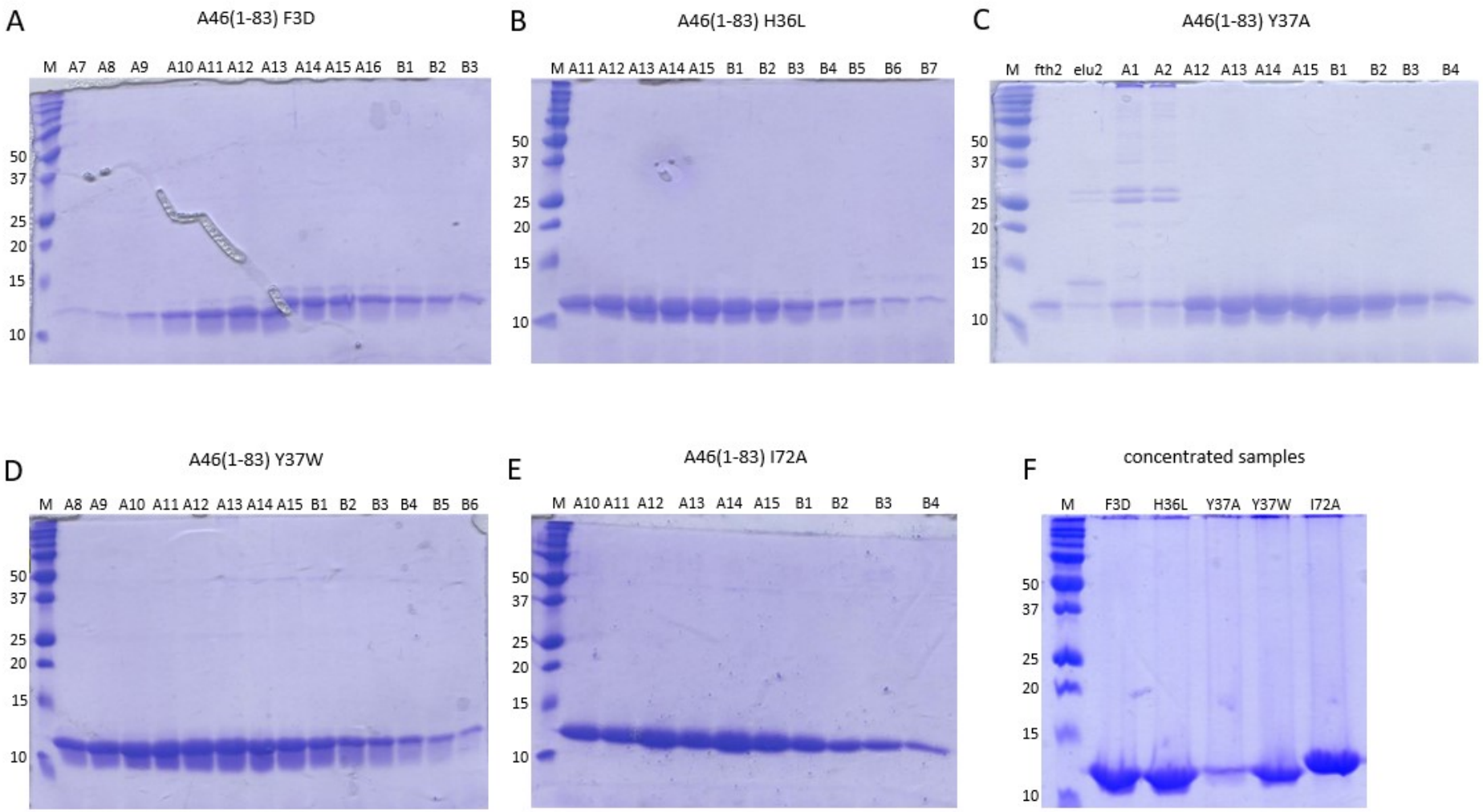

Figure 10 - SDS gels of the fractions of interest from the size exclusion runs of all constructs as well as the final concentrated samples. ***(A)*** *SEC fractions of the F3D construct* ***(B)*** *SEC fractions of the H36L construct* ***(C)*** *SEC fractions of the Y37A construct* ***(D)*** *SEC fractions of the Y37W construct* ***(E)*** *SEC fractions of the I72A construct* ***(F)*** *All samples after the final concentration loaded in a dilution of 1:5 with dH_2O. M = marker (4 µl)*

3.2 Purification of MBP-His_{10}-TEV-A46 (1-240)

To be able to carry out *in vitro* pulldown experiments of A46 and TRAM, we first had to purify the full-length A46 protein. Full-length A46 was expressed as a fusion construct with the MBP tag, as described previously by Fedosyuk et al. (Fedosyuk et al., 2014). The sequence of the construct is given below in Fig. 12. The four additional amino acid residues at the N-terminus of A46 had been found to increase solubility and to also facilitate protein crystallization.

MAEEGKLVIWINGDKGYNGLAEVGKKFEKDTGIKVTVEHPDKLEEKFPQVAATGDGP
DIIFWAHDRFGGYAQSGLLAEITPDKAFQDKLYPFTWDAVRYNGKLIAYPIAVEALSLIY
NKDLLPNPPKTWEEIPALDKELKAKGKSALMFNLQEPYFTWPLIAADGGYAFKYENGKY
DIKDVGVDNAGAKAGLTFLVDLIKNKHMNADTDYSIAEAAFNKGETAMTINGPWAWSN
IDTSKVNYGVTVLPTFKGQPSKPFVGVLSAGINAASPNKELAKEFLENYLLTDEGLEAVN
KDKPLGAVALKSYEEELAKDPRIAATMENAQKGEIMPNIPQMSAFWYAVRTAVINAASG
RQTVDEALKDAQTNSSSNNNNNNNNNNLGIEGRHHHHHHHHHHENLYFQGGSQQM
AFDISVNASKTINALVYFSTQQNKLVIRNEVNDTHYTVEFDRDKVVDTFISYNRHNDTIEI
RGVLPEETNIGCAVNTPVSMTYLYNKYSFKLILAEYIRHRNTISGNIYSALMTLDDLAIKQ
YGDIDLLFNEKLKVDSDSGLFDFVNFVKDMICCDSRIVVALSSLVSKHWELTNKKYRC
MALAEHISDSIPISELSRLRYNLCKYLRGHTESIEDKFDYFEDDDSSTCSAVTDRETDV

MW = 72.55 kDa / pI = 5.32

Figure 11 - Amino acid sequence of the MBP-His_{10}-TEV-4N-A46 (1-240) construct. The TEV cleavage site is marked in blue, the four additional residues at the N-terminus of A46 are marked in green. MW = molecular weight; pI = isoelectric point. MW and pI were obtained by entering the sequence in the Expasy ProtParam online tool.

We analyzed fractions of the different steps of the on-batch His-affinity purification on an SDS gel to check whether we could obtain the fusion protein in the elution. The gel showed that we were able to obtain the protein from the chromatography, along with smaller protein impurities (Fig. 13 A). Subsequently, we dialyzed the elution together with TEV protease to cleave off the tag and afterwards purified the sample again by on-batch His-affinity chromatography as described in 2.4.9.2. The corresponding SDS gels showed that we had successfully cleaved a majority of the protein of interest from the tag (Fig. 13 B) and that we were able to remove the TEV-protease as well as the majority of the MBP tag from our sample by the second His-affinity chromatography. There was, however, still a small fraction of the uncleaved fusion protein as well as of the cleaved MBP tag present in our sample after this step of purification (Fig. 13 C). We subsequently dialyzed the sample against the A46 FL dialysis buffer 2 and performed a size exclusion chromatography to further purify A46 (1-240). The chromatogram revealed four distinct peaks at a retention volume of 50-80 ml, indicating that A46 is

present in different oligomeric states (Fig. 14 A). We ran fractions lying within these peaks on an SDS gel to understand which fractions would contain the protein of interest (Fig. 14 B). Based on the result, we decided to concentrate fractions B10-C4 to an end volume of 300µl to remove most of the protein impurities which were present in the other fractions. Spectrophotometric analysis of the OD_{280} revealed a protein concentration of 2.96 mg/ml.

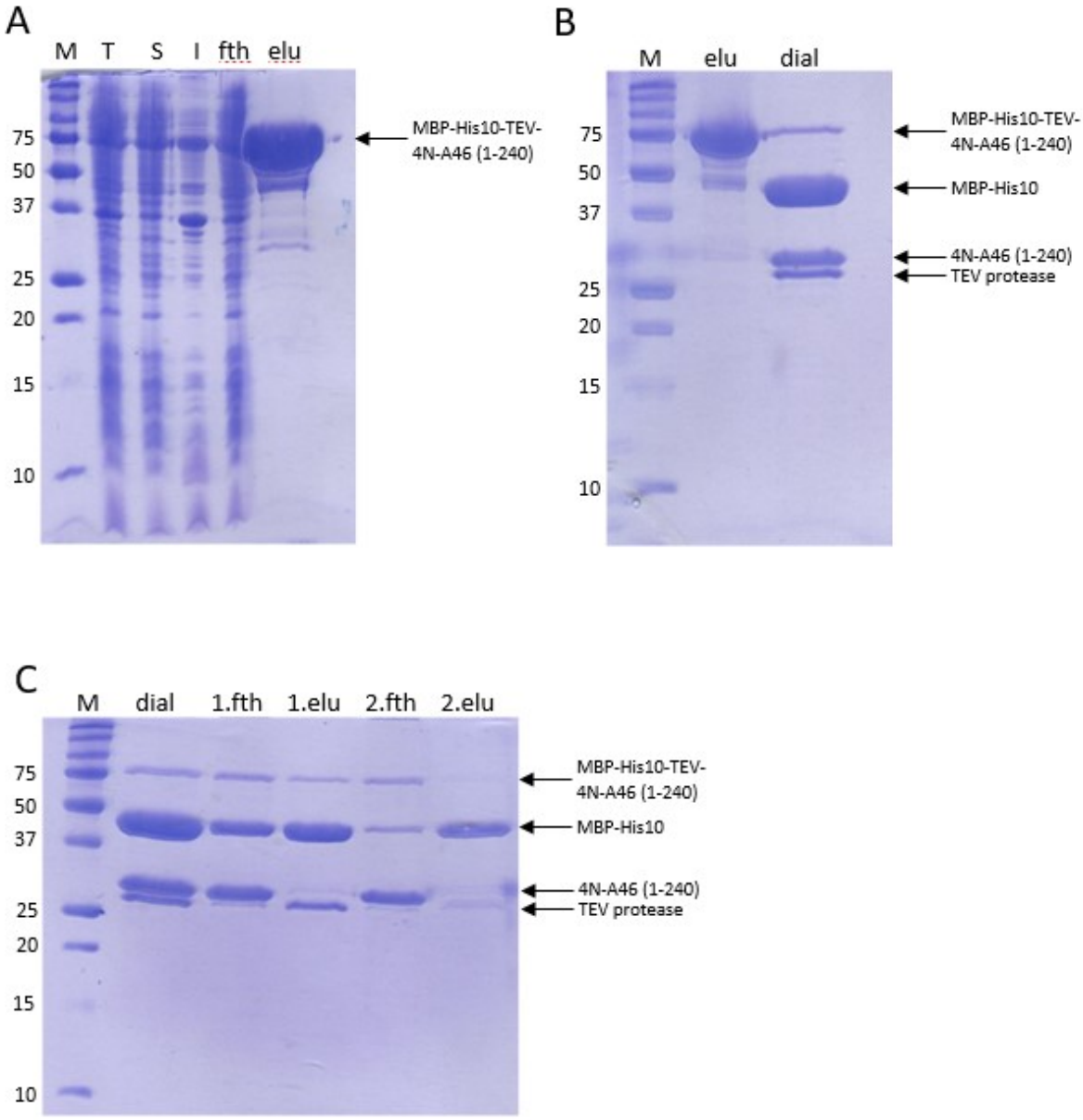

Figure 12 - Fractions of the different purification steps of A46 (1-240) prior to size exclusion. ***(A)*** *His-trap of cleared cell lysate* ***(B)*** *elution of the first His-trap and sample after overnight dialysis with TEV protease* ***(C)*** *dialyzed sample and fractions of the second His-trap to purify the protein of interest from TEV protease and tag. M = marker (4 µl); T = total (0.5 µl); S = soluble (0.5 µl); I = insoluble (0.5 µl); fth = flowthrough (0.5 µl in A, 6.5 µl in C); elu = elution (6.5 µl in A and C, 3.5 µl in B); dial = dialyzed sample (6.5 µl)*

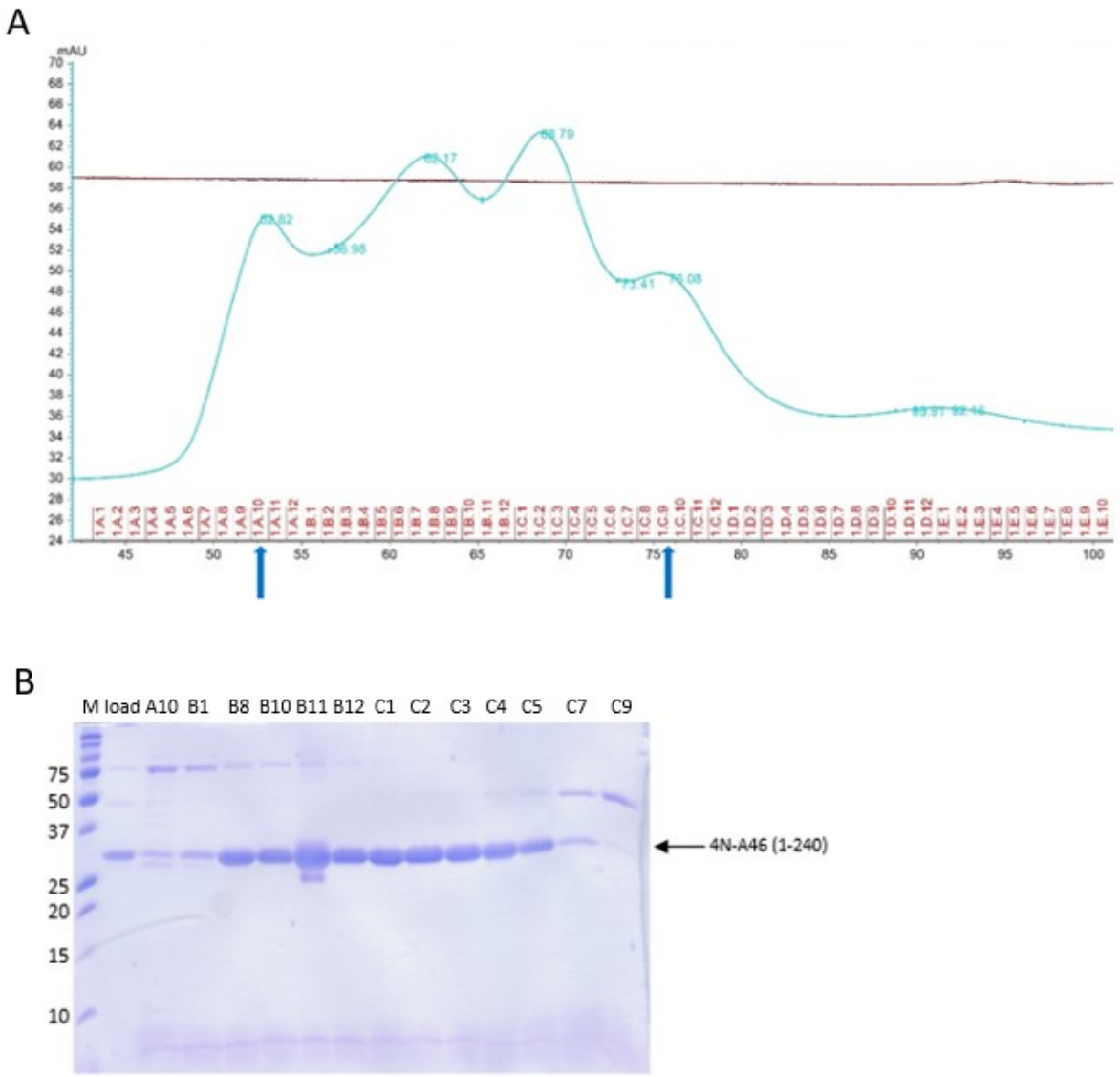

Figure 13 - Size exclusion carried out with the cleaved A46 (1-240) sample. ***(A)*** *chromatogram obtained on the ÄKTA pure, UV absorption in light blue, conductivity in brown. The blue arrows indicate the range in which fractions were analyzed* ***(B)*** *SDS gel of the sample obtained after the second His-trap (**load**) and the size exclusion fractions of interest.* ***M*** *= marker (4 µl); amount of sample loaded for load: 6.5 µl; for all SEC fractions: 30 µl*

3.3 Solubilization trials of TIR/TRIF and trx-TIR/TRIF

To find suitable conditions for the expression of soluble TIR/TRIF protein, we performed test expressions with varying expression conditions, cell strains, IPTG concentrations and lysis buffers. SoluBL21 and BL21 LysS are *E. coli* cell strains commonly used for expression of insoluble proteins or proteins that exhibit a toxic effect on the cells that produce them. Lowering the temperature of the expression as well as the IPTG concentration used to induce the cells can also lead to greater amounts of soluble protein. Lastly, the composition of the buffer that is used to resuspend the cells has an enormous impact on the solubility of the protein outside of cells. While the pH of the solution should

not be close to the pI of the protein, ionic strength, stabilizing molecules such as glycerol and reducing agents such as β-mercaptoethanol can play an important role in whether a protein will be soluble in a specific solution. The protein here was expressed as a His_{10}-TEV-TIR/TIF fusion construct. Cells were opened in a French press and on-batch His-affinity chromatography was performed to purify the protein. We subsequently analyzed the fractions of the different purification steps on SDS-PAGE gels to check whether we could obtain TIR/TRIF in the elution fractions. We were, however, not able to obtain the protein in a soluble state under any of the conditions tested. An example of a typical SDS gel after on-batch His-affinity chromatography is given in Fig. 16 A. Therefore, we decided to fuse the TIR/TRIF sequence to the trx-tag as described in chapter 2.3.14, since the fusion with the trx-tag has often proven to be a convenient way to solubilize otherwise insoluble proteins (Terpe, 2003; Esposito and Chatterjee, 2006). The amino acid sequence of His_6-trx-TEV-His_{10}-TEV-TIR/TRIF is given below in Fig. 15.

MKHHHHHHPMSDKIIHLTDDSFDTDVLKADGAILVDFWAEWCGPCKMIAPILD
EIADEYQGKLTVAKLNIDQNPGTAPKYGIRGIPTLLLFKNGEVAATKVGALSKGQ
LKEFLDANLAGSGSGSENLYFQGAMGHHHHHHHHHHENLYFQGESSSEQKF
YNFVILHARADEHIALRVREKLEALGVPDGATFCEDFQVPGRGELSCLQDAIDH
SAFIILLLTSNFDCRLSLHQVNQAMMSNLTRQGSPDCVIPFLPLESSPAQLSSDT
ASLLSGLVRLDEHSQIFARKVANTFKPHRLQARKAMWRKEQD

His_{10}-TEV-TIR/TRIF: MW = 20.27 kDa / pI = 6.45

His_6-trx-TEV-His_{10}-TEV-TIR/TRIF: MW = 34.60 kDa / pI = 6.20

Figure 14 - Amino acid sequence of the His_6-trx-TEV-His_{10}-TEV-TIR/TRIF construct. TEV cleavage sites are marked in blue. MW = molecular weight; pI = isoelectric point. MW and pI were obtained by entering the sequence in the Expasy ProtParam online tool.

After we had obtained the correct plasmid, we again performed test expressions in varying conditions. However, as before, the protein remained insoluble even when fused to the trx-tag. A summary of the different expression conditions teste is given in table 6. An example of an SDS gel of fractions obtained during the purification of the various test expressions of His_6-trx-TEV-His_{10}-TEV-TIR/TRIF is depicted in Fig. 16 B.

Table 6 - All combinations of TRIF constructs, expression conditions and lysis buffers tested during test expression trials

Trial number	Construct	*E. coli* strain	IPTG concentration (mM)	Expression conditions	Resuspension buffer	Cold shock
1	TIR/TRIF	BL21	0.5	4h, 23°C	L1	-
2	TIR/TRIF	BL21	0.1	4h, 23°C	L1	-

3	TIR/TRIF	BL21	0.25	4h, 23°C	L1	-
4	TIR/TRIF	BL21	0.25	4h, 23°C	20mM Tris pH 8.5, 500mM NaCl, 25mM imidazole, 10mM BME, 5% glycerol	-
5	TIR/TRIF	BL21	0.5	4h, 23°C	20mM Tris pH 8.5, 500mM NaCl, 25mM imidazole, 10mM BME, 5% glycerol	-
6	TIR/TRIF	BL21	0.5	overnight, 16°C	L1	yes
7	TIR/TRIF	BL21	0.25	overnight, 16°C	L1	yes
8	TIR/TRIF	BL21	0.1	overnight, 16°C	L1	yes
9	TIR/TRIF	BL21	0.05	overnight, 16°C	L1	yes
10	TIR/TRIF	BL21 LysS	0.2	overnight, 16°C	L1	yes
11	TIR/TRIF	SoluBL21	0.2	overnight, 16°C	L1	yes
12	Trx-TIR/TRIF	BL21	0.1	overnight, 16°C	L1	yes
13	Trx-TIR/TRIF	BL21	0.2	overnight, 16°C	L1	yes
14	Trx-TIR/TRIF	BL21	0.05	overnight, 16°C	L1	yes
15	Trx-TIR/TRIF	BL21	0.1	4h, 23°C	L1	-
16	Trx-TIR/TRIF	BL21	0.2	4h, 23°C	L1	-

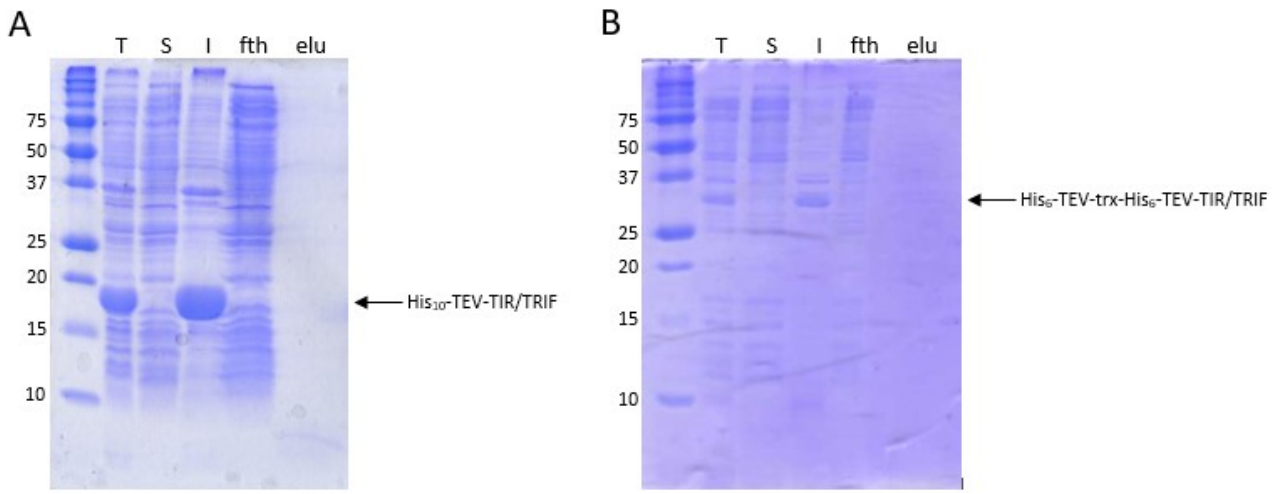

Figure 15 -Examples of SDS gels of cleared cell lysates purified on on-batch His-affinity chromatography. ***(A)*** *Example of a purification trial with TIR/TRIF (trial number 5)* ***(B)*** *example of a purification trial with trx-TIR/TRIF (trial number 14). M = marker (4 µl); T = total (0.5 µl); S = soluble (0.5 µl); I = insoluble (0.5 µl); fth = flowthrough (0.5 µl in A, 6.5 µl in C); elu = elution (6.5 µl in A and C, 3.5 µl in B); dial = dialyzed sample (6.5 µl)*

3.4 Expression and purification of trx-TIR/TRIF (396-545)

Since none of our previous attempts at solubilizing the TIR/TRIF protein were successful, we decided to investigate whether shortening the construct would have a positive influence on solubility. As described in chapter 2.3.14, we created a version of TIR/TRIF with a deletion of nine amino acids on the N-terminus fused to the trx-tag. The sequence of the resulting product is given below in Fig. 17.

MKHHHHHHPMSDKIIHLTDDSFDTDVLKADGAILVDFWAEWCGPCKMIAPILD
EIADEYQGKLTVAKLNIDQNPGTAPKYGIRGIPTLLLFKNGEVAATKVGALSKGQ
LKEFLDANLAGSGSGSENLYFQGAMAHHHHHHENLYFQGNFVILHARADEHIA
LRVREKLEALGVPDGATFCEDFQVPGRGELSCLQDAIDHSAFIILLLTSNFDCRL
SLHQVNQAMMSNLTRQGSPDCVIPFLPLESSPAQLSSDTASLLSGLVRLDEHSQ
IFARKVANTFKPHRLQARKAMWRKEQD

MW = 32.98 kDa / pI = 6.15

Figure 16 - Amino acid sequence of the His_6-trx-TEV-His_6-TEV-TIR/TRIF (396-545) construct. TEV cleavage sites are marked in blue. MW = molecular weight; pI = isoelectric point. MW and pI were obtained by entering the sequence in the Expasy ProtParam online tool.

Additionally, we decided to co-express this construct with the chaperone pG-Tf2 (Chaperone Plasmid Set, Takara) since coexpression of an insoluble protein with a chaperone can lead to solubilization of the former (Rodrigo et al., 2014; Veisi et al., 2015) For this, we transformed BL21 cells with the pG-Tf2 plasmid and made them competent following the usual protocol. Subsequently, we transformed the trx-TIR/TRIF (396-545) plasmid into these BL21 pG-Tf2 cells and did another test expression with two different lysis buffers (see chapter 2.4.9.3). The SDS gel showed that a small fraction of the produced protein could be obtained in both elutions (Fig. 18). We therefore pooled those elutions and dialyzed them overnight against 50mM Tris pH 8.0, 10mM BME, 25mM imidazole together with TEV protease to cleave off the trx-tag. The product was concentrated and further purified by size exclusion chromatography. However, the chromatogram and the corresponding SDS gel of the fractions that showed UV absorption peaks revealed that the protein eluted at a volume that corresponded to a higher molecular mass than a monomer (Fig. 19 A). Furthermore, other bigger proteins were present in all fractions that TIR/TRIF was found in (Fig. 19 B). We concluded that the protein had likely aggregated with chaperones or other proteins of higher size during the course of the purification and therefore decided to focus on our experiments on TRAM and A46 for the remainder of the thesis.

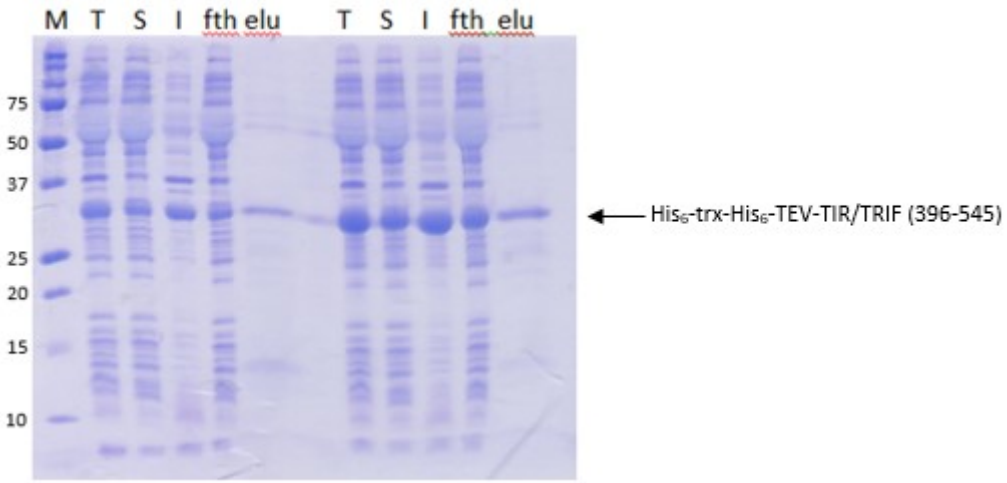

Figure 17 - SDS gel of the fractions obtained from His-affinity chromatography of the cleared cell lysate. The construct could partially be solubilized and obtained in the elution fraction. M = marker (4 µl); T = total (0.5 µl); S = soluble (0.5 µl); I = insoluble (0.5 µl); fth = flowthrough (0.5 µl in A, 6.5 µl in C); elu = elution (6.5 µl)

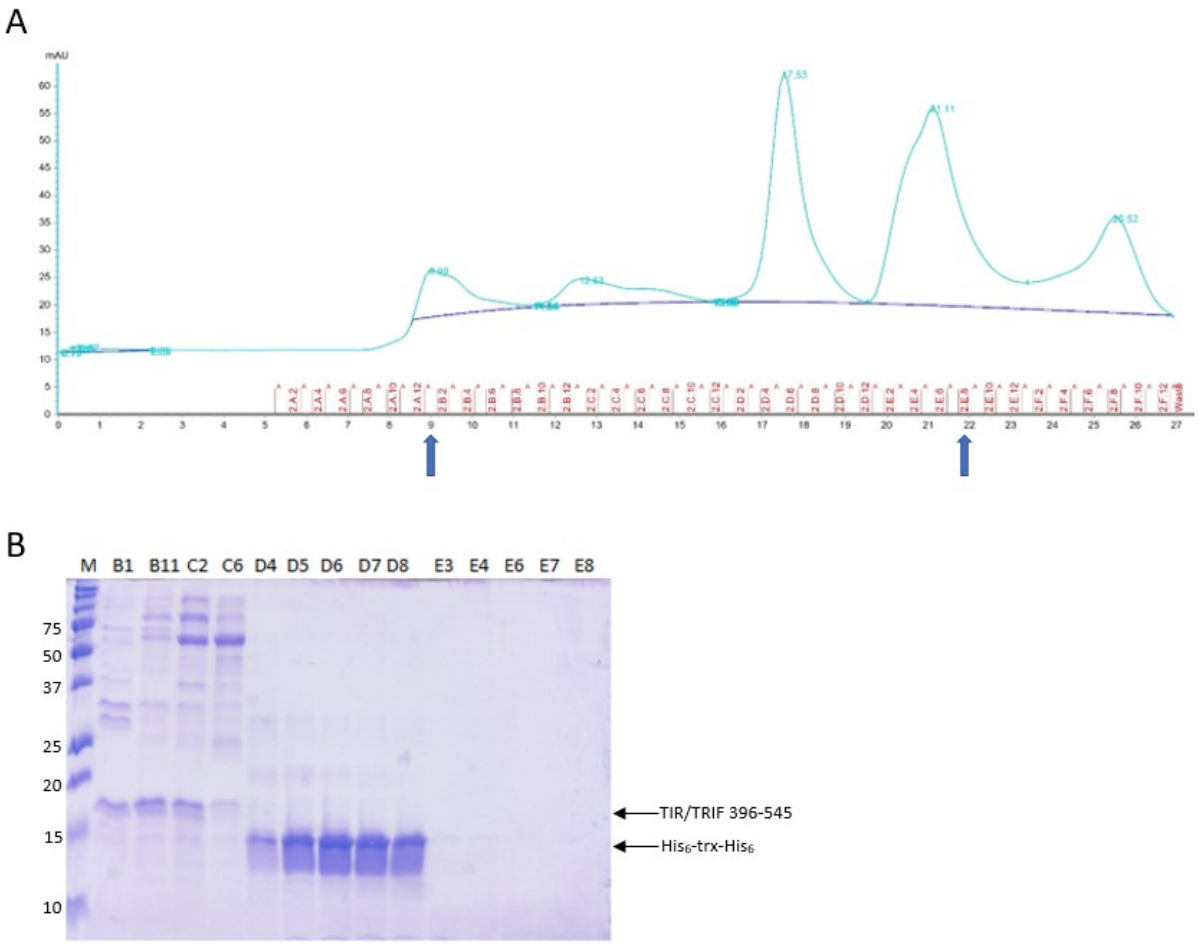

*Figure 18 – Size exclusion chromatogram and SDS gel of the size exclusion fractions of interest of the TIR/TRIF (396-545) construct. **(A)** Size exclusion chromatogram of TIR/TRIF (396-545) that had previously been cleaved off the trx-tag with TEV protease. The blue arrows indicate the range in which fractions were analyzed on an SDS gel. **(B)** Corresponding SDS gel of the analyzed fractions. The protein of interest and the tag are marked with arrows. As can be seen, TIR/TRIF (396-545) could not be purified and eluted earlier than proteins of similar size together with proteins of larger size that may be chaperones.*

3.5 TRAM full-length purification trials

To study interactions between TRAM and A46 in coexpression experiments as well as in *in vitro* pulldown experiments, we first had to establish a protocol for purifying soluble TRAM protein. A pET-11d vector containing the sequence for full-length TRAM with a C-terminal, TEV-cleavable His_{10} tag cloned between the NcoI and BamHI restriction sites was ordered from GenScript to perform test expressions. The amino acid sequence of the construct is given below in Fig. 20.

MGIGKSKINSCPLSLSWGKRHSVDTSPGYHESDSKKSEDLSLCNVAEHSNTTE
GPTGKQEGAQSVEEMFEEEAEEEVFLKFVILHAEDDTDEALRVQNLLQDDFGI
KPGIIFAEMPCGRQHLQNLDDAVNGSAWTILLLTENFLRDTWCNFQFYTSLMNS
VNRQHKYNSVIPMRPLNNPLPRERTPFALQTINALEEESRGFPTQVERIFQESVY
KTQQTIWKETRNMVQRQFIAENLYFQGHHHHHHHHHHH

MW = 29.14 kDa / pI = 5.62

Figure 19 - Amino acid sequence of the TRAM-TEV-His_{10} construct. The TEV cleavage site is marked in blue. MW = molecular weight; pI = isoelectric point. MW and pI were obtained by entering the sequence in the Expasy ProtParam online tool.

E. coli cells were transformed with this vector and various test expressions were carried out using different *E. coli* strains, expression conditions and resuspension buffers (see table 7). Subsequently, on-batch His-trap purifications were carried out to isolate the construct of interest and fractions of the different purification steps were loaded on SDS gels to check whether the protein could be obtained. However, even though TRAM was overexpressed in all cases, we could not obtain soluble protein under any of the conditions tested. An example of an SDS gel of fractions obtained during the purification of a test expression is depicted in Fig. 21.

Table 7 - All combinations of expression conditions and lysis buffers tested during test expressions of TRAM-TEV-His_{10}

Trial number	*E. coli* strain	IPTG concentration (mM)	Expression conditions	Resuspension buffer	Cold shock
1	BL21	0.5	4h, 23°C	TRAM trial buffer	-
2	BL21	0.5	4h, 23°C	20mM Tris pH 7.4, 100mM NaCl, 25mM imidazole, 10mM BME, 5% glycerol	-
3	BL21	0.5	4h, 23°C	20mM Tris pH 8.5, 500mM NaCl, 25mM imidazole, 10mM BME, 5% glycerol	-
4	BL21	0.5	4h, 23°C	20mM Tris pH 7.4, 500mM NaCl, 25mM imidazole, 10mM BME, 5% glycerol	-
5	BL21	0.25	overnight, 16°C	TRAM trial buffer	yes
6	BL21	0.5	overnight, 16°C	TRAM trial buffer	yes
7	BL21	0.1	overnight, 16°C	TRAM trial buffer	yes
8	BL21	0.05	overnight, 16°C	TRAM trial buffer	yes
9	BL21	0.2	overnight, 16°C	TRAM trial buffer	yes
10	SoluBL21	0.2	overnight, 16°C	TRAM trial buffer	yes

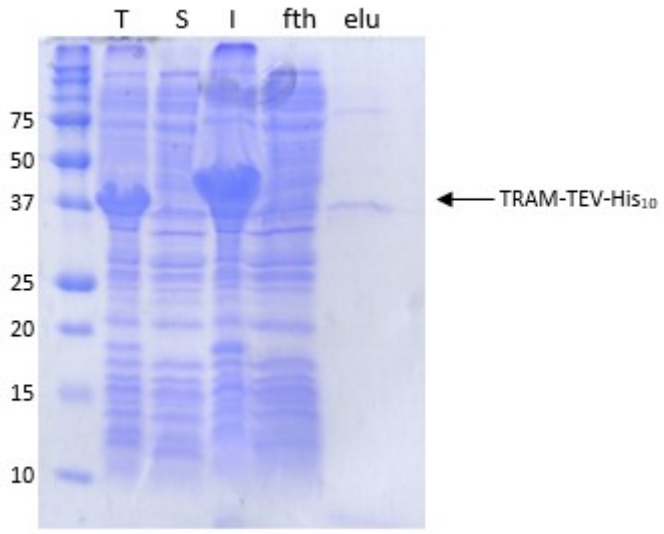

Figure 20 - Example of an SDS gel of a cleared cell lysate purified from a TRAM-TEV-His_{10} expression on on-batch His-affinity chromatography (trial number 6). The protein of interest is highly expressed but almost completely insoluble. M = marker (4 µl); T = total (0.5 µl); S = soluble (0.5 µl); I = insoluble (0.5 µl); fth = flowthrough (0.5 µl in A, 6.5 µl in C); elu = elution (6.5 µl in A and C, 3.5 µl in B)

3.6 Expression and purification of a C-terminally truncated version TRAMΔ5-TEV-His_6

Since our purification trials with the original full-length TRAM construct hardly yielded any soluble protein, we decided to follow the approach of Ullah et al. and produce a version of TRAM lacking the 5 last amino acids on its C-terminus, since this construct had been shown to be soluble (Ullah et al., 2015). We performed PCR and ligation as described in chapter 2.3.13 to create a TRAMΔ5-TEV-His_6 construct for further purification trials. The results of the sequencing showed that we had successfully obtained the pET-11d vector containing the desired TRAMΔ5-TEV-His6 sequence (Fig. 22).

MGIGKSKINSCPLSLSWGKRHSVDTSPGYHESDSKKSEDLSLCNVAEHSNTTE
GPTGKQEGAQSVEEMFEEEAEEEVFLKFVILHAEDDTDEALRVQNLLQDDFGI
KPGIIFAEMPCGRQHLQNLDDAVNGSAWTILLLTENFLRDTWCNFQFYTSLMNS
VNRQHKYNSVIPMRPLNNPLPRERTPFALQTINALEEESRGFPTQVERIFQESVY
KTQQTIWKETRNMVQENLYFQGHHHHHH

MW = 27.98 kDa / pI = 5.27

Figure 21 - Amino acid sequence of the TRAMΔ5-TEV-His_6 construct. The TEV cleavage site is marked in blue. MW = molecular weight; pI = isoelectric point. MW and pI were obtained by entering the sequence in the Expasy ProtParam online tool.

The construct was expressed in BL21 or B834 *E. coli* cells that were induced with 0.25mM IPTG. Both a 4-hour expression on 23°C and an overnight expression on 16°C were tried initially. The proteins were resuspended in TRAM lysis buffer and subsequently purified on an on-batch His-trap as described in materials and methods. The SDS gel showed that soluble TRAMΔ5-TEV-His_6 protein could be obtained in the elution fractions of both samples, and that the yield was slightly higher when expressing on 16°C overnight (Fig. 23). We therefore employed this method for all further purifications of TRAMΔ5-TEV-His_6. It is notable that, although the molecular weight of the construct is approximately 28 kDa, the protein runs close to the 37 kDa band on SDS gels. This is seen also in expressions of TRAM in mammalian cells and may indicate post-translational modifications of the protein that cause it to migrate slower through the gel. The sample obtained from the elution of the His-trap was dialyzed overnight and further purified by size exclusion chromatography to remove impurities caused by other proteins. The chromatogram showed a distinct peak at a retention volume of 85-100ml (Fig. 24 A). Fractions of this peak as well as of the two smaller peaks at lower retention volumes were run on an SDS gel to check for proteins of the correct molecular weight. The results showed that the prominent peak seen in the chromatogram contained our protein of interest along with small amounts of impurities, while the two smaller peaks contained proteins of higher molecular weight (Fig. 24 B).

Therefore, fractions D9-E7 were concentrated. Final concentrations of TRAM were 3.82 mg/ml from 2L of expression.

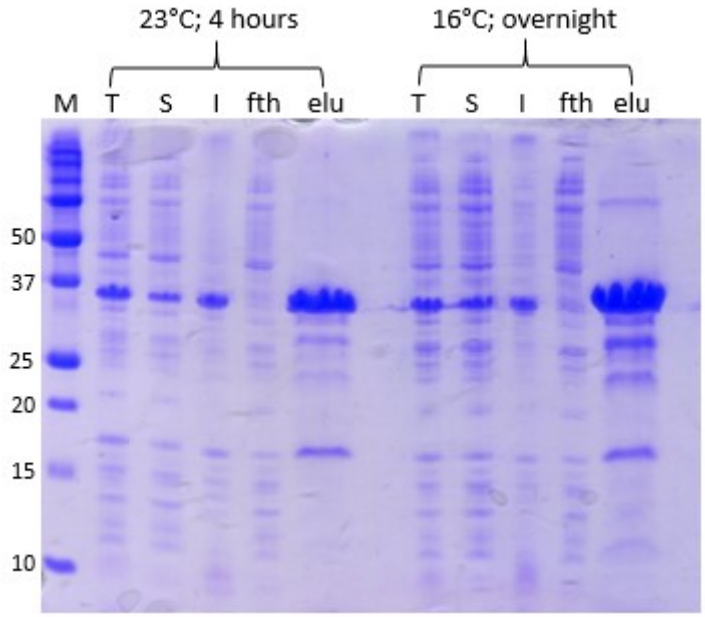

Figure 22 – SDS gel of the fractions obtained from on-batch His affinity chromatography of TRAMΔ5-TEV-His_6 expressions. The construct was partly soluble and could be obtained in the elution fraction. The protein yield was slightly higher for the overnight expression carried out at 16°C. M = marker (4 µl); T = total (0.5 µl); S = soluble (0.5 µl); I = insoluble (0.5 µl); fth = flowthrough (0.5 µl in A, 6.5 µl in C); elu = elution (6.5 µl in A and C, 3.5 µl in B)

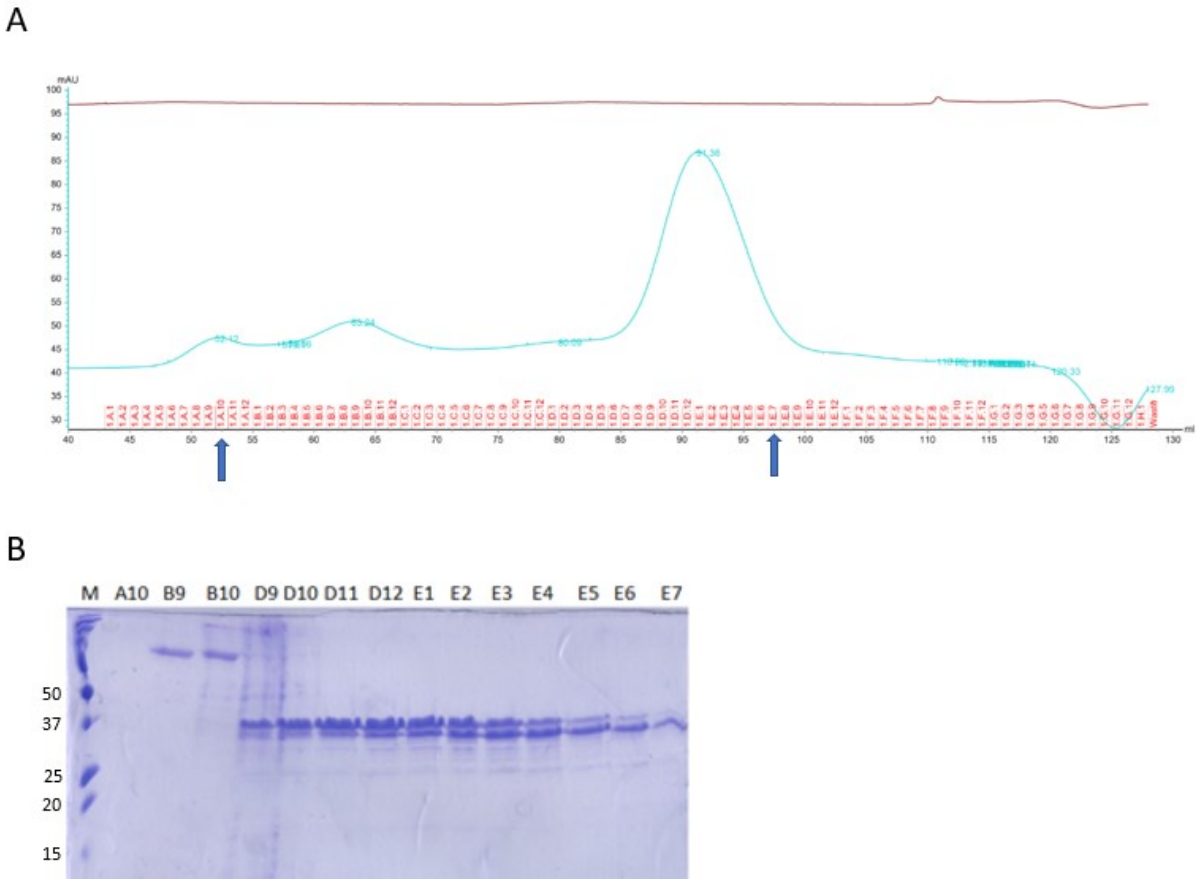

*Figure 23 - Size exclusion chromatogram and corresponding SDS gel of the purification of TRAMΔ5-TEV-His$_6$. **(A)** Size exclusion chromatogram of the dialyzed sample. The UV absorption curve is shown in light blue, the conductivity of the solution in brown. The arrows indicate the range in which fractions were analyzed on an SDS gel. **(B)** SDS gel of the fractions of interest. TRAMΔ5-TEV-His$_6$ was present exlusively in the biggest peak seen on the chromatogram.The second band visible on the gel is likely caused by a specific N-terminal degradation of the protein.*

As can be seen in Fig. 24, TRAMΔ5-TEV-His$_6$ showed two distinct bands on the SDS gel after size exclusion chromatography. This may be because of a specific N-terminal degradation occurring during the expression of the protein or later during the course of the purification. Both bands could be detected by Western blotting with anti-His antibodies, suggesting that they both were His-tagged (data not shown).

3.7 TRAM-A46 coexpression

After we confirmed that the TRAMΔ5-TEV-His$_6$ construct is partially soluble, we wanted to test whether a coexpression of this construct together with A46 (1-240)-myc in *E. coli* would lead to the formation of a stable complex between these two proteins that could be pulled down and purified. The TRAM construct bears a His-tag and is therefore retained on a His-affinity column. Thus, A46 (1-240)-myc should be washed off the column during the washing steps. Should a stable complex between TRAM and A46 be formed, A46 would be retained on the column by TRAM and could afterwards be co-eluted.

We expressed both proteins from the same cells in the BL21 and B834 *E. coli* strains and purified the cell lysate through on-batch His-affinity chromatography. The SDS gel showed that TRAM was obtained in both elutions. A46, however, could not clearly be identified on the gel due to no significant overexpression of the protein. While a band directly under that of TRAM could possibly have been A46, also a very faint band below might also have corresponded to the viral protein (Fig. 25 A). To ascertain the fractions in which A46 could be found, we performed an anti-myc Western blot with the samples obtained from the His-affinity chromatography. Interestingly, A46 was expressed in both cell strains, but was not present in the elution of the BL21 sample, whereas it was eluted in the sample of the B834 expression (Fig. 25 B). The signal on the top of the membrane is often seen in Western blots with full-length A46 and could represent an aggregation of protein that cannot enter the separation gel. We subsequently decided to pool these elutions together to obtain the maximum amount of both TRAM and A46 in one sample and then dialyze them against the buffer used for resuspension of the cells without imidazole. Afterwards, we concentrated the sample and examined it by size exclusion chromatography. The chromatogram showed one distinct peak at a retention volume of 85-100ml, resembling the chromatogram of TRAMΔ5-TEV-His_6 (data not shown). We loaded the fractions lying within this peak on an SDS gel and did an anti-myc Western blot to detect whether A46 was present in the fractions in question. However, the protein could not be detected on the membrane (data not shown), likely because it had precipitated during the dialysis or was extensively diluted during the size exclusion run to be seen on the Western blot.

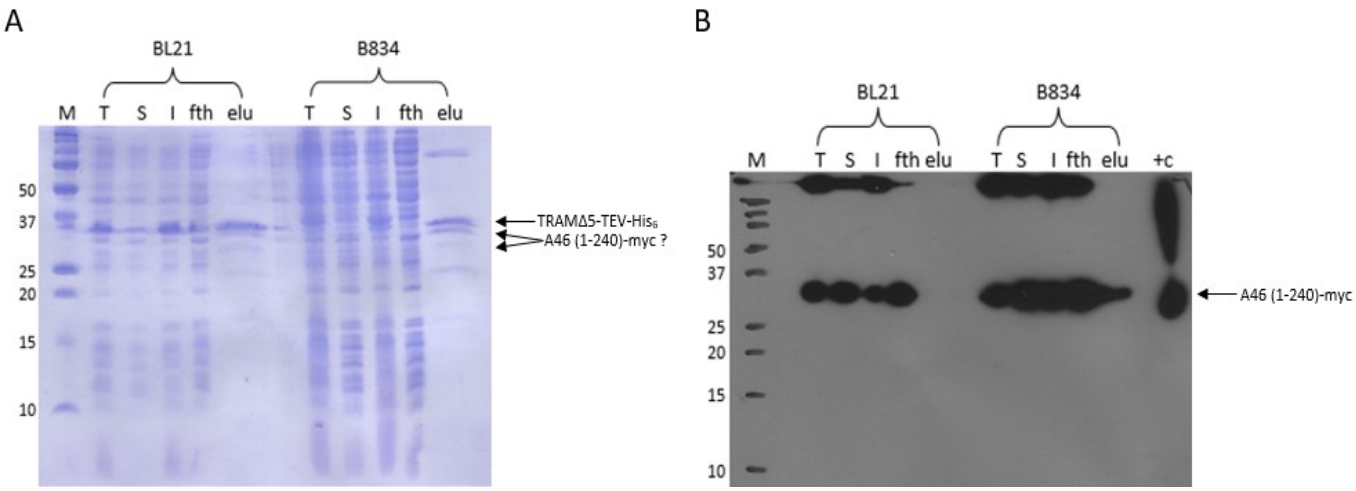

Figure 24 – SDS gel and Western blot of the coexpressions of TRAMΔ5-TEV-His_6 and A46 (1-240)-myc in BL21 and B834 E. coli cells. ***(A)*** *SDS gel showing the fractions obtained during His-affinity chromatography. TRAM was overexpressed and could be obtained in the elutions of both samples. A46 did not show overexpression and could not be doubtlessly identified.* ***(B)*** *anti-myc Western blot of the same samples. A46 was expressed in both cell strains, but was only eluted in the B834 sample. . M = marker (4 µl); T = total (0.5 µl); S = soluble (0.5 µl); I = insoluble (0.5 µl); fth = flowthrough (0.5 µl in A, 6.5 µl in C); elu = elution (6.5 µl)*

3.8 *In vitro* complex formation between A46 and TRAM

To investigate whether A46 and TRAM would form a complex *in vitro*, we mixed purified TRAMΔ5-TEV-His_6 and non-tagged A46 (1-240) together and dialyzed them against various buffers as described in materials and methods. Subsequently, we performed small-scale His-affinity chromatography to purify TRAM and analyzed the obtained fractions from the different purification steps on SDS-PAGE to learn whether A46 would co-elute with TRAM, indicating an interaction between the two proteins. A46 was not present in any of the elution fractions under the conditions tested (data not shown), indicating that formation of a stable complex between the two proteins did not occur. However, we observed that in all buffers tested, the amount of A46 recovered from the sample after dialysis but before His-trap was low compared to the total amount of A46 used in these experiments. An example is shown in Fig. 26. Therefore, A46 was lost in great amounts during dialysis, either because it precipitated due to sub-optimal buffer conditions or because it stuck to the wall or membrane of the dialysis tubes and could therefore not be found in the solution anymore.

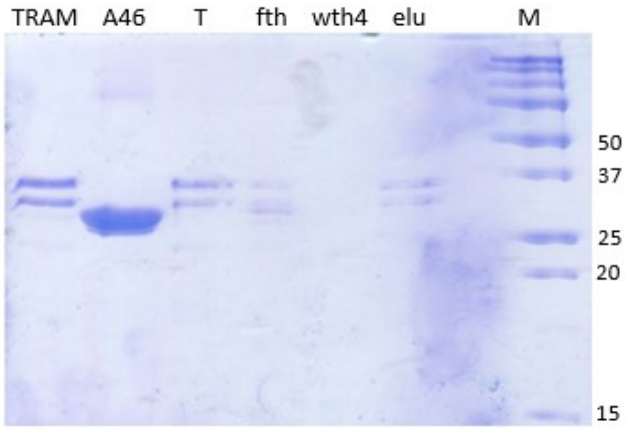

Figure 25 - SDS gel of the fractions taken from the in vitro pulldown experiment compared to the total amounts of both purified proteins used in the experiment. A46 is lost from the solution during dialysis. TRAM is present in two distinct bands, likely because of a specific N-terminal degradation.

3.9 Effect of A46 on the subcellular localization of TRAM in mammalian cells

A46 has been shown to bind to TRAM in pull-down experiments performed with mammalian cells (Sofiya Fedosyuk, unpublished data). Thus, we wanted to examine whether this interaction would lead to the dislocation of TRAM within living mammalian cells. Under physiological conditions, TRAM is localized to the cellular membrane via an N-terminal myristoylation that serves as a membrane anchor and is crucial for NF-κB activation (Rowe et al., 2006). It is therefore possible that A46 brings about a

dissociation of TRAM from the membrane, thereby sequestering or inhibiting its function in the TLR signaling pathway. To test whether the subcellular localization of TRAM in mammalian cells would change in the presence of A46, we co-transfected HiExp cells with TRAM-FLAG as well as with varying amounts of either the myc-tagged N-terminus, the C-terminus or the full-length variant of A46 and subsequently performed subcellular fractionation with the cultured cells. The obtained fractions were analyzed by Western blotting. γ- tubulin and α-calnexin blots were made to examine whether the same amount of proteins had been loaded in all fractions. The results showed that, as expected, TRAM was present in much greater amount in the membrane fraction than in the cytosol. This becomes evident when comparing the exposure times of the films to the developed membranes. While a signal for cytosolic TRAM was seen only after five minutes, the membrane-associated protein could be clearly detected after less than 30 seconds. No A46 variant showed a significant change in the distribution of TRAM between the membrane and the cytosol and TRAM remained predominantly in the membrane fraction in the presence of all A46 constructs. Furthermore, the N-terminus of A46 seemed to be localized in much greater amounts to the cytosol than to the membrane, whereas the C-terminus and the full-length A46 were found in the cytosol and membrane fractions in equal amounts (Fig. 27).

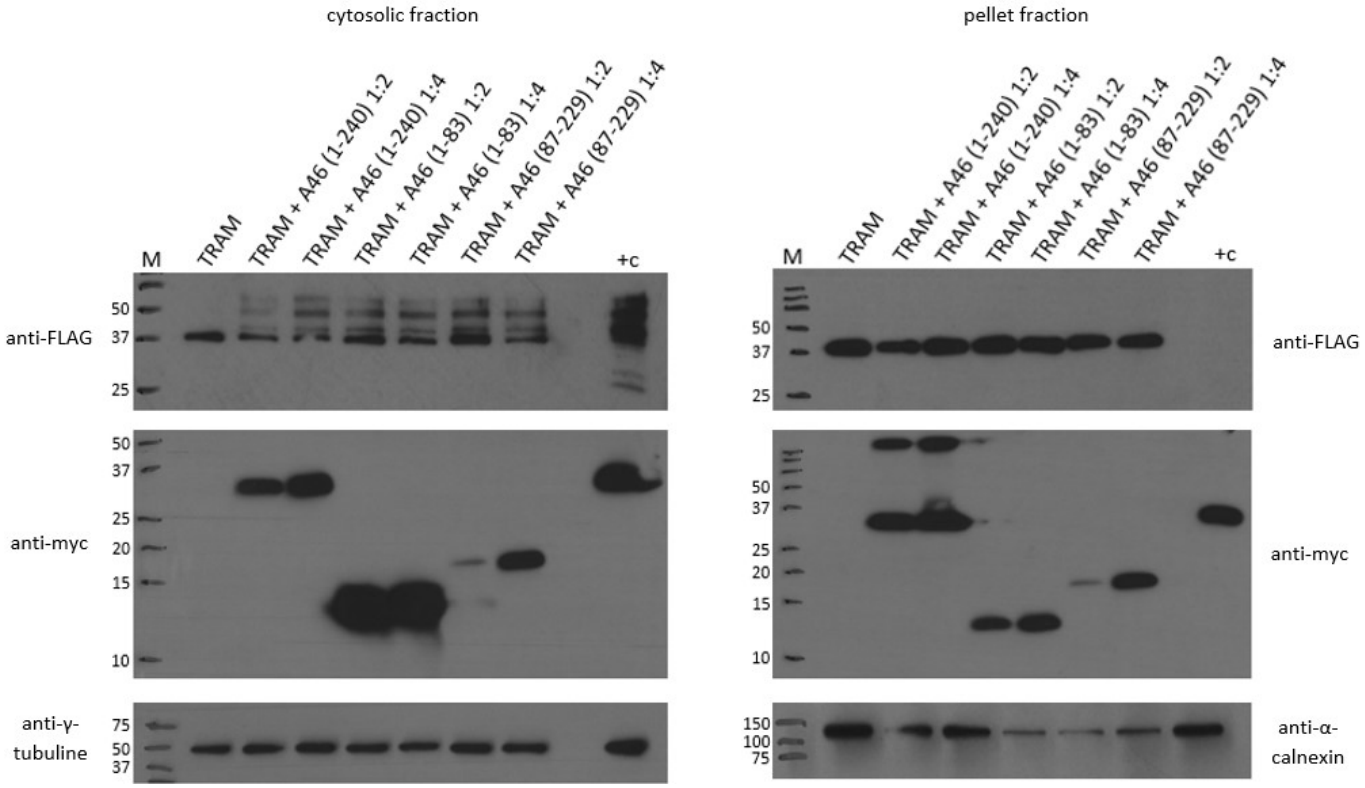

Figure 26 - Western Blots of the cytosolic (left side) and membrane fractions (right side) of all co-transfections of TRAM with different A46 constructs as well as the single transfection with TRAM as a control. Top left: anti-FLAG blot with 5 minutes exposure time; middle left: anti-myc blot with 5 seconds exposure time; bottom left: control anti-γ-tubuline blot with 5 minutes exposure time; top right: anti-FLAG blot with 30 seconds exposure time; middle right: anti-myc blot with 5 seconds exposure time; bottom right; control anti-α-calnexin blot with 4 minutes exposure kit and 1/10 Femto kit used. +c = positive controls

3.10 Subcellular localization and expression levels of A46 domains in mammalian cells

Knowledge about the localization of full-length A46 as well as its C- and N-terminal domains within mammalian cells could help us gain a better understanding of their possible modes of action in interfering with the TLR signaling pathway. To this end, we examined the subcellular localization following the fractionation protocol described previously. Two wells of a six-well plate were used per condition. In the first experiment, we separated the cytosol from the pellet fraction containing nuclei, mitochondria and cell membranes. The western blots suggested that full-length A46 and the C-terminal domain were found in both fractions while the N-terminal domain localized exclusively to the cytosol. Furthermore, the N-terminus appeared to be expressed to a much higher extent that the other two constructs (Fig. 28).

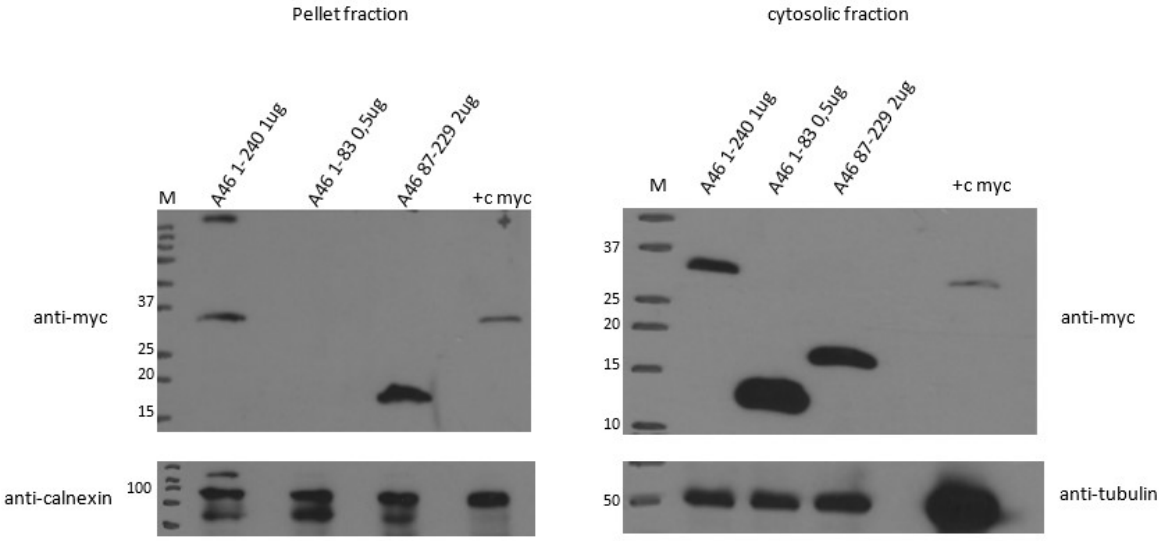

Figure 27 – Western Blots of the membrane (left side) and cytosolic fractions (right side) of the transfections with different A46 constructs. The N-terminus of A46 localizes solely to the cytosol, whereas the C-terminus is found both in the cytosol and the cellular membranes. The full-length A46 is also found in both fractions. There is a notable overexpression of the N-terminus compared to the other two constructs. Anti-α-calnexin and anti-γ-tubulin western blots were made as a control to see whether the same amount of protein had been loaded in all fractions.

We subsequently repeated the experiment, but this time fractionated into nuclei, mitochondria, cytosol and cellular membranes. Again, we observed overexpression of the N-terminus compared to the C-terminus and full-length A46. As before, the N-terminus was mainly present in the cytosol, with small amounts being found in the mitochondria and membrane fractions as well. In contrast, the C-terminus was present in the cytosol and the cellular membranes to approximately the same extent, but not in the nuclei or in the mitochondria. Full-length A46 showed a distribution pattern with characteristics of both domains, being present in the cytosol and membranes in approximately the same amounts and to a lesser extent also in the mitochondria (Fig. 29).

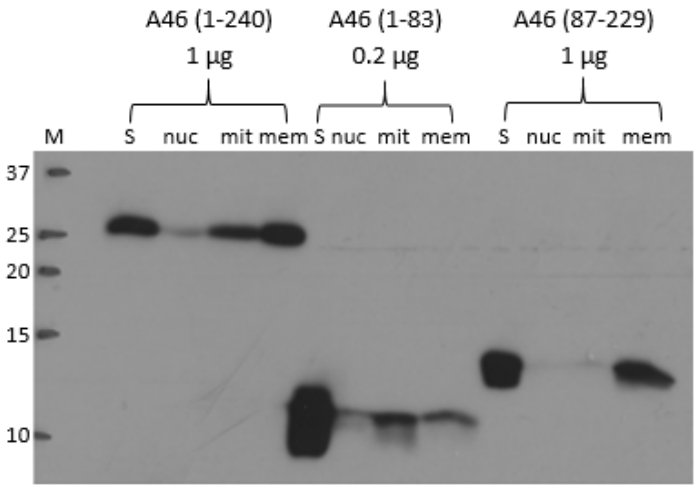

Figure 28 – anti-myc Western blot of cytosolic (S), nuclear (nuc), mitochondrial (mit) and cellular membrane (mem) fractions of HiExp cells transfected with the different A46 constructs. While the N-terminus is mainly present in the membranes and to a small portion also in the mitochondria, the C-terminus localizes to the cytosol and cellular membranes in comparable amounts. The full-length A46 protein unites the localization characteristics of its two domains, localizing to the cytosol, the cellular membranes and in smaller amounts to the mitochondria. All three constructs seem to be absent from the nuclear fraction.

As a next step, we performed the experiment again, however this time transfecting with 0.02 and 0.05 µg DNA of the N-terminus while still using 1ug of DNA of the other two constructs to reach a similar level of expression of all constructs. The results suggested that 0.02µg of DNA encoding for the N-terminus of A46 is not a sufficient amount to reach protein expression, while the amount of cytosolic N-terminus protein resulting from transfection of 0.05 µg respective DNA equals the amount of cytosolic full-length A46 after transfection with 1 µg of the respective DNA. While again the N-terminus was present only exclusively in the cytosol, this time both the full-length A46 and the C-terminus were found in all fractions in comparable amounts (Fig. 30). Therefore, these results are not consistent with the previous experiment concerning the localization of full-length A46 and its C-terminus to nuclei and mitochondria in mammalian cells.

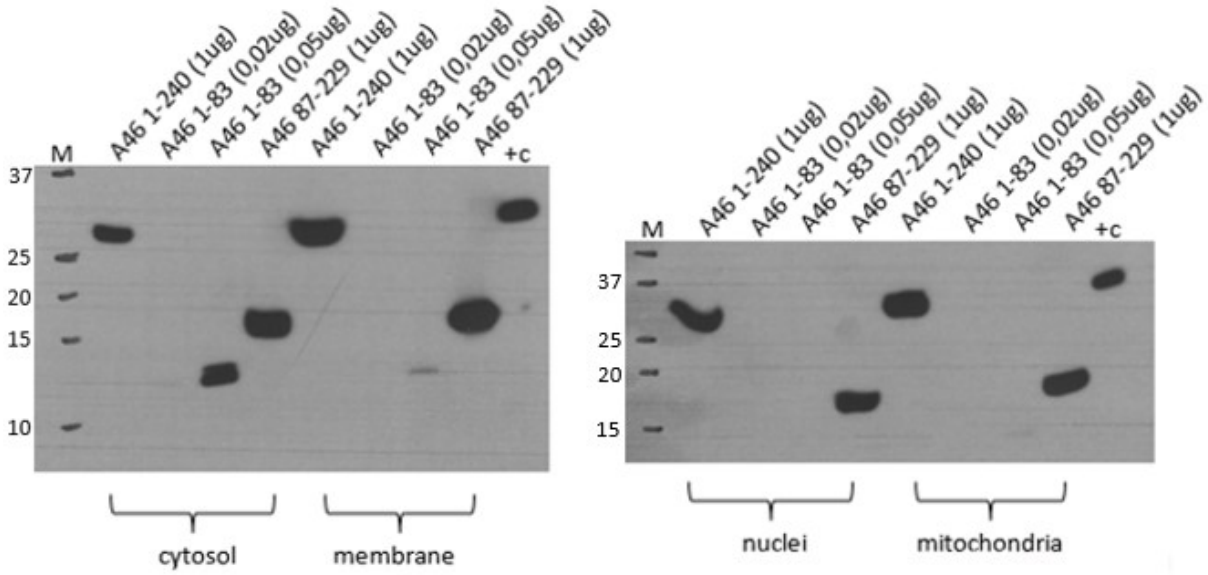

Figure 29 – anti-myc Western of cytosolic, nuclear, mitochondrial and cellular membrane fractions of HiExp cells transfected with the different A46 constructs. As seen before, the N-terminus of A46 localizes only to the cellular membranes. In contrast to the last experiment, however, Full-length A46 as well as the C-terminus are found in all fractions in comparable amounts. 0.05 µg DNA of A46 (1-83) is not enough to induce protein expression while 0.05µg lead to comparable amounts of soluble protein that are comparable with the other two constructs.

4. Discussion

4.1 Purification of N-terminal mutants of A46

A46 is a protein of VACV that is expressed early during infection and functions to inhibit the TLR signaling pathway by binding to TLR4 as well as to the adaptor proteins MyD88, Mal, TRIF and TRAM. This in turn prevents downstream signaling (Stack et al., 2005; Brady and Bowie, 2014). While the C-terminus of A46 was shown to adopt a Bcl-2-like fold (Fedosyuk et al., 2014), the crystal structure of the N-terminal domain was solved two years later, which revealed a β-sandwich that is assembled from two A46 N-termini and possesses a hydrophobic cavity that can bind myristic acid (Fedosyuk et al., 2016). In the light of these findings, we wished to express and purify versions of the A46 N-terminus that had point mutations in the hydrophobic pocket to test whether they would impair the viral protein's ability to bind fatty acids. We successfully expressed and purified the five mutant proteins F3D, H36L, Y37A, Y37W and I72A. Fig. 31 shows a view of the β-sandwich accommodating a molecule of myristic acid.

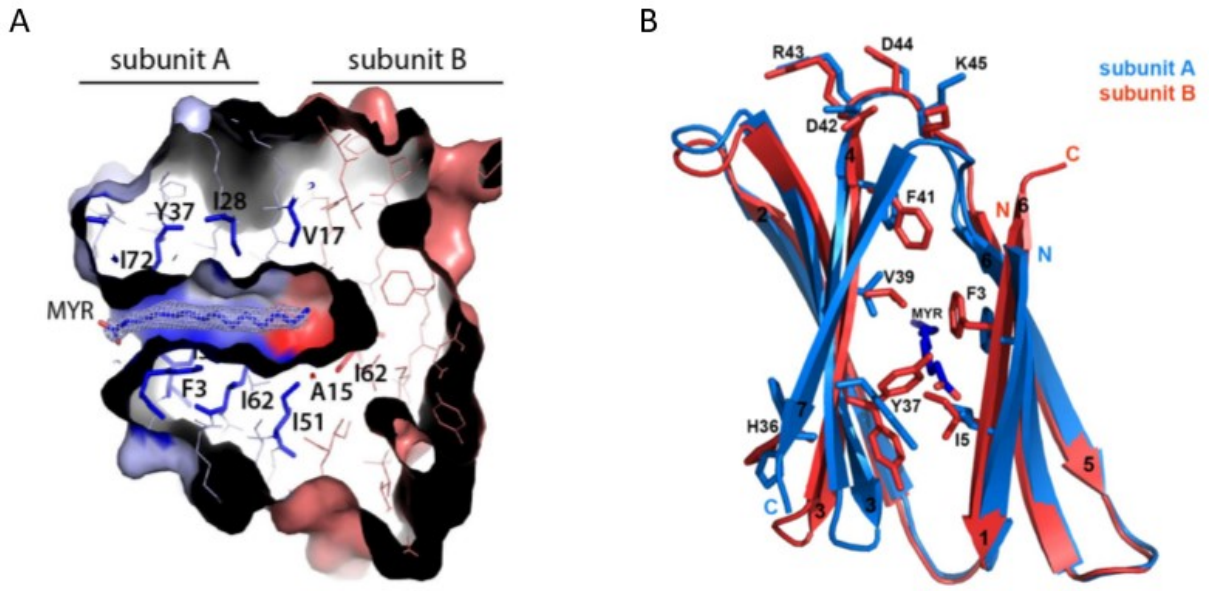

Figure 30 – Model of the β-sandwich with a molecule of myristic acid bound. (A) Model showing the location of some of the investigated amino acid residues and the myristic acid in longitudinal section. (B) Superimposition of the subunits A and B that make up the β-sandwich. Residues of interest which lie in the hydrophobic cavity or take different positions in either subunit are shown as sticks.

These mutant proteins were subsequently tested for their lipid content by mass spectrometry by Terry K. Smith (University of St. Andrews). The lipid content of all mutant proteins was reduced compared to the wild type, with the I72A mutant exhibiting the lowest amounts. These results are described in more detail in the paper to which this thesis contributed (Fedosyuk et al., 2016). Overall, the N-

terminus of A46 is a model for an exciting new lipid-binding protein fold and it will be interesting to investigate its potential function for the virus.

4.2 TRAM solubilization

TRAM is a mammalian adaptor protein of the TLR signaling pathway and necessary for the interaction between TLR4 and TRIF (Oshiumi et al., 2003a; Oshiumi et al., 2003b). As it is one of the proteins targeted by A46 (Stack and Bowie, 2012), our aim was to find conditions suitable for expressing and purifying TRAM for subsequent binding studies with A46. We tried to obtain soluble protein using a variety of different expression conditions and buffer compositions. However, TRAM remained insoluble even though it was overexpressed in *E. coli* in all the conditions tested. We subsequently looked for ways to overcome the issue of insolubility. Enokizono et al. described the expression and purification of A C117H mutant of the TIR-domain of TRAM (Enokizono et al., 2013). However, introducing this mutation into the protein was not possible in our case, since the cysteine 117 residue lies in the BB loop crucial for interaction with A46 and has also been shown to abrogate downstream signaling (Enokizono et al., 2013). Purification of full-length TRAM with an N-terminal poly-His-tag was also reported (Ullah et al., 2015). However, since an N-terminal His-tag might interfere with the binding between TRAM and A46, using this construct also was not an option for us. Therefore, we decided to follow another approach presented by the above authors, who obtained soluble protein of truncated versions of TRAM. Indeed, we were able to successfully obtain soluble TRAMΔ5-TEV-His_6 protein. Since the three most C-terminal amino acids in TRAM are phenylalanine, isoleucine and alanine and therefore all hydrophobic, their removal likely improves the solubility of the protein. Interestingly, a second band migrating closely below the one of TRAM can be observed on SDS gels of TRAM sample preparations. This second protein is co-purified together with TRAM, suggesting that it could represent TRAM which has undergone specific N-terminal degradation, either by proteases present in the cell lysate or induced by the conditions during the purification. It is unlikely that the lower band represents a natural *E. coli* protein which is rich in histidines and has a very similar molecular weight as TRAM and therefore cannot be separated from it during the purification. Even though multiple proteins expressed by *E. coli* have been reported to be able to bind to nickel affinity columns and to only be washed off at concentrations of 55mM imidazole (Bolanos-Garcia and Davies, 2006), it is very unlikely that one of these proteins is over-expressed to almost the same extent as our TRAM construct. Mass spectrometry analysis of this slightly smaller protein will be required to gain certainty about its nature and to identify a possible cleavage site in the N-terminus, which would allow for the identification of the cause of this observation.

4.3 TRIF solubilization

TRIF is the mammalian adaptor protein which transmits signals by TLR3 and TLR4 by binding either directly to the receptor in the case of TLR3, or through the additional adaptor protein TRAM in the case of TLR4 (Oshiumi et al., 2003a; Oshiumi et al., 2003b; Yamamoto et al., 2002). Our aim was to obtain the TIR domain of this protein in a soluble form for binding studies with A46. As with TRAM, we tested various expression conditions and buffer compositions, however, His_{10}-TEV-TIR-TRIF remained insoluble, even though it was highly overexpressed. Therefore, we tried fusing this construct to the trx-tag, a common protein tag used for solubilization. However, also the fusion construct was not soluble. Next, we created a shortened version of TIR-TRIF fused to the trx tag and co-expressed it with the pG-Tf2 chaperone in an attempt to improve solubility. This way, soluble protein could be obtained, however, it eluted too soon on size exclusion to be a monomer, suggesting that the protein had likely aggregated. A study by Tatematsu et al. in 2010 found that the N-terminal domain of TRIF interacts with its TIR domain, likely to prevent downstream signaling in the absence of TLR pathway stimuli, and that the lack of this N-terminal domain promotes homo-oligomerization of TRIF molecules via its TIR domain (Tatematsu et al., 2010). Consistent with this finding, TRIF homo-oligomerization, mediated by the TIR domain and the C-terminal region of TRIF, was reported to be critical for the activation of IRF3 and NF-κB through the TRIF-dependent pathway (Funami et al., 2008). Furthermore, these authors reported that the overexpression of TRIF in HeLa cells leads to the formation of so-called signalosomes, proteinaceous structures which contain TRIF, likely in an oligomerized state (Funami et al., 2007; Funami et al., 2008). Together, these studies identify a possible reason for our inability to obtain soluble monomeric TIR-TRIF. The protein may have oligomerized since the N-terminus, which normally masks the TIR domain, was missing. This would explain why the protein eluted so early from the size exclusion column, and could potentially also be the reason why we struggled with its solubilization. Future experiments should therefore be conducted with a version of TRIF that contains both the N-terminal domain and the TIR domain, to assess whether this construct would be better suited for purification and potential binding studies with A46.

4.4 TRAM-A46 co-expression and *in vitro* binding

To investigate whether TRAM and A46 would form a complex in *E. coli* cells, we co-expressed a C-terminally myc-tagged version of full-length A46 with the truncated TRAM protein which was soluble. The SDS gel showed the presence of the TRAM construct, as well as other bands which could potentially correspond to A46. Indeed, we could detect A46 in the different steps of the purification and in one of the elutions from the His-affinity chromatography, however, A46 was lost during the subsequent

dialysis and size exclusion chromatography, indicating that no stable complex between the proteins had formed. The SDS gel of the His-affinity chromatography shows that only small amounts of the proteins which could be A46 were obtained, indicating that the expression conditions were sub-optimal. Since TRAM and A46 alone should be expressed at very different conditions as described in 2.4.9.2 and 2.4.9.4, finding a good compromise that allows both proteins to be properly over-expressed might prove to be challenging. Furthermore, the buffers used to resuspend the cells and purify the proteins vary greatly in their ionic strength. Since buffer composition is absolutely crucial for the solubilization and correct folding of proteins, A46 might have precipitated during the dialysis because the buffer used was not suitable to keep it soluble. Another reason for the poor expression of A46 might be the construct itself. While the full-length variant of A46 that we purified on its own had four additional amino acids and an MBP-tag on its N-terminus for solubilization, the construct we used in the co-expression experiments lacked these features and instead was only fused to a C-terminal myc-tag. We removed the MBP tag because it may have interfered with the binding of A46 to TRAM. This could, however, have induced poor expression of the protein compared to the MBP-tagged variant. For these reasons, the co-expression should be repeated with a myc-tagged construct of A46 that has the four additional amino acids on its N-terminus to determine whether this improves A46 expression and potential complex formation. It will also be important to test various expression conditions and buffer compositions to find a good compromise that will allow the over-expression and purification of soluble TRAM and A46 together.

We also investigated the ability of TRAM and A46 to form a complex *in vitro* by mixing both purified proteins, dialyzing them together against various buffers and subsequently performing pull-down experiments on Ni-NTA beads. Surprisingly, A46 could not be detected in the samples after dialysis anymore. This observation could be explained by two possible scenarios: Either A46 precipitated during dialysis because of sub-optimal buffer compositions, or it bound to the wall of the dialysis tubes and could therefore not be found in the solution anymore. This indicates that a potential complex between TRAM and A46 is not stable enough to prevent A46 from precipitating or interacting with the tube walls. As a next approach, purified A46 alone should be dialyzed against various buffers, preferably also using different sets of dialysis tubes, to find conditions suitable for keeping it in the solution. Once such conditions are found, the *in vitro* complex formation with TRAM could be repeated.

Another interesting approach would be to perform in vitro complex formation experiments with myristoylated TRAM. This protein lacks its myristoylation when expressed in *E. coli*, since the bacteria do not possess a cytosolic enzyme that can attach this fatty acid to proteins (Glück et al., 2010). However, researchers reported that expressing human N-myristoyltransferase together with a protein

of interest that has an N-terminal myristoylation site leads to myristoylation of this protein in *E. coli* if myristic acid is added to the expression medium (Glück et al., 2010). Using this approach, we tried to produce myristoylated TRAM. However, mass spectrometry analysis of the purified protein revealed that the myristoylation was not successful, likely because the myristic acid was not truly dissolved upon addition to the expression medium. By improving this step of the purification protocol in the future, it should nevertheless be possible to obtain myristoylated TRAM. Subsequently, it could be tested whether this modification has any effects on *in vitro* complex formation with A46.

4.5 Effects of A46 on intracellular TRAM localization

As described before, TRAM is myristoylated in vivo in mammalian cells and this modification anchors TRAM to the cellular membrane, a crucial process for the protein to function properly in the TLR signaling pathway (Rowe et al., 2006). We knew that the N-terminus of A46 binds myristic acid, so we hypothesized that A46 might inhibit TRAM by binding to its myristate, therefore pulling it out of the membrane into the cytoplasm and thus disrupting its function. To test this assumption, we co-transfected mammalian cells with TRAM and either A46 full-length or its C- or N-terminus and subsequently performed subcellular fractionation. We then used Western blotting to see where TRAM and A46 would be localized, respectively, and whether the simultaneous expression of both proteins had any effects on the localization of TRAM. As expected, TRAM localized primarily to the membrane, however, neither the full-length A46 nor its C- or N-terminus seemed to delocalize TRAM from the membrane to the cytosol. This result suggests that A46 does not inhibit TRAM by binding to its myristate, but rather only to TRAM itself, for example to the BB loop of its TIR domain, as a study by Stack and Bowie showed (Stack and Bowie, 2012). One should consider, however, that our transfection method leads to very high intracellular concentrations of the proteins of interest. This is potentially problematic for several reasons: First, it is difficult to compare intensities on a Western blot if there is too much signal. This also means that subtle changes in intensity might be overlooked because they are too weak to stand out against a very strong signal. Second, high protein expression may lead to artifacts in the subcellular fractionation because of insufficient washing of the fractions, and therefore proteins might be observed in compartments to which they do not localize in the cells. Finally, it cannot be excluded that non-physiological amounts of proteins alter or inhibit their intrinsic functions. For these reasons, it will be useful to repeat these experiments with a transfection method that leads to lower intracellular concentrations of the target proteins to verify the results obtained in this thesis.

As of now, the exact interaction sites between A46 and TRAM are not fully known. It will be an interesting challenge to identify them in the future and to create a molecular model of these interactions.

4.6 Intracellular localization of A46 domains

To gain a better understanding of where A46 is localized in the host's cells, we performed subcellular fractionation on cells that had been transfected with either the full-length protein or the N- or C-terminus, respectively. While the N-terminus localized primarily to the cytosol, the C-terminus and the full-length protein were present in the membrane and cytosolic fraction to approximately the same extent. However, we obtained contradictory results concerning the possible localization to the nucleus and the mitochondria. This is likely due to the high expression level of the constructs in the cells, and our washing steps may not have been sufficient to remove artifacts of the A46 proteins from all fractions. As with our co-transfection experiments with TRAM, these experiments should be repeated with a transfection method that yields lower intracellular concentrations of the proteins of interest to obtain more reliable results.

We saw clearly, however, that the N-terminus of A46 does not localize to the cellular membrane, and that it is the C-terminus that seems to anchor A46 there. Thus, the hydrophobic cavity of the N-terminal β-sandwich does not bind lipids of the cellular membrane. It will be interesting to investigate how the Bcl-2-like C-terminus of A46 mediates binding to the membrane.

Lastly, our results show that the N-terminus of A46 is expressed approximately twenty times more than the C-terminus and the full-length protein. This could potentially be because of the lower toxicity of the N-terminal construct to the cells. It was recently shown that the A46 N-terminus on its own could not inhibit IL-1 mediated activation of NF-κB, in contrast to the C-terminus and the full-length protein (Fedosyuk et al., 2016). Because of this, cells might be able to tolerate higher intracellular concentrations of the A46 N-terminus. This finding should be kept in mind when performing transfections with variants of A46 in the future.

4.7 Conclusion

In this thesis, we purified five mutants of the A46 N-terminus, which were subsequently found to have lower levels of myristic acid bound than the wild-type protein.

Moreover, a potential complex between A46 and TRAM is likely not stable enough to be purified under the conditions we tested. The fact that A46 does not seem to change the subcellular localization of TRAM indicates that the viral protein likely does not bind to the myristate of TRAM. Elucidating the

physiological function of the hydrophobic cavity of the N-terminus of A46 will be an interesting future challenge.

Finally, we showed that A46 is anchored to the cellular membrane via its Bcl-2-like C-terminus, while the N-terminus is strictly cytosolic. Further investigations may shed light on the molecular basis of this unsuspected interaction.

5. Appendix

5.1 List of amino acids

Amino acid	3-letter code	1-letter code
Alanine	Ala	A
Arginine	Arg	R
Asparagine	Asn	N
Aspartic acid	Asp	D
Cysteine	Cys	C
Glutamic acid	Glu	E
Glutamine	Gln	Q
Glycine	Gly	G
Histidine	His	H
Isoleucine	Ile	I
Leucine	Leu	L
Lysine	Lys	K
Methionine	Met	M
Phenylalanine	Phe	F
Proline	Pro	P
Serine	Ser	S
Threonine	Thr	T
Tryptophan	Trp	W
Tyrosine	Tyr	Y
Valine	Val	V

5.2 List of abbreviations

Abbreviation	Full name
+ c	positive control
°C	degrees Celsius
µg	micrograms
µl	microliters
APS	ammonium persulfate
BCA	bicinchoninic acid
BME	β-mercaptoethanol
CIP	calf intestinal alkaline phosphatase
conc	concentrated
dH_2O	distilled water
dial	dialysis
DMEM	Dulbecco's Modified Eagle Medium
DNA	deoxyribonucleic acid
DNase	deoxyribonuclease
dsDNA	double-stranded DNA
DTT	dithiothreitol
EDTA	ethylenediaminetetraacetic acid
elu	elution
FL	full length
fth	flowthrough
I	insoluble
IL	interleukin
INF	interferon
IRF	Interferon regulatory factor
IPTG	isopropyl β-D-1 thiogalactopyranoside
LB	Luria Bertani broth

M	marker; membrane fraction
MBP	maltose binding protein
min	minutes
mit	mitochondrial fraction
µl	microliters
ml	milliliters
mM	millimoles
MPXV	Monkeypox virus
MW	molecular weight
NP-40	Nonidet P-40
nuc	nuclear fraction
OD_{600}	optical density at wavelength 600nm
P	pellet
PAGE	polyacrylamide gel electrophoresis
PBS	phosphate buffered saline
PBST	phosphate buffered saline with Tween 20
PCR	polymerase chain reaction
pI	isoelectric point
PVDF	polyvinyl difluoride
rpm	revolutions per minute
S	soluble
SDS	sodium dodecylsulfate
Sec	seconds
T	total
TAE	Tris-acetate-EDTA
TBS	Tris buffered saline
TBST	Tris buffered saline with Tween 20
TEMED	tetramethylethylenediamine
TEV	Tobacco Etch virus // cleavage site of TEV protease

TIR	Toll-Interleukin receptor
TLR	Toll-like receptor
TRAM	TRIF-related adapter molecule
TRIF	TIR-domain-containing adapter-inducing interferon-β
trx	thioredoxin
UV	ultraviolet light
VACV	Vaccinia virus
VARV	Variola virus
VETF	Vaccinia virus early transcription factor
VITFs	Vaccinia virus intermediate transcription factors
wth	washthrough

References

http://viralzone.expasy.org

Aderem A, Ulevitch RJ. Toll-like receptors in the induction of the innate immune response. *Nature*. 2000;406(6797):782-787.

Akira S, Takeda K. Toll-like receptor signalling. *Nat Rev Immunol*. 2004;4:499-511.

Ansarah-Sobrinho C, Moss B. Role of the I7 protein in proteolytic processing of vaccinia virus membrane and core components. *J Virol*. 2004;78(12):6335-6343.

Appleyard G, Hapel AJ, Boulter EA. An antigenic difference between intracellular and extracellular rabbitpox virus. *J Gen Virol*. 1971;13(1):9-17.

Armstrong JA, Metz DH, Young MR. The Mode of Entry of Vaccinia Virus into L Cells. *J Gen Virol*. 1973;21(3):533-537.

Bahar MW, Graham SC, Chen RAJ, Cooray S, Smith GL, Stuart DI, Grimes JM. How vaccinia virus has evolved to subvert the host immune response. *J Struct Biol*. 2011;175(2):127-134.

Baldick CJ, Keck JG, Moss B. Mutational analysis of the core, spacer, and initiator regions of vaccinia virus intermediate-class promoters. *J Virol*. 1992;66(8):4710-4719.

Baroudy BM, Venkatesan S, Moss B. Incompletely base-paired flip-flop terminal loops link the two DNA strands of the vaccinia virus genome into one uninterrupted polynucleotide chain. *Cell.* 1982;28(2):315-324

Barquet N, Domingo P. Smallpox: the triumph over the most terrible of the ministers of death. *Ann Intern Med.* 1997;127(8 Pt 1):635-642.

Belongia EA, Naleway AL. Smallpox vaccine: the good, the bad, and the ugly. *Clin Med Res*. 2003;1(2):87-92.

Bisht H, Weisberg AS, Szajner P, Moss B. Assembly and disassembly of the capsid-like external scaffold of immature virions during vaccinia virus morphogenesis. *J Virol*. 2009;83(18):9140-9150.

Blancou J, Kieny MP, Lathe R, Lecocq JP, Pastoret PP, Soulebot JP, Desmettre P. Oral vaccination of the fox against rabies using a live recombinant vaccinia virus. *Nature.* 1986;322(6077):373-375.

Bolanos-Garcia VM, Davies OR. Structural analysis and classification of native proteins from E. coli commonly co-purified by immobilised metal affinity chromatography. *Biochim Biophys Acta*. 2006;1760(9):1304-1313.

B**owie A, Kiss-Toth E, Symons JA, Smith GL, Dower SK, O'Neill LAJ.** A46R and A52R from vaccinia virus are antagonists of host IL-1 and toll-like receptor signaling. *Proc Natl Acad Sci U S A*. 2000;97(18):10162-10167.

Boyle KA, Arps L, Traktman P. Biochemical and genetic analysis of the vaccinia virus D5 protein: Multimerization-dependent ATPase activity is required to support viral DNA replication. *J Virol*. 2007;81(2):844-859.

Boyle KA, Stanitsa ES, Greseth MD, Lindgren JK, Traktman P. Evaluation of the role of the vaccinia virus uracil DNA glycosylase and A20 proteins as intrinsic components of the DNA polymerase holoenzyme. *J Biol Chem*. 2011;286(28):24702-24713.

Brady G, Bowie AG. Innate immune activation of NFκB and its antagonism by poxviruses. *Cytokine Growth Factor Rev.* 2014;25(5):611-620.

Brochier B, Costy F, Pastoret PP. Elimination of fox rabies from Belgium using a recombinant vaccinia-rabies vaccine: an update. *Vet Microbiol*. 1995;46(1-3):269-279.

Broyles SS. Vaccinia virus transcription. *J Gen Virol*. 2003;84(9):2293-2303.

Broyles SS, Moss B. Sedimentation of an RNA polymerase complex from vaccinia virus that specifically initiates and terminates transcription. *Mol Cell Biol*. 1987;7(1):7-14.

Broyles SS, Yuen L, Shuman S, Moss B. Purification of a factor required for transcription of vaccinia virus early genes. *J Biol Chem*. 1988;263(22):10754-10760.

Burns K, Janssens S, Brissoni B, Olivos N, Beyaert R, Tschopp J. Inhibition of Interleukin 1 Receptor/Toll-like Receptor Signaling through the Alternatively Spliced, Short Form of MyD88 Is Due to Its Failure to Recruit IRAK-4. *J Exp Med*. 2003;197(2):263-268.

Cairns J. The initiation of vaccinia infection. *Virology*. 1960;11(3):603-623.

Carter GC, Law M, Hollinshead M, Smith GL. Entry of the vaccinia virus intracellular mature virion and its interactions with glycosaminoglycans. *J Gen Virol*. 2005;86(5):1279-1290.

Challberg MD, Englund PT. Purification and properties of the deoxyribonucleic acid polymerase induced by vaccinia virus. *J Biol Chem*. 1979;254(16):7812-7819.

Chang A, Metz DH. Further investigations on the mode of entry of vaccinia virus into cells. *J Gen Virol.* 1976;32(2):275–282

Chang SJ, Chang YX, Izmailyan R, Tang YL, Chang W. Vaccinia virus A25 and A26 proteins are fusion suppressors for mature virions and determine strain-specific virus entry pathways into HeLa, CHO-K1, and L cells. *J Virol*. 2010;84(17):8422-8432.

Chen RAJ, Jacobs N, Smith GL. Vaccinia virus strain Western Reserve protein B14 is an intracellular virulence factor. *J Gen Virol*. 2006;87(6):1451-1458.

Chen RAJ, Ryzhakov G, Cooray S, Randow F, Smith GL. Inhibition of IκB kinase by vaccinia virus virulence factor B14. *PLoS Pathog*. 2008;4(2):e22.

Chiu WL, Lin CL, Yang MH, Tzou DLM, Chang W. Vaccinia virus 4c (A26L) protein on intracellular mature virus binds to the extracellular cellular matrix laminin. *J Virol*. 2007;81(5):2149-2157.

Chung CS, Hsiao JC, Chang YS, Chang W. A27L protein mediates vaccinia virus interaction with cell surface heparan sulfate. *J Virol*. 1998;72(2):1577-1585.

Condit RC, Moussatche N, Traktman P. In a nutshell: structure and assembly of the vaccinia virion. *Adv Virus Res*. 2006;66:31-124.

Cyrklaff M, Risco C, Fernández JJ, Jiménez MV, Estéban M, Baumeister W, Carrascosa JL. Cryo-electron tomography of vaccinia virus. *Proc Natl Acad Sci U S A*. 2005;102(8):2772-2777.

Da Fonseca FG, Wolffe EJ, Weisberg A, Moss B. Effects of deletion or stringent repression of the H3L envelope gene on vaccinia virus replication. *J Virol*. 2000;74(16):7518-7528.

Dales S. The uptake and development of vaccinia virus in strain L cells followed with labeled viral deoxyribonucleic acid. *J Cell Biol.* 1963;18(1):51-72.

Dales S, Mosbach EH. Vaccinia as a model for membrane biogenesis. *Virology.* 1968;35(4):564-583.

Dales S, Siminovitch L. The development of vaccinia virus in Earle's L strain cells as examined by electron microscopy. *J Biophys Biochem Cytol*. 1961;10(4):475-503.

Davison AJ, Moss B. Structure of vaccinia virus early promoters. *J Mol Biol.* 1989a;210(4):749-69.

Davison AJ, Moss B. Structure of vaccinia virus late promoters. *J Mol Biol.* 1989b;210(4):771-84.

DeLange AM, McFadden G. Sequence-nonspecific replication of transfected plasmid DNA in poxvirus-infected cells. *Proc Natl Acad Sci U S A*. 1986;83(3):614-618.

De Silva FS, Lewis W, Berglund P, Koonin EV, Moss B. Poxvirus DNA primase. *Proc Natl Acad Sci U S A.* 2007;104(47):18724-18729.

Dharmawardhane S, Schürmann A, Sells MA, Chernoff J, Schmid SL, Bokoch GM. Regulation of macropinocytosis by p21-activated kinase-1. *Mol Biol Cell*. 2000;11(10):3341-3352.

DiPerna G, Stack J, Bowie AG, Boyd A, Kotwal G, Zhang Z, Arvikar S, Latz E, Fitzgerald KA, Marshall WL. Poxvirus protein N1L targets the I-κB kinase complex, inhibits signaling to NF-κB by the tumor necrosis factor superfamily of receptors, and inhibits NF-κB and IRF3 signaling by toll-like receptors. *J Biol Chem*. 2004;279(35):36570-36578.

Doms RW, Blumenthal R, Moss B. Fusion of intra-and extracellular forms of vaccinia virus with the cell membrane. *J Virol*. 1990;64(10):4884-4892.

Dubochet J, Adrian M, Richter K, Garces J, Wittek R. Structure of intracellular mature vaccinia virus observed by cryoelectron microscopy. *J Virol*. 1994;68(3):1935-1941.

Ellison KS, Peng W, McFadden G. Mutations in active-site residues of the uracil-DNA glycosylase encoded by vaccinia virus are incompatible with virus viability. *J Virol*. 1996;70(11):7965-7973.

Ember SWJ, Ren H, Ferguson BJ, Smith GL. Vaccinia virus protein C4 inhibits NF-κB activation and promotes virus virulence. *J Gen Virol*. 2012;93(Pt 10):2098-2108.

Enokizono Y, Kumeta H, Funami K, Horiuchi M, Sarmiento J, Yamashita K, Standley DM, Matsumoto M, Seya T, Inagaki F. Structures and interface mapping of the TIR domain-containing adaptor molecules involved in interferon signaling. *Proc Natl Acad Sci U S A*. 2013;110(49):19908-19913.

Esposito D, Chatterjee DK. Enhancement of soluble protein expression through the use of fusion tags. *Curr Opin Biotechnol*. 2006;17(4):353-358.

Evans E, Klemperer N, Ghosh R, Traktman P. The vaccinia virus D5 protein, which is required for DNA replication, is a nucleic acid-independent nucleoside triphosphatase. *J Virol*. 1995;69(9):5353-5361.

Fedosyuk S. Structural studies of VACV A46 and TBEV NS2B/3 proteins as an approach to elucidate virus-host interactions. 2014. *Dissertation*

Fedosyuk S, Bezerra GA, Radakovics K, Smith TK, Sammito M, Bobik N, Round A, Ten Eyck LF, Djinović-Carugo K, Usón I, Skern T. Vaccinia virus immunomodulator A46: A lipid and protein-binding scaffold for sequestering host TIR-domain proteins. *PLoS Pathog*. 2016;12(12):e1006079.

Fedosyuk S, Grishkovskaya I, de Almeida Ribeiro E, Skern T. Characterization and structure of the vaccinia virus NF-κB antagonist A46. *J Biol Chem*. 2014;289(6):3749-3762.

Fenner F, Wittek R, Dumbell KR. The Orthopoxviruses. *Academic Press, Inc*. 1989.

Fenner F, Henderson DA, Arita I, Ježek Z, Ladnyi ID. Smallpox and its eradication. *History Of International Public Health, No.6*; World Health Organization, Geneva. 1988.

Fitzgerald KA, Palsson-McDermott EM, Bowie AG, Jefferies CA, Mansell AS, Brady G, Brint E, Dunne A, Gray P, Harte MT, McMurray D, Smith DE, Sims JE, Bird TA, O'Neill LA. Mal (MyD88-adapter-like) is required for Toll-like receptor-4 signal transduction. *Nature*. 2001;413(6851):78-83.

Fitzgerald KA, Rowe DC, Barnes BJ, Caffrey DR, Visintin A, Latz E, Monks B, Pitha PM, Golenbock DT. LPS-TLR4 Signaling to IRF-3/7 and NF-κB involves the Toll adapters TRAM and TRIF. *J Exp Med*. 2003a;198(7):1043-1055.

Fitzgerald KA, McWhirter SM, Faia KL, Rowe DC, Latz E, Golenbock DT, Coyle AJ, Liao SM, Maniatis T. IKKε and TBK1 are essential components of the IRF3 signaling pathway. *Nat Immunol*. 2003b;4(5):491-496.

Franklin E, Khan AR. Poxvirus antagonism of innate immunity by Bcl-2 fold proteins. *J Struct Biol*. 2013;181(1):1-10.

Freuling CM, Hampson K, Selhorst T, Schröder R, Meslin FX, Mettenleiter TC, Müller T. The elimination of fox rabies from Europe: determinants of success and lessons for the future. *Philos Trans R Soc Lond B Biol Sci.* 2013;368(1623):20120142.

Funami K, Sasai M, Ohba Y, Oshiumi H, Seya T, Matsumoto M. Spatiotemporal mobilization of Toll/IL-1 receptor domain-containing adaptor molecule-1 in response to dsRNA. *J Immunol*. 2007;179(10):6867-6872.

Funami K, Sasai M, Oshiumi H, Seya T, Matsumoto M. Homo-oligomerization is essential for Toll/interleukin-1 receptor domain-containing adaptor molecule-1-mediated NF-κB and interferon regulatory factor-3 activation. *J Biol Chem*. 2008;283(26):18283-18291.

Garcia AD, Moss B. Repression of vaccinia virus Holliday junction resolvase inhibits processing of viral DNA into unit-length genomes. *J Virol*. 2001;75(14):6460-6471.

Gershon PD, Moss B. Early transcription factor subunits are encoded by vaccinia virus late genes. *Proc Natl Acad Sci U S A*. 1990;87(11):4401-4405.

Ghosh S, May MJ, Kopp EB. NF-κB and Rel proteins: evolutionarily conserved mediators of immune responses. *Annu Rev Immunol*. 1998;16:225-260.

Glück JM, Hoffmann S, Koenig BW, Willbold D. Single vector system for efficient N-myristoylation of recombinant proteins in *E. coli*. *PLoS One*. 2010;5(4):e10081.

Goebel SJ, Johnson GP, Perkus ME, Davis SW, Winslow JP, Paoletti E. The complete DNA sequence of vaccinia virus. *Virology.* 1990;179(1):247-266, 517-63.

González JM, Esteban M. A poxvirus Bcl-2-like gene family involved in regulation of host immune response: sequence similarity and evolutionary history. *Virol J*. 2010;7:59.

Goldufsky J, Sivendran S, Harcharik S, Pan M, Bernardo S, Stern RH, Friedlander P, Ruby CE, Saenger Y, Kaufman HL. Oncolytic virus therapy for cancer. *Oncolytic Virother*. 2013;2:31-46.

Graham SC, Bahar MW, Cooray S, Chen RAJ, Whalen DM, Abrescia NGA, Alderton D, Owens RJ, Stuart DI, Smith GL, Grimes JM. Vaccinia virus proteins A52 and B14 share a Bcl-2-like fold but have evolved to inhibit NF-κB rather than apoptosis. *PLoS Pathog*. 2008;4(8):e1000128.

Griffiths G, Wepf R, Wendt T, Locker JK, Cyrklaff M, Roos N. Structure and assembly of intracellular mature vaccinia virus: isolated-particle analysis. *J Virol.* 2001;75(22):11034-11055.

Hansson GK, Edfeldt K. Toll to be paid at the gateway to the vessel wall. *Arterioscler Thromb Vasc Biol*. 2005;25(6):1085-1087.

Harte MT, Haga IR, Maloney G, Gray P, Reading PC, Bartlett NW, Smith GL, Bowie A, O'Neill LAJ. The poxvirus protein A52R targets Toll-like receptor signaling complexes to suppress host defense. *J Exp Med*. 2003;197(3):343-351.

Henderson DA, Moss B. Recombinant Vaccinia Virus Vaccines. In: *Vaccines, 3rd edition.* Philadelphia: Saunders; 1999.

Henderson DA, Inglesby TV, Bartlett JG, Ascher MS, Eitzen E, Jahrling PB, Hauer J, Layton M, McDade J, Osterholm MT, O'Toole T, Parker G, Perl T, Russell PK, Tonat K. Smallpox as a biological weapon: medical and public health management. Working Group on Civilian Biodefense. *JAMA.* 1999; 281(22):2127-2137.

Heuser J. Deep-etch EM reveals that the early poxvirus envelope is a single membrane bilayer stabilized by a geodetic "honeycomb" surface coat. *J Cell Biol*. 2005;169(2):269-283.

Hollinshead M, Vanderplasschen A, Smith GL, Vaux DJ. Vaccinia virus intracellular mature virions contain only one lipid membrane. *J Virol*. 1999;73(2):1503-1517.

Howard AR, Senkevich TG, Moss B. Vaccinia virus A26 and A27 proteins form a stable complex tethered to mature virions by association with the A17 transmembrane protein. *J Virol*. 2008;82(24):12384-12391.

Hruby DE. Vaccinia virus vectors: New strategies for producing recombinant vaccines. *Clin Microbiol Rev*. 1990;3(2):153-170.

Hughes AL, Friedman R. Poxvirus genome evolution by gene gain and loss. *Mol Phylogenet Evol.* 2005;35(1):186-195

Hultmark D. Macrophage differentiation marker MyD88 is a member of the Toll/IL-1 receptor family. *Biochem Biophys Res Commun.* 1994;199(1): 144–146

Ichihashi Y, Oie M, Tsuruhara T. Location of DNA-binding proteins and disulfide-linked proteins in vaccinia virus structural elements. *J Virol*. 1984;50(3):929-938.

Ishii K, Moss B. Role of vaccinia virus A20R protein in DNA replication: construction and characterization of temperature-sensitive mutants. *J Virol*. 2001;75(4):1656-1663.

Jacobs BL, Langland JO, Kibler KV, Denzler KL, White SD, Holechek SA, Wong S, Huynh T, Baskin CR. Vaccinia virus vaccines: past, present and future. *Antivir Res*. 2009;84(1):1-13.

Jain A, Kaczanowska S, Davila E. IL-1 receptor-associated kinase signaling and its role in inflammation, cancer progression, and therapy resistance. *Front Immunol*. 2014;5:553.

Joklik WK. The poxviruses. *Bacteriol Rev*. 1966;30(1):33-66.

Jones EV, Moss B. Mapping of the vaccinia virus DNA polymerase gene by marker rescue and by cell-free translation of selected RNA. *J Virol*. 1984;49(1):72-77.

Kalverda AP, Thompson GS, Vogel A, Schröder M, Bowie AG, Khan AR, Homans SW. Poxvirus K7 protein adopts a Bcl-2 fold: biochemical mapping of its interactions with human DEAD box RNA helicase DDX3. *J Mol Biol*. 2009;385(3):843-853.

Karin M, Ben-Neriah Y. Phosphorylation meets ubiquitination: the control of NF-κB activity. *Annu Rev Immunol*. 2000;18:621-663.

Kates JR, McAuslan BR. Poxvirus DNA-dependent RNA polymerase. *Proc Natl Acad Sci U S A.* 1967;58(1):134-141.

Katsafanas GC, Moss B. Linkage of transcription and translation within cytoplasmic poxvirus DNA factories provides a mechanism to coordinate viral and usurp host functions. *Cell Host Microbe*. 2007;2(4):221-228.

Keck JG, Baldick CJ Jr, Moss B. Role of DNA replication in vaccinia virus gene expression: a naked template is required for transcription of three late trans-activator genes. *Cell.* 1990;61(5):801-809.

Kim Y, Lee H, Heo L, Seok C, Choe J. Structure of vaccinia virus A46, an inhibitor of TLR4 signaling pathway, shows the conformation of VIPER motif. *Protein Sci*. 2014;23(7):906-914.

Kirn DH, Thorne SH. Targeted and armed oncolytic poxviruses: a novel multi-mechanistic therapeutic class for cancer. *Nat Rev Cancer*. 2009;9(1):64-71.

Kollewe C, Mackensen AC, Neumann D, Knop J, Cao P, Li S, Wesche H, Martin MU. Sequential autophosphorylation steps in the interleukin-1 receptor-associated kinase-1 regulate its availability as an adapter in interleukin-1 signaling. *J Biol Chem*. 2004;279(7):5227-5236.

Kretzschmar M, Wallinga J, Teunis P, Xing S, Mikolajczyk R. Frequency of adverse events after vaccination with different vaccinia strains. *PLoS Med*. 2006;3(8):e272.

Lemaitre B, Nicolas E, Michaut L, Reichhart JM, Hoffmann JA. The dorsoventral regulatory gene cassette *spätzle/Toll/cactus* controls the potent antifungal response in Drosophila adults. *Cell*. 1996;86(6):973-983.

Li S, Strelow A, Fontana EJ, Wesche H. IRAK-4: A novel member of the IRAK family with the properties of an IRAK-kinase. *Proc Natl Acad Sci U S A*. 2002;99(8):5567-5572.

Liu L, Cooper T, Howley PM, Hayball JD. From crescent to mature virion: Vaccinia virus assembly and maturation. *Viruses*. 2014;6(10):3787-3808.

Locker JK, Kuehn A, Schleich S, Rutter G, Hohenberg H, Wepf R, Griffiths G. Entry of the two infectious forms of vaccinia virus at the plasma membane is signaling-dependent for the IMV but not the EEV. *Mol Biol Cell*. 2000;11(7):2497-2511.

Lysakova-Devine T, Keogh B, Harrington B, Nagpal K, Halle A, Golenbock DT, Monie T, Bowie AG. Viral inhibitory peptide of TLR4, a peptide derived from vaccinia protein A46, specifically inhibits TLR4 by directly targeting MyD88 adaptor-like and TRIF-related adaptor molecule. *J Immunol*. 2010;185(7):4261-4271.

Maloney G, Schröder M, Bowie AG. Vaccinia virus protein A52R activates p38 mitogen-activated protein kinase and potentiates lipopolysaccharide-induced interleukin-10. *J Biol Chem*. 2005;280(35):30838-30844.

Matho MH, Maybeno M, Benhnia MREI, Becker D, Meng X, Xiang Y, Crotty S, Peters B, Zajonc DM. Structural and biochemical characterization of the vaccinia virus envelope protein D8 and its recognition by the antibody LA5. *J Virol*. 2012;86(15):8050-8058.

Mayr A. Smallpox vaccination and bioterrorism with pox viruses. *Comp Immunol Microbiol Infect Dis. 2003;26(5-6):423-430.*

McCraith S, Holtzman T, Moss B, Fields S. Genome-wide analysis of vaccinia virus protein-protein interactions. *Proc Natl Acad Sci U S A*. 2000;97(9):4879-4884.

Medzhitov R, Preston-Hurlburt P, Janeway Jr CA. A human homologue of the *Drosophila* Toll protein signals activation of adaptive immunity. *Nature*. 1997;388(6640):394-397.

Medzhitov R, Janeway Jr C. Innate immune recognition: mechanisms and pathways. *Immunol Rev*. 2000;173:89-97.

Mercer J, Helenius A. Vaccinia virus uses macropinocytosis and apoptotic mimicry to enter host cells. *Science*. 2008;320(5875):531-535.

Mercer J, Knébel S, Schmidt FI, Crouse J, Burkard C, Helenius A. Vaccinia virus strains use distinct forms of macropinocytosis for host-cell entry. *Proc Natl Acad Sci U S A*. 2010;107(20):9346-9351.

Minnigan H, Moyer RW. Intracellular location of rabbit poxvirus nucleic acid within infected cells as determined by in situ hybridization. *J Virol*. 1985;55(3):634-643.

Morgan C. Vaccinia virus reexamined: development and release. *Virology.* 1976;73(1):43-58.

Morgan JR, Cohen LK, Roberts BE. Identification of the DNA sequences encoding the large subunit of the mRNA-capping enzyme of vaccinia virus. *J Virol*. 1984;52(1):206-214.

Moss B. Vaccinia virus: a tool for research and vaccine development. *Science.* 1991;252(5013):1662-1667.

Moss B. Poxvirus cell entry: how many proteins does it take? *Viruses*. 2012;4(5):688-707.

Moss B. Poxvirus DNA replication. *Cold Spring Harb Perspect Biol*. 2013;5(9):a010199.

Moyer RW, Graves RL. The mechanism of cytoplasmic orthopoxvirus DNA replication. *Cell.* 1981;27(2 Pt 1):391-401.

Muzio M, Ni J, Feng P, Dixit VM. IRAK (Pelle) family member IRAK-2 and MyD88 as proximal mediators of IL-1 signaling. *Science*. 1997;278(5343):1612-1615.

Nalca A, Rimoin AW, Bavari S, Whitehouse CA. Reemergence of monkeypox: prevalence, diagnostics, and countermeasures. *Clin Infect Dis*. 2005;41(12):1765-1771.

Niles EG, Seto J. Vaccinia virus gene D8 encodes a virion transmembrane protein. *J Virol*. 1988;62(10):3772-3778.

Oeckinghaus A, Ghosh S. The NF-κB family of transcription factors and its regulation. *Cold Spring Harb Perspect Biol*. 2009;1(4):a000034

O'Neill LAJ, Bowie AG. The family of five: TIR-domain-containing adaptors in Toll-like receptor signalling. *Nat Rev Immunol*. 2007;7(5):353-364.

Oshiumi H, Matsumoto M, Funami K, Akazawa T, Seya T. TICAM-1, an adaptor molecule that participates in Toll-like receptor 3–mediated interferon-β induction. *Nat Immunol*. 2003a;4(2):161-167.

Oshiumi H, Sasai M, Shida K, Fujita T, Matsumoto M, Seya T. TIR-containing adapter molecule (TICAM)-2, a bridging adapter recruiting to Toll-like receptor 4 TICAM-1 that induces interferon-β. *J Biol Chem*. 2003b;278(50):49751-49762.

Pahl HL. Activators and target genes of Rel/NF-κB transcription factors. *Oncogene*. 1999;18(49):6853-6866.

Panicali D, Paoletti E. Construction of poxviruses as cloning vectors: insertion of the thymidine kinase gene from herpes simplex virus into the DNA of infectious vaccinia virus. *Proc Natl Acad Sci U S A*. 1982;79(16):4927-4931.

Payne LG, Kristenson K. Mechanisms of vaccinia virus release and its specific inhibition by N_1-isonicotinoyl-N_2-3-methyl-4-chlorobenzoylhydrazine. *J Virol.* 1979;32(2):614-622.

Pedley CB, Cooper RJ. The assay, purification and properties of vaccinia virus-induced uncoating protein. *J Gen Virol*. 1987;68(4):1021-1028.

Perkus ME, Piccini A, Lipinskas BR, Paoletti E. Recombinant vaccinia virus: immunization against multiple pathogens. *Science.* 1985;229(4717):981–984.

Qin L, Favis N, Famulski J, Evans DH. Evolution of and evolutionary relationships between extant vaccinia virus strains. *J Virol*. 2015;89(3):1809-1824.

Risco C, Rodríguez JR, López-Iglesias C, Carrascosa JL, Esteban M, Rodríguez D. Endoplasmic reticulum-Golgi intermediate compartment membranes and vimentin filaments participate in vaccinia virus assembly. *J Virol*. 2002;76(4):1839-1855.

Rodriguez D, Rodriguez JR, Esteban M. The vaccinia virus 14-kilodalton fusion protein forms a stable complex with the processed protein encoded by the vaccinia virus A17L gene. *J Virol*. 1993;67(6):3435-3440.

Rodríguez JR, Risco C, Carrascosa JL, Esteban M, Rodríguez D. Characterization of early stages in vaccinia virus membrane biogenesis: implications of the 21-kilodalton protein and a newly identified 15-kilodalton envelope protein. *J Virol*. 1997;71(3):1821-1833.

Rodrigo WWP, Dassanayake RS, Karunanayake EH, Gunawardene YINS, Weerasena OVDSJ. Heterologous expression, chaperone mediated solubilization and purification of parasitic nematode-specific growth factor-like protein of *Setaria digitata*. *Asian Pac J Trop Med*. 2014;7(2):85-92.

Roper RL, Payne LG, Moss B. Extracellular vaccinia virus envelope glycoprotein encoded by the A33R gene. *J Virol*. 1996;70(6):3753-3762.

Rowe DC, McGettrick AF, Latz E, Monks BG, Gay NJ, Yamamoto M, Akira S, O'Neill LA, Fitzgerald KA, Golenbock DT. The myristoylation of TRIF-related adaptor molecule is essential for Toll-like receptor 4 signal transduction. *Proc Natl Acad Sci U S A*. 2006;103(16):6299-6304.

Sambrook J, Shatkin AJ. Polynucleotide ligase activity in cells infected with simian virus 40, polyoma virus, or vaccinia virus. *J Virol*. 1969;4(5):719-726.

Sánchez-Sampedro L, Perdiguero B, Mejías-Pérez E, García-Arriaza J, Di Pilato M, Esteban M. The evolution of poxvirus vaccines. *Viruses*. 2015;7(4):1726-1803.

Sato S, Sugiyama M, Yamamoto M, Watanabe Y, Kawai T, Takeda K, Akira S. Toll/IL-1 receptor domain-containing adaptor inducing IFN-β (TRIF) associates with TNF receptor-associated factor 6 and TANK-binding kinase 1, and activates two distinct transcription factors, NF-κB and IFN-regulatory factor-3, in the Toll-like receptor signaling. *J Immunol*. 2003;171(8):4304-4310.

Schmelz M, Sodeik B, Ericsson M, Wolffe EJ, Shida H, Hiller G, Griffiths G. Assembly of vaccinia virus: the second wrapping cisterna is derived from the trans Golgi network. *J Virol*. 1994;68(1):130-147.

Schmidt FI, Bleck CKE, Reh L, Novy K, Wollscheid B, Helenius A, Stahlberg H, Mercer J. Vaccinia virus entry is followed by core activation and proteasome-mediated release of the immunomodulatory effector VH1 from lateral bodies. *Cell Rep*. 2013;4(3):464-476.

Schnierle BS, Gershon PD, Moss B. Cap-specific mRNA (nucleoside-$O^{2'}$-)-methyltransferase and poly(A) polymerase stimulatory activities of vaccinia virus are mediated by a single protein. *Proc Natl Acad Sci U S A*. 1992;89(7):2897-2901.

Schröder M, Baran M, Bowie AG. Viral targeting of DEAD box protein 3 reveals its role in TBK1/IKKε-mediated IRF activation. *EMBO J*. 2008;27(15):2147-2157.

Seet BT, Johnston JB, Brunetti CR, Barrett JW, Everett H, Cameron C, Sypula J, Nazarian SH, Lucas A, McFadden G. Poxviruses and immune evasion. *Annu Rev Immunol*. 2003;21:377-423.

Senkevich TG, Bruno D, Martens C, Porcella SF, Wolf YI, Moss B. Mapping vaccinia virus DNA replication origins at nucleotide level by deep sequencing. *Proc Natl Acad Sci U S A*. 2015;112(35):10908-10913.

Shackelton LA, Holmes EC. The evolution of large DNA viruses: combining genomic information of viruses and their hosts. *Trends Microbiol.* 2004;12(10):458-465

Sharma S, tenOever BR, Grandvaux N, Zhou GP, Lin R, Hiscott J. Triggering the interferon antiviral response through an IKK-related pathway. *Science*. 2003;300(5622):1148-1151.

Singh K, Gittis AG, Gitti RK, Ostazeski SA, Su HP, Garboczi DN. The vaccinia virus H3 envelope protein, a major target of neutralizing antibodies, exhibits a glycosyltransferase fold and binds UDP-Glucose. *J Virol*. 2016;90(10):5020-5030.

Slack JL, Schooley K, Bonnert TP, Mitcham JL, Qwarnstrom EE, Sims JE, Dower SK. Identification of two major sites in the type I interleukin-1 receptor cytoplasmic region responsible for coupling to pro-inflammatory signaling pathways. *J Biol Chem*. 2000;275(7):4670-4678.

Smith GL, Law M. The exit of vaccinia virus from infected cells. *Virus Res.* 2004;106(2):189-197.

Smith GL, McFadden G. Smallpox: anything to declare? *Nat Rev Immunol*. 2002;2(7):521-527.

Smith GL, Benfield CTO, Maluquer de Motes C, Mazzon M, Ember SWJ, Ferguson BJ, Sumner RP. Vaccinia virus immune evasion: mechanisms, virulence and immunogenicity. *J Gen Virol*. 2013;94(11):2367-2392.

Sodeik B, Doms RW, Ericsson M, Hiller G, Machamer CE, van't Hof W, van Meer G, Moss B, Griffiths G. Assembly of vaccinia virus: Role of the intermediate compartment between the endoplasmic reticulum and the Golgi stacks. *J Cell Biol*. 1993;121(3):521-541.

Soulat D, Bürckstümmer T, Westermayer S, Goncalves A, Bauch A, Stefanovic A, Hantschel O, Bennett KL, Decker T, Superti-Furga G. The DEAD-box helicase DDX3X is a critical component of the TANK-binding kinase 1-dependent innate immune response. *EMBO J*. 2008;27(15):2135-2146.

Stack J, Bowie AG. Poxviral protein A46 antagonizes Toll-like receptor 4 signaling by targeting BB loop motifs in Toll-IL-1 receptor adaptor proteins to disrupt receptor:adaptor interactions. *J Biol Chem*. 2012;287(27):22672-22682.

Stack J, Haga IR, Schröder M, Bartlett NW, Maloney G, Reading PC, Fitzgerald KA, Smith GL, Bowie AG. Vaccinia virus protein A46R targets multiple Toll-like-interleukin-1 receptor adaptors and contributes to virulence. *J Exp Med*. 2005;201(6):1007-1018.

Stuart DT, Upton C, Higman MA, Niles EG, McFadden G. A poxvirus-encoded uracil DNA glycosylase is essential for virus viability. *J Virol*. 1993;67(5):2503-2512.

Szajner P, Weisberg AS, Lebowitz J, Heuser J, Moss B. External scaffold of spherical immature poxvirus particles is made of protein trimers, forming a honeycomb lattice. *J Cell Biol*. 2005;170(6):971-981.

Takeda K, Kaisho T, Akira S. Toll-like receptors. *Annu Rev Immunol*. 2003;21:335-376.

Tatematsu M, Ishii A, Oshiumi H, Horiuchi M, Inagaki F, Seya T, Matsumoto M. A molecular mechanism for Toll-IL-1 receptor domain-containing adaptor molecule-1-mediated IRF-3 activation. *J Biol Chem*. 2010;285(26):20128-20136.

Terpe K. Overview of tag protein fusions: from molecular and biochemical fundamentals to commercial systems. *Appl Microbiol Biotechnol*. 2003;60(5):523-533.

Thorne SH, Hwang TH, Kirn DH. Vaccinia virus and oncolytic virotherapy of cancer. *Curr Opin Mol Ther.* 2005;7(4):359-365.

Tolonen N, Doglio L, Schleich S, Locker JK. Vaccinia virus DNA replication occurs in endoplasmic reticulum-enclosed cytoplasmic mini-nuclei. *Mol Biol Cell*. 2001;12(7):2031-2046.

Tooze J, Hollinshead M, Reis B, Radsak K, Kern H. Progeny vaccinia and human cytomegalovirus particles utilize early endosomal cisternae for their envelopes. *Eur J Cell Biol.* 1993;60(1):163-178.

Townsley AC, Weisberg AS, Wagenaar TR, Moss B. Vaccinia virus entry into cells via a low-pH-dependent endosomal pathway. *J Virol*. 2006;80(18):8899-8908.

Townsley AC, Moss B. Two distinct low-pH steps promote entry of vaccinia virus. *J Virol*. 2007;81(16):8613-8620.

Traktman P, Sridhar P, Condit RC, Roberts BE. Transcriptional mapping of the DNA polymerase gene of vaccinia virus. *J Virol*. 1984;49(1):125-131.

Traktman P, Liu K, DeMasi J, Rollins R, Jesty S, Unger B. Elucidating the essential role of the A14 phosphoprotein in vaccinia virus morphogenesis: construction and characterization of a tetracycline-inducible recombinant. *J Virol*. 2000;74(8):3682-3695.

Tulman ER, Delhon G, Afonso CL, Lu Z, Zsak L, Sandybaev NT, Kerembekova UZ, Zaitsev VL, Kutish GF, Rock DL. Genome of horsepox virus. *J Virol*. 2006;80(18):9244-9258.

Ullah MO, Valkov E, Ve T, Williams S, Mas C, Mansell A, Kobe B. Recombinant production of functional full-length and truncated human TRAM/TICAM-2 adaptor protein involved in Toll-like receptor and interferon signaling. *Protein Expr Purif*. 2015;106:31-40.

Ullah MO, Sweet MJ, Mansell A, Kellie S, Kobe B. TRIF-dependent TLR signaling, its functions in host defense and inflammation, and its potential as a therapeutic target. *J Leukoc Biol*. 2016;100(1):27-45.

Unger B, Mercer J, Boyle KA, Traktman P. Biogenesis of the vaccinia virus membrane: genetic and ultrastructural analysis of the contributions of the A14 and A17 proteins. *J Virol*. 2013;87(2):1083-1097.

Vanderplasschen A, Smith GL. A novel virus binding assay using confocal microscopy: demonstration that the intracellular and extracellular vaccinia virions bind to different cellular receptors. *J Virol*. 1997;71(5):4032-4041.

Vanderplasschen A, Mathew E, Hollinshead M, Sim RB, Smith GL. Extracellular enveloped vaccinia virus is resistant to complement because of incorporation of host complement control proteins into its envelope. *Proc Natl Acad Sci U S A*. 1998;95(13):7544-7549.

Veisi K, Farajnia S, Zarghami N, Khoram Khorshid HR, Samadi N, Ahdi Khosroshahi S, Zarei Jaliani H. Chaperone-assisted soluble expression of a humanized anti-EGFR ScFv antibody in *E. Coli. Adv Pharm Bull*. 2015;5(Suppl 1):621-627.

Vos JC, Stunnenberg HG. Derepression of a novel class of vaccinia virus genes upon DNA replication. *EMBO J*. 1988;7(11):3487-3492.

Wang C, Deng L, Hong M, Akkaraju GR, Inoue J, Chen ZJ. TAK1 is a ubiquitin-dependent kinase of MKK and IKK. *Nature*. 2001;412(6844):346-351.

Wang DR, Hsiao JC, Wong CH, Li GC, Lin SC, Yu SS, Chen W, Chang W, Tzou DL. Vaccinia viral protein A27 is anchored to the viral membrane via a cooperative interaction with viral membrane protein A17. *J Biol Chem*. 2014;289(10):6639-6655.

Ward BM. Visualization and characterization of the intracellular movement of vaccinia virus intracellular mature virions. *J Virol*. 2005;79(8):4755-4763.

Wei CM, Moss B. Methylated nucleotides block 5'-terminus of vaccinia virus messenger RNA. *Proc Natl Acad Sci U S A*. 1975;72(1):318-322.

Wesche H, Henzel WJ, Shillinglaw W, Li S, Cao Z. MyD88: An adapter that recruits IRAK to the IL-1 receptor complex. *Immunity*. 1997;7(6):837-847.

Whitbeck JC, Foo CH, de Leon MP, Eisenberg RJ, Cohen GH. Vaccinia virus exhibits cell-type-dependent entry characteristics. *Virology.* 2009;385(2):383-391.

Wittek R, Moss B. Tandem repeats within the inverted terminal repetition of vaccinia virus DNA. *Cell.* 1980;1:277-284.

Xu Y, Tao X, Shen B, Horng T, Medzhitov R, Manley JL, Tong L. Structural basis for signal transduction by the Toll/interleukin-1 receptor domains. *Nature*. 2000;408(6808):111-115.

Yamamoto M, Sato S, Mori K, Hoshino K, Takeuchi O, Takeda K, Akira S. Cutting edge: a novel Toll/IL-1 receptor domain-containing adapter that preferentially activates the IFN-β promoter in the Toll-like receptor signaling. *J Immunol*. 2002;169(12):6668-6672.

Yoneyama M, Suhara W, Fukuhara Y, Fukuda M, Nishida E, Fujita T. Direct triggering of the type I interferon system by virus infection: activation of a transcription factor complex containing IRF-3 and CBP/p300. *EMBO J*. 1998;17(4):1087-1095.

Yu L, Wang L, Chen S. Endogenous toll-like receptor ligands and their biological significance. *J Cell Mol Med*. 2010;14(11):2592-2603.

Yu Z, Huang Z, Lung ML. Subcellular fractionation of cultured human cell lines. *Bio-protocol. 2013;*3(9):e754.

Zakay-Roness Z, Bernkopf H. Effect of active and ultraviolet-irradiated inactive vaccinia virus on the development of Shay leukemia in rats. *Cancer Res*. 1964;24:373-378.

Zonov E, Kochneva G, Yunusova A, Grazhdantseva A, Richter V, Ryabchikova E. Features of the antitumor effect of vaccinia virus Lister strain. *Viruses*. 2016;8(1):20.